CHAPTER 4. PAVEMENT PERFORMANCE

4.1 Introduction

The main purpose of this study has been to investigate relationships between higher strength and associated properties of concrete, its effect on pavement performance, and its added resistance to chemical and physical deterioration. In the context of increasing strength, the objective is to identify the key concrete properties and mix characteristics associated with the improved pavement performance.

The preliminary evaluation of the effects of PCC strength on pavement performance levels, based on the LTPP database, indicated that some of the primary pavement deterioration mechanisms are hidden within the foundation layer properties and climate/traffic parameters. See chapter 1. Therefore, a detailed field investigation was undertaken to isolate the effects and the mechanisms of PCC on JPCP deterioration from the effects of foundation and environmental factors.

The review of the LTPP database and other available information from various SHA's revealed only a few in-service concrete pavements of high strength (45 to 50 MPa or above) and sufficient age (> 20 to 25 years) in different climatic zones for evaluation in this study. Three out of the fifteen test sections selected for detailed field and laboratory investigation had high in-service compressive strength. These three sections were located in different climatic zones. The Washington State LTPP section 53-3812, in the WNF zone, was selected as it had the highest field compressive strength of 75 MPa (10,875 lbf/in^2) and had excellent long-term performance. The higher strength JPCP near Tracy, California, 06-CS3, located in the DNF zone, had field compressive strength of about 58 MPa (8,410 lbf/in^2). The third high strength project was the Wisconsin LTPP section 55-3008 located in the WF zone, with a field compressive strength of 62 MPa (8,990 lbf/in^2).

In each of these climate zones, other projects were selected to cover a range in strength levels and performance. The complete test matrix includes seven projects from the DNF and DF zones, five from the WF zone, and three from the WNF zone. Chapter 3 presents key pavement information, climate data, PCC properties, and summary site and petrographic descriptions. Appendixes A through E provide the detailed results obtained by the project team and include field surveys, mechanical properties (strength and stiffness), air void characteristics and concrete composition, permeability, mix compositions, and additional petrographic analysis.

The selected 15 test sections span the low, medium and high strength range for jointed plain concrete pavements found in the LTPP database as discussed in section 5.1.

4.1.1 Pavement Distress at the Time of Field Testing

Summary distress survey results, collected during the field investigation portion of this project, are shown in table 4.1.1 and 4.1.2. At the time of field testing, 10 out of the 15 sections had not developed any significant amount of distress in terms of joint faulting,

spalling and transverse cracking. The fifteen pavements represent a range in concrete strength, joint spacing, traffic levels, age, and climatic regions. Eight sections represent pavements, which have low long-term distress. They are 20 to 25 years old or older. Five sections were 22 years old or older and have developed various distress types and levels. The remaining two sections were included because they have developed the highest amount of joint faulting and joint spalling in the LTPP database. The Wisconsin LTPP section 55-3008 had developed an average of 9.0 mm joint faulting. The Iowa LTPP section 19-3006 had the highest amount of joint spalling in the database with 20 out of 23 joints in the high level spalling category. For a JPCP on CTB, this section had also developed a significant amount of joint faulting with an average of 4.2 mm. In addition, 5 of its 22 slabs had developed low severity transverse cracking.

Among the investigated pavements was an older California PCC pavement experimental project, which was constructed in 1971. Four different pavement designs were included to study the effect of joint spacing, slab thickness, PCC strength, and base type (CTB versus LCB) on pavement performance (Wells and Nokes, 1991). They are undoweled JPCP designs with random, skewed, and nonsealed transverse joints. All sections have a 137 mm (5.4 in.) base with three sections resting on cement treated base (CTB) and one section resting on lean concrete base (LCB). All sections have a 610 mm (24 in.) aggregate subbase. In this project three northbound sections were selected for detailed field and laboratory investigation, as their original design had not been altered. They include the control section, the higher PCC strength section, and the thickened section. The latter is also an LTPP section (06-7456). The experimental sections had carried substantial heavy vehicle loading (about 16 million ESAL's) at time of investigation.

The experimental test road is of major interest to this project as the effect of increased PCC strength on pavement performance can be evaluated relative to a control section. The higher design strength was achieved by increasing the cement content from 307 to 418 kg/m^3 (5½ to 7½ sacks per yd^3). It will be shown that increasing the cement content instead of reducing the w/c ratio has had a detrimental effect on pavement performance. For the control section, 06-CS1, seven slabs were cracked, averaging about 21 percent slab cracking for the section. Of the 32 slabs in test section 06-CS3, 23 had developed low to medium-severity full lane-width transverse cracking. The thickened test section, 06-7456, had developed a significant amount of joint faulting (2.6 mm) for a JPCP on CTB, but without the associated transverse cracking. Only one slab out of 33 had transverse cracking.

The following sections discuss the major findings on the development of faulting, spalling, and transverse cracking. Faulting and spalling are evaluated in terms of development over an extended period of time, and the data represent the time-series of distress available in the LTPP database combined with the last distress survey conducted at time of field testing. The observed transverse cracking is discussed based on intermittent and permanent loss of support.

Table 4.1.1 *Observed faulting determined in this study and overall foundation stiffness. (The joint spacings can be found in table 3.1.1.)*

Climate	Section ID	Age (Years)	Traffic (KESAL)	Base Type	Joint LTE System	Joints (#)	Ave. Faulting (mm)	Subgrade Stiffness (CBR)
DNF	06-3017	20	3900	CTB	Agg.	31	0.6	86
	06-3021	24	5250	CTB	Agg.	33	1.6	46
	06-7456	25	16000	CTB	Agg.	33	2.6	NA
	06-CS1	26	16000	CTB	Agg.	33	0.0	74
	06-CS3	26	16000	CTB	Agg.	32	1.1	72
	06-I10	51	>16000[1]	CTB	Agg.	33	1.6	67
DF	53-3019	11	6200	Granular	Agg.	43	0.4	57
WF	19-3006	22	3975	CTB	Dowels	23	4.2	6
	19-3055	28	4265	Granular	Agg.	25	2.9	10
	27-4054	25	10700	Granular	Dowels	19	2.7	NA
	39-3801	13	4685	CTB	Dowels	25	0.4	44
	55-3008	22	15220	Granular	Agg.	34	9.0	7
WNF	53-3011	20	8935	Granular	Agg.	43	2.2	83
	53-3812	33	12765	Granular	Agg.	34	1.0	81
	13-GA1-5/6	25	23025	CTB/ATB	Dowels	26	2.0	4

[1] estimated.

Table 4.1.2 *Observed joint spalling and transverse cracking in this study.*

Climate	Section ID	Age (years)	Traffic (KESAL)	No. of Joints	Transverse Joint Spalling Indicated in levels of low, moderate, and high. (L,M,H)						Transverse Slab Cracking Indicated in levels of low, moderate, and high. (L,M,H)					
					L (m)	No.	M (m)	No.	H (m)	No.	L (m)	No.	M (m)	No.	H (m)	No.
DNF	06-3017	20	3900	31	0.5	3	0	0	0	0	0	0	0	0	0	0
	06-3021	24	5250	33	5.4	24	0	0	0	0	6.9	2	0	0	0	0
	06-7456	25	16000	33	1.9	4	0	0	0	0	0	1	0	0	0	0
	06-CS1	26	16000	33	3.2	20	0	0	0	0	23.6	7	0	0	0	0
	06-CS3	26	16000	32	1.4	11	0	0	0	0	82	23	0	0	0	0
	06-I10	51	>16000[1]	33	2.7	22	0	0	0	0	28.6	8	0	0	0	0
DF	53-3019	11	6200	43	10.0	42	0	0	0	0	0	0	0	0	0	0
WF	19-3006	22	3975	23	24.1	20	4.0	7	25	20	18.5	5	0	0	0	0
	19-3055	28	4265	25	19.0	24	0	0	0	0	0	0	0	0	0	0
	27-4054	25	10700	19	9.5	16	0	0	0	0	2.4	1	0	0	0	0
	39-3801	13	4685	25	8.6	25	0	0	0	0	0	0	0	0	0	0
	55-3008	22	15220	34	47.5	33	0	0	0	0	4	1	0	0	0	0
WNF	53-3011	20	8935	43	11.1	41	0	0	0	0	0	0	0	0	0	0
	53-3812	33	12765	34	10.4	30	0	0	0	0	0	0	0	0	0	0
	13-GA1-5/6	25	23025	26	0	0	0	0	0	0	0	0	0	0	0	0

[1] estimated.

4.2 Joint and Crack Faulting

Faulting can be caused either by slab settlement or by the accumulation of loose material beneath the slab near the approach joints. This distress type is important as it controls the ride quality. Observations of faulted joints by Neal et al. (1985) show that a thicker accumulation occurs under the approach slab (upstream side of the joint), causing this end to lift. Material accumulates under the approach slab when the leave slab deflects from wheel loading. When the leave slab is deflected by wheel load, the fines and free water under the joints are ejected towards the approach joint side, where the fines accumulate and gradually lift up the joint, causing faulting. In order to create this type of joint or crack faulting, these factors must occur simultaneously: heavy vehicle loading, free water at the slab-base interface, fines and/or erodible base material, poor load transfer, and curling/warping.

Analysis of field and laboratory data showed that Wisconsin section 55-3008 had developed the highest amount of joint faulting in the LTPP database due to slab settlement and pumping. The JPCP rests on a granular base over a very soft foundation. The data and surface profile measurements using the dipstick device suggest that the substantial pavement upward curvature in the higher strength PCC has occurred over time, and that the foundation has been able to conform to the slab's shape as it settled. In this case the faulting had developed without transverse cracking and corner breaks, indicating that the slab settlement did not induce permanent loss of slab support by the foundation. The data suggests that the foundation had been able to conform to the slab's shape as it settled.

The data obtained for the experimental test sections near Tracy in California showed that these sections developed faulting as a result of pumping erosion with associated accumulation of fines near the approach joint. The erosion had formed a gap under the leave slab and the slab had de-bonded from the base. This condition, combined with temperature curling, can over time induce fatigue transverse cracking starting at the top of the slab. The cracking phenomenon is discussed in detail in section 4.3.

The following sections include a discussion of the variation of joint and crack faulting along a test section, and a discussion on the development of faulting for JPCP's depending on traffic and foundation characteristics.

4.2.1 Joint Faulting from Slab Settlement or Pumping Erosion

Slab Settlement of the Wisconsin Section 55-3008

Surface elevation profiles for the Wisconsin section 55-3008 show joint faulting of 4.3 to 15.2 mm. Figure 4.2.1 shows a faulted joint in this section. Despite the severe faulting, only 1 out of 33 slabs for the 153-m test section has developed transverse cracking of low severity. See also table 4.1.2. Figure 4.2.2 shows the surface elevation profiles for three 30-m sections starting at the beginning of the test section. The surface profiles were obtained in the direction of traffic for both the outer and the inner wheel-paths using the Dipstick device. The 153-m section was measured in increments of 0.3 m (1 ft) starting

at the white painted marker located in this case 0.9 m (3 ft) before the beginning of the first transverse joint. A zero beginning elevation was selected at the start point for both the outer and the inner wheel paths, and the site design slopes were removed as well in order to show small changes in elevation profiles. These results show quantitatively the amount of faulting of each joint. Also, the slabs are noticeably rotated from faulting at the joints with the approach side of the joint turned upward and the leave side of the joint turned downward. Furthermore, the profiles also show that the slabs are of varying length and that only one slab is cracked (located 75 to 80 m from the start of the test section).

In addition to the rotation, the slabs are curved upward at approach joints, consistent with pumping of fines in the presence of water from the leave side to the approach side of a joint. The foundation is forgiving, which has allowed the slab to settle and develop substantial permanent upward curved shape, thereby reducing loss of support. Excellent agreement was obtained between the profiles in the outer and inner wheel paths.

Figure 4.2.1 *Faulted transverse joint in test section 55-3008.*

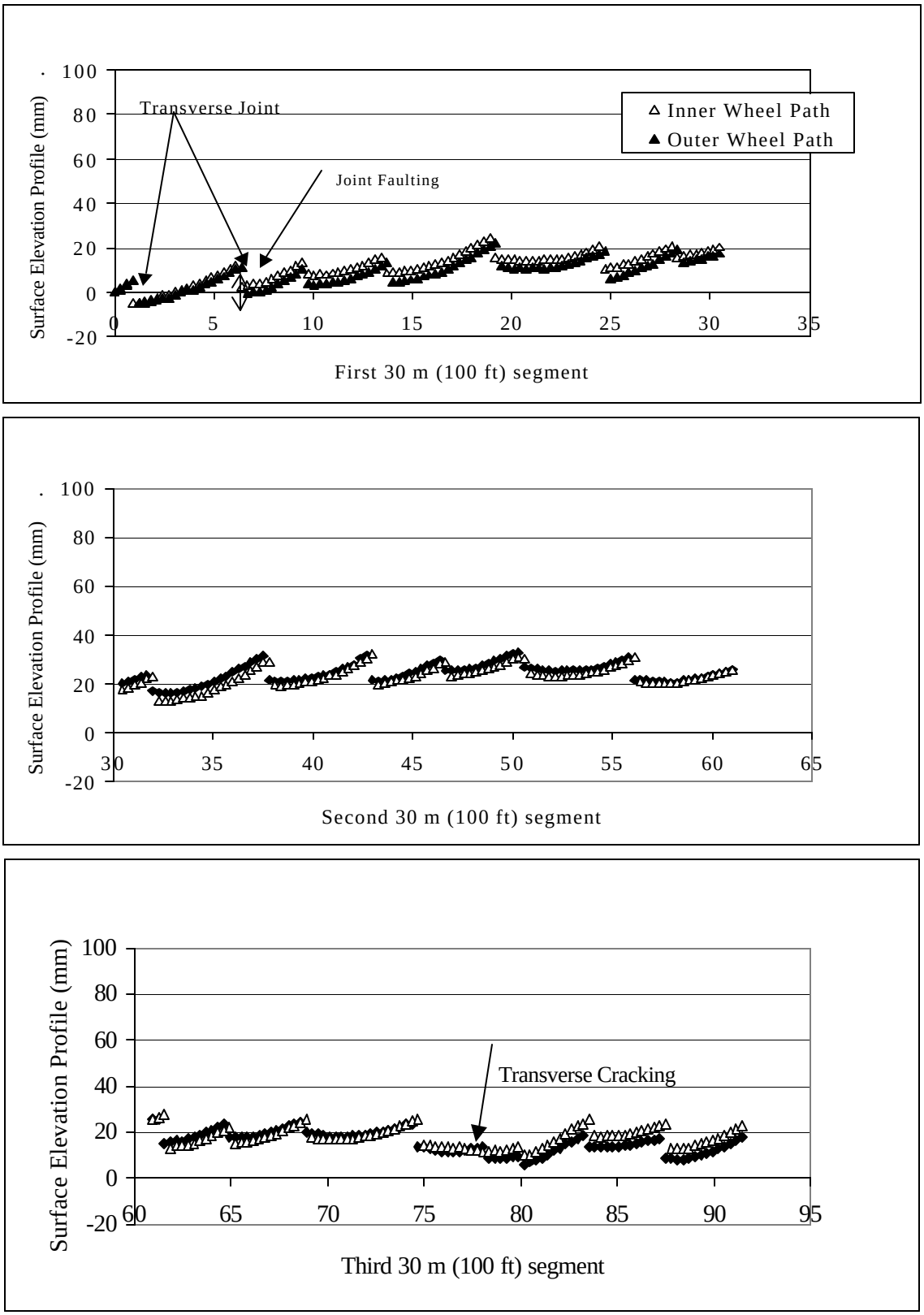

Figure 4.2.2 *Surface profiles for test section 55-3008 with random joint spacing.*

Pumping Erosion on Experimental Test Road near Tracy, California

Surface staining on the shoulder close to joints from pumping was evident for the Tracy Test Road sections 06-CS1 and 06-CS3 as seen from figure 4.2.3. Surface elevation profiles of individual slabs show the effects of pumping with a tendency for the approach side of each transverse joint to develop a permanent concave upward shape. See figure 4.2.4 for Tracy Test Road Section 06-7456. Neal et al. (1985) studied this buildup of fines under slabs in detail. They used tracer sand under the pavement and the shoulder to locate movement of fines, and demonstrated that the source of fines was the adjacent shoulder and the CTB surface. This is consistent with figure 4.2.5, which shows a depressed shoulder. Pumping erosion leads to de-bonding of the CTB from the concrete slab.

Figure 4.2.3 *Surface staining on the shoulder close to joints from Tracy Test Road (06-CS1).*

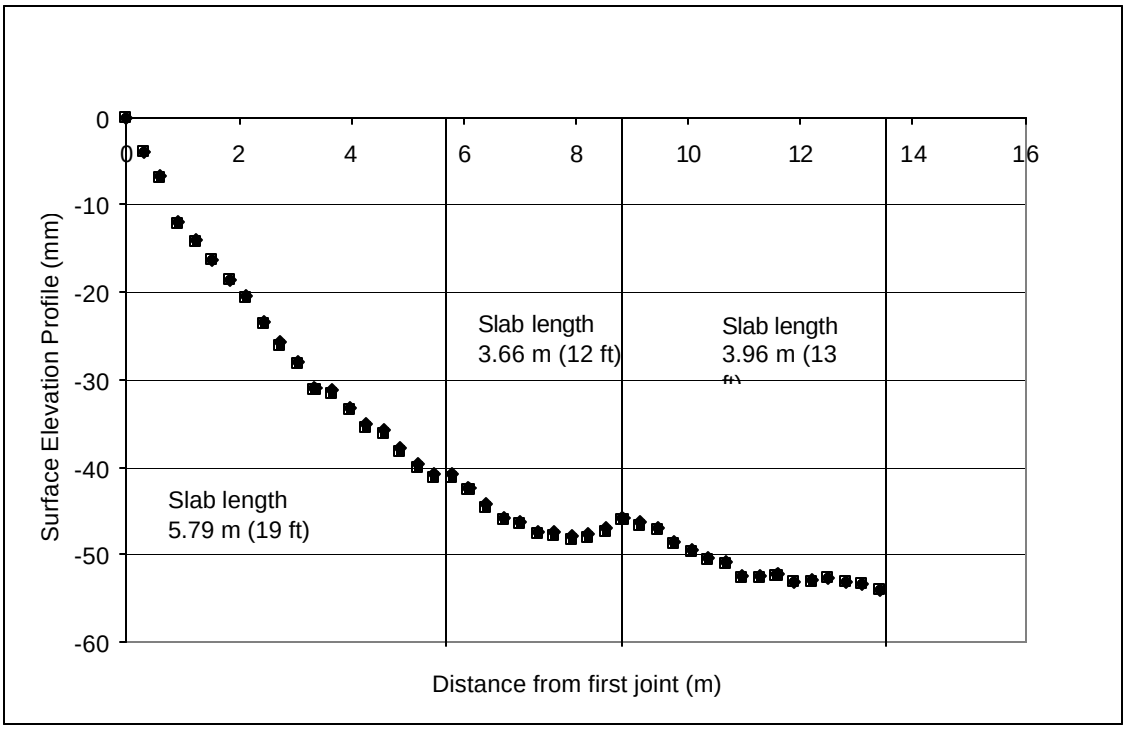

Figure 4.2.4 *Surface elevation profiles for 06-7456 at Tracy. The design slope is not extracted from the profiles.*

Figure 4.2.5 *Depressed shoulder in test section 06-CS3 from pumping of fines. Transverse cracking in outer and inner lane.*

4.2.2 Individual Joint/Crack Faults versus Section Average

Faulting is typically evaluated in terms of one single average section value. The drawback of using one average value is that it can obscure the true faulting, as both negative and positive faulting values occur.

Figures 4.2.6, 4.2.7, and 4.2.8 illustrate the variability in joint faulting measured along the outer wheel path in the direction of traffic for the 153-m test section as illustrated for three different projects. The test sections are 06-I-10, 06-7456 and 06-CS3 in California. Fault measurements were made using the Georgia Faultmeter. The typical coefficient of variation for this distress type is about 50 percent. Note that no clear relation between joint spacing and the level of faulting has been detected from the faulting data.

The effect of environment on faulting is noticeable for the 51 year old I-10 project in San Bernadino Co., California. For this project fault measurements were conducted near the inner wheel path to avoid a section exposed to surface grinding. The faulting data along this test section illustrate the effect of local conditions on overall faulting. See figure 4.2.6. In the first 120 m of the 153-m test section the joint and crack faulting varies between –1.5 and 4.2 mm. However, at the bridge overpass on Etiwanda Ave. the faulting data stabilizes at a level of 1 mm. This is substantially smaller compared to the rest of the test section. It is believed that the reduced faulting is associated with the absence of water under the bridge overpass. Free water is one of the necessary components for faulting development due to pumping erosion. This agrees with findings by Wells (1993). He also showed that traffic and climate are the major factors with respect to joint fault development for several California JPCP's, and that a stable non-erodible LCB tends to reduce fault development. Wells and Nokes (1991) showed, based on fault measurements, that the PCC pavement on LCB of the experimental test sections on I-5, near Tracy, was most resistant to pumping erosion. This was confirmed by a recent investigation by Caltrans on the performance of these sections (Long and Shatnawi, 2000).

It is important to determine fault measurements for each joint and crack along a project length and to monitor the fault development over time as transverse cracks relieve slab stress. The presence of cracks may skew the average project fault value downward as faulting of cracks has not developed over the same time period as that of the joints. Crack faulting may even be negative (i.e. approach crack side lower than leave side) due to slab rotation. This is illustrated for section 06-CS3 in figure 4.2.7. The fault values for this section vary between -2.5 and 5.6 mm with an average value of 1.1 mm. However, the majority of the crack fault data falls below the section average. In addition, it is noticeable that the thickened section at the Tracy Test Road, 06-7456, has a higher overall section fault of about 2.6 mm, and that the fault data ranges from about -1 to 9 mm, see figure 4.2.8. It is suggested that the higher joint faulting is because these thicker slabs have not yet cracked. Furthermore, these sections with variable joint spacing (3.6 to 5.8 m) did not show any correlation between slab length and faulting, which indicates that joint faulting is a local problem controlled by pumping. See figure 4.2.9. This is also

in agreement with surface profile measurements for the three project sections 06-CS1, 06-CS3, and 06-7456.

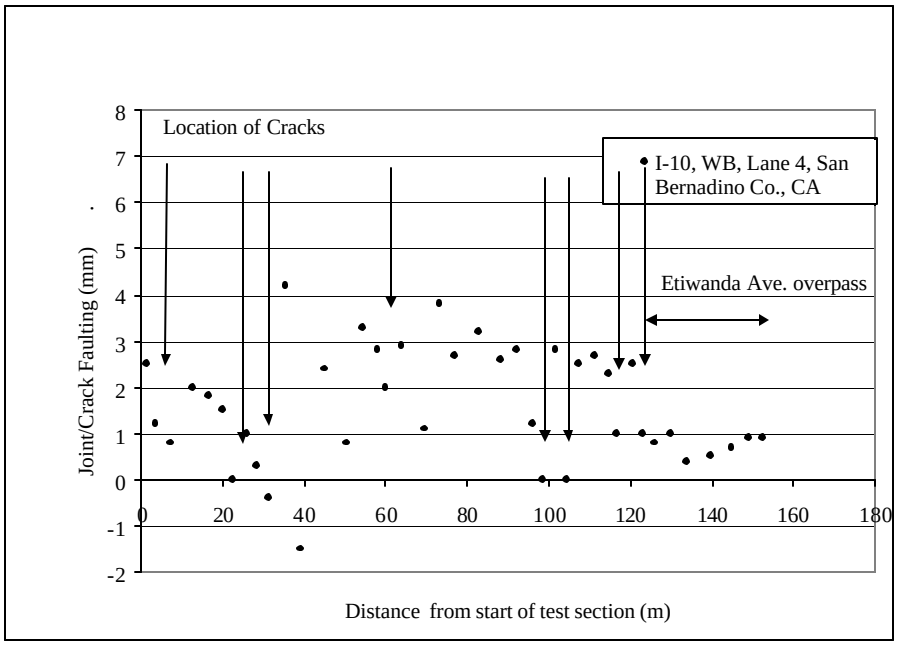

Figure 4.2.6 *Joint/crack faulting measured along the outer wheel path in the direction of traffic for the 153-m test section, 06-I10 in California.*

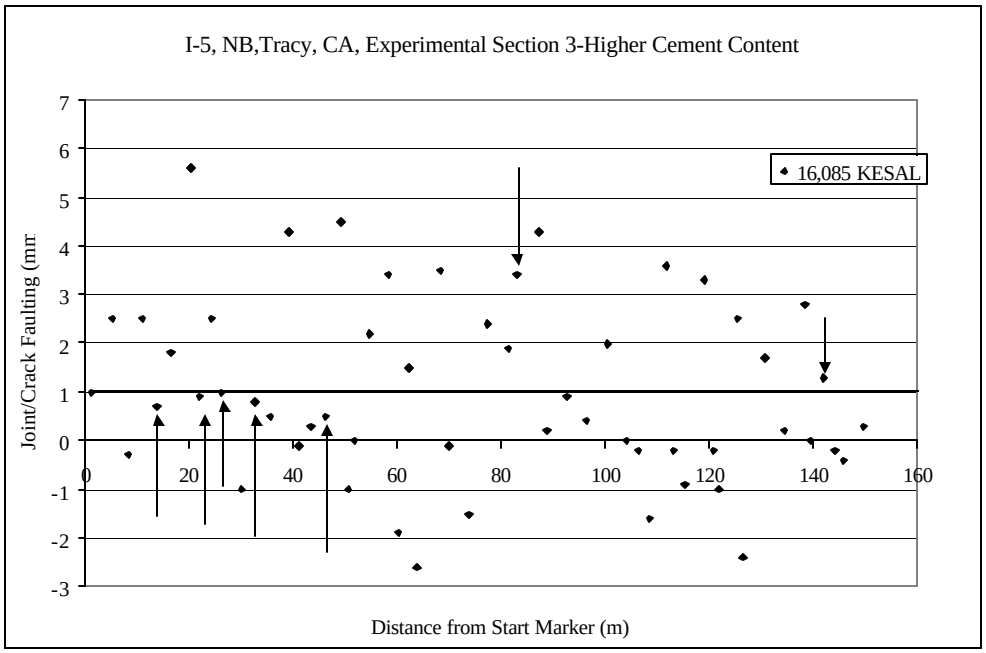

Figure 4.2.7 *Joint/crack faulting measured along the outer wheel path in the direction of traffic for the 153-m test section, experimental test road 06-CS3 near Tracy, California.*

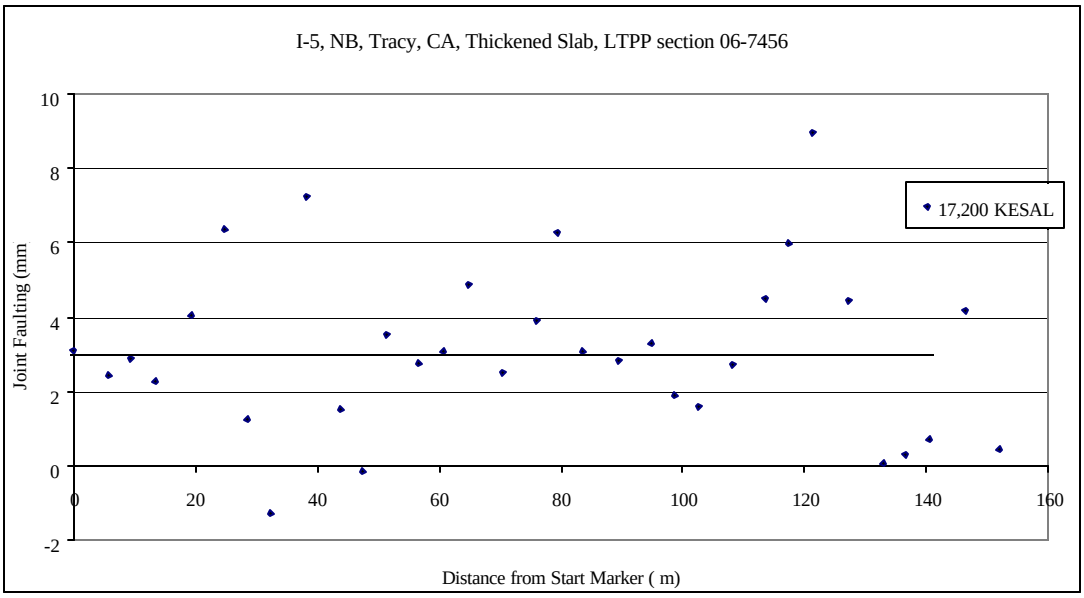

Figure 4.2.8 *Joint/crack faulting measured along the outer wheel path in the direction of traffic for the 153-m test section experimental test road 06-7456 near Tracy, California.*

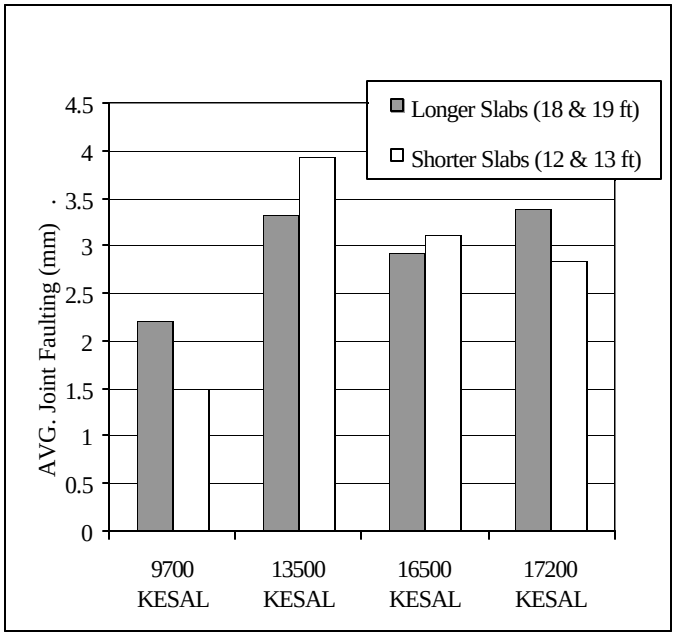

Figure 4.2.9 *Joint faulting for slabs of various lengths for experimental test road 06-7456 near Tracy, California at different cumulative traffic levels.*

In cases where pumping erosion does not occur, fault development for substantial traffic loading (17,000 KESAL's) is negligible for JPCP's on CTB or ATB. This is shown in figures 4.2.10 and 4.2.11 for the Georgia experimental test sections 13-GA1-5 (JPCP on CTB) and 13-GA1-6 (JPCP on ATB).

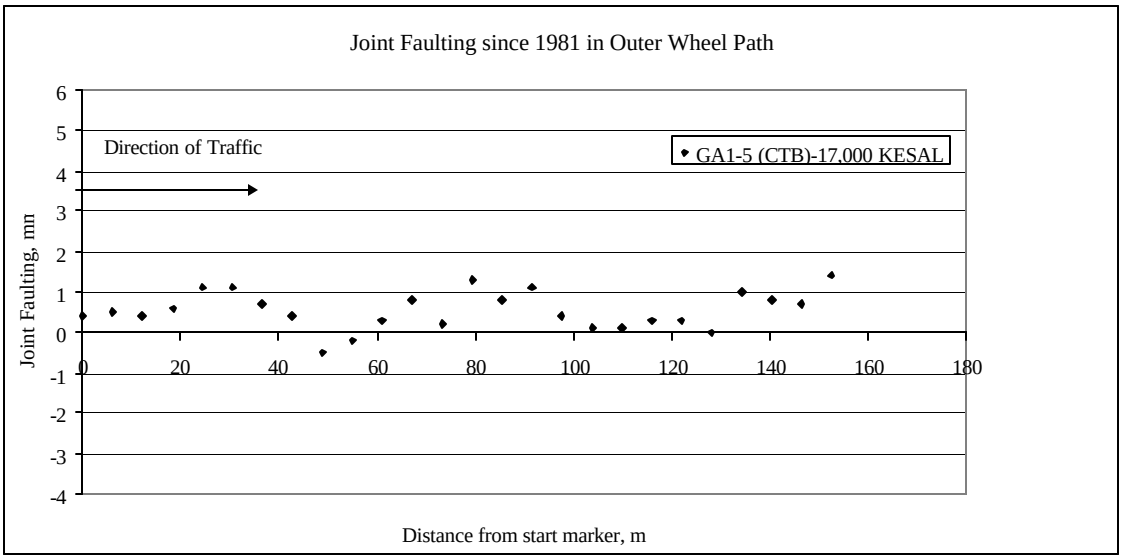

Figure 4.2.10 *Joint faulting measured along the outer wheel path in the direction of traffic for the 153-m test section Georgia Test Road section 13-GA1-5.*

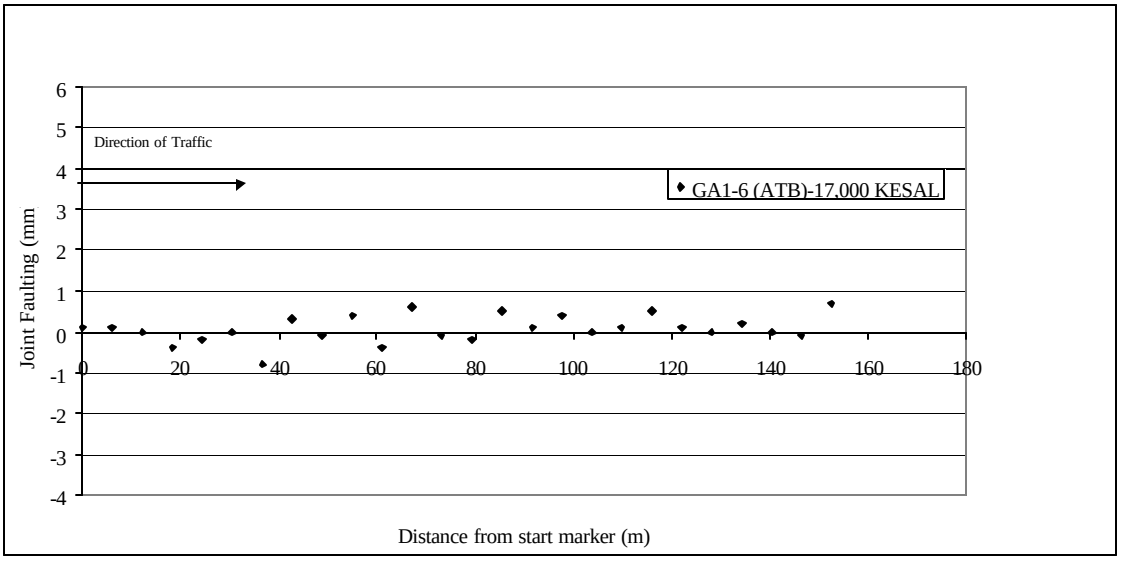

Figure 4.2.11 *Joint faulting measured along the outer wheel path in the direction of traffic for the 153-m test section Georgia Test Road section 13-GA1-6.*

4.2.3 Development of Faulting

Faulting is primarily controlled by the cumulative traffic and base type, and faulting is linearly related to cumulative ESAL's. For granular bases, the rate of faulting increases substantially with decreasing subgrade CBR. Faulting of a JPCP on CTB increases with pumping, and the rate of faulting is controlled by the CTB and not the subgrade CBR. This is shown in figures 4.2.12 and 4.2.13. Overall the observed trend is in agreement with other studies.

Figure 4.2.12 shows the fault development versus traffic for pavements on granular bases. The data represent the time-series of distress available in the LTPP database combined with the last distress survey conducted at time of field testing. The data show a high degree of faulting for section 55-3008 versus traffic. The most plausible reason is settlement of the slab on the soft sandy lean clay subgrade (CBR=7). The rate of increase follows the same trend as section 19-3055, which rests on a foundation with similar characteristics. However, section 19-3055 has not yet experienced the high traffic of section 55-3008.

For other sections on granular bases, where the foundation is much stiffer, faulting develops at a much lower rate. When the faulting of these sections (in figure 4.2.12) is compared to the faulting of sections on stiff CTB's (in figure 4.2.13) the rate of development is found to be similar. Thus, the rate of faulting appears to be independent of base type provided there is uniform stiff support for the pavement slab.

Figure 4.2.13 shows the faulting development versus traffic for sections on CTB's. It can be seen that the overall rate of faulting development is very low. However, there is also a relation between faulting development and the occurrence of pumping in these sections. Pumping of CTB foundations leads to loss of slab support and higher vertical slab displacement. Loss of slab support on a stiff foundation such as a CTB can result in premature transverse cracking, as will be discussed later.

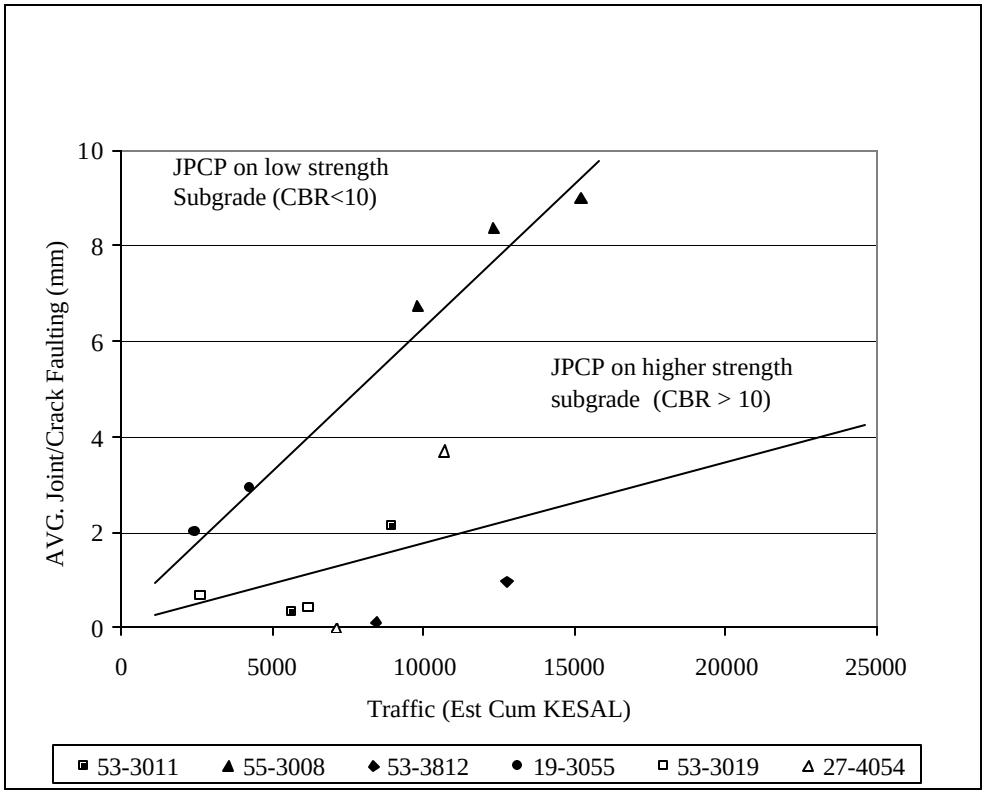

Figure 4.2.12 *Faulting development versus traffic for JPCP on granular bases.*

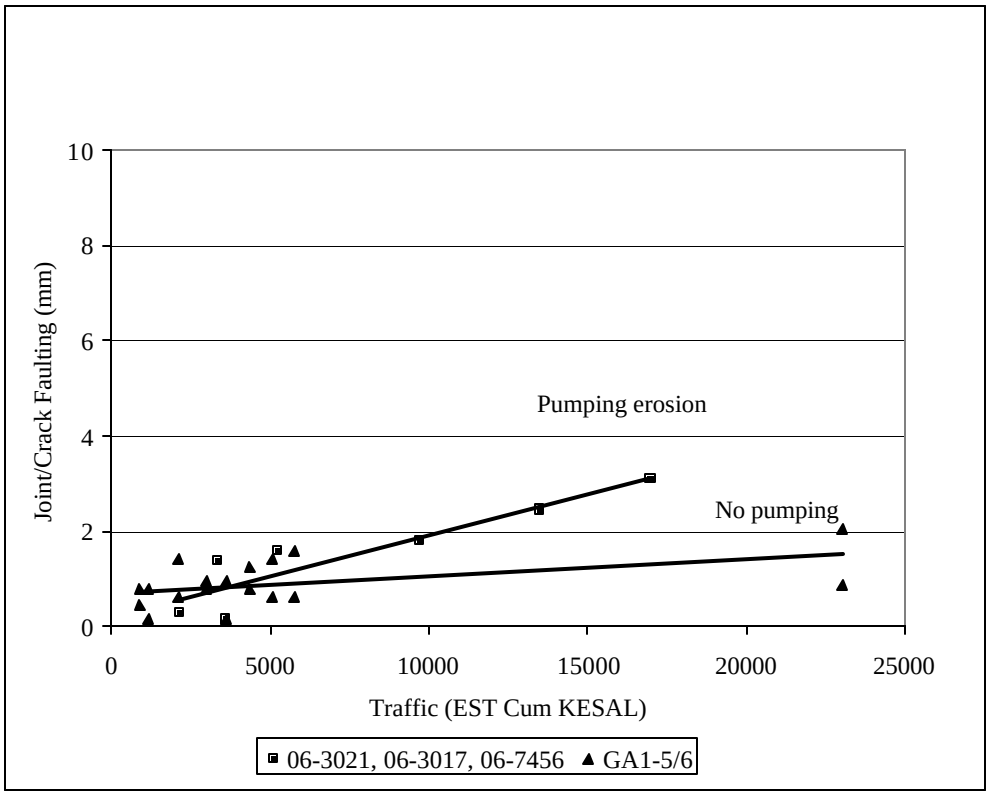

Figure 4.2.13 *Faulting development versus traffic for JPCP on CTB.*

4.2.4 Aggregate Interlock and Pavement Performance

Joint and crack load transfer efficiency (LTE) is often quantified using a relative measure of the deflections on either side of the crack or joint. Several formulas have been developed for quantifying LTE based on slab deflections. The LTE measure proposed by Ioannides and Korovesis (1990) is applied. The equation is:

$$LTE = \frac{d_u}{d_l} \cdot 100\% \qquad (4.2.1)$$

where LTE = load transfer (%)

δ_u = deflection of the unloaded side of the crack or joint (mm), and

δ_l = deflection on the loaded side of the crack or joint (mm).

In this study the LTE was obtained at joints and the values are tabulated in table 4.2.1. Most of the sites have an average site LTE exceeding the suggested 60 percent limit for medium and heavy truck traffic (Smith et al., 1990).

The LTE data show that there is greater variation in LTE values with lower average LTE for a project. This indicates that local joint phenomena are controlling the behavior. The key factors that affect LTE are faulting, spalling, pumping-erosion, crack width, and coarse aggregate type (e.g. Colley and Humphrey, 1967; Nowlen, 1968; Bruinsma et al., 1995; Abdel-Maksoud et al., 1998; and Buch et al., 2000).

One site worth noting is test section 06-I10, in California, where all LTE values were high (78 to 95 percent.) This concrete had very large gravel-like aggregates with a maximum size of 50 to 62 mm. The use of these aggregates would be expected to yield very high load transfer even at large joint openings (e.g. Colley and Humphrey, 1967; Nowlen, 1968; and Abdel-Maksoud et al., 1998).

In general, the LTE is low for the test sections where pumping erosion occurs and only aggregate interlock provides the shear load transfer. The experimental test road near Tracy with the three sections (06-7456 thicker slab, 06-CS1 control section, and 06-CS3 higher cement content) show that the 06-7456 had maintained high LTE compared to the other two sections. The loss of LTE on those sections is likely related to pumping erosion and faulting. However, when LTE is only determined at one point in time the values can only indicate an overall trend, as the coarse aggregate characteristics and the crack width also affect LTE.

The two undoweled Washington sections 53-3011 and 53-3019 on granular bases both have low average LTE of about 34 to 46 percent. However, these sections hardly developed any faulting. It is likely that the high subgrade stiffness and the good subsurface drainage prevented severe fault development in these sections. The subgrade CBR values were on the order of 57 to 83, see table 4.1.1. Table 4.1.2 shows that all joints had started to develop spalling, which is typical for joints with very low LTE.

The lower joint LTE values are associated with fracture through rather than around the coarse aggregates. See also figure 3.1.29. The high early strength in these concretes has likely contributed to the fracture of the coarse aggregates. In such cases, LTE is not improved by using larger size coarse aggregates.

The Iowa test section 19-3055 has also maintained very high joint load transfer (average 86 percent) through its 28 years of service life. This is remarkable since it is an undoweled JPCP's on granular bases over a foundation with relative low subgrade stiffness (CBR of 10). However, the excellent performance is likely due to the low traffic volume, and the avoidance of pumping-erosion and faulting. See figure 4.2.12.

Table 4.2.1 *Average load transfer and its variation along with key design and coarse aggregate information.*

Climate Region	LTPP		Aggregate Characteristics		Traffic (KESAL)	Base Type	Joint Load Transfer System	Load Transfer Efficiency (LTE)			
	State	Section	Max. Aggregate Size[1] (mm)	Type				Section Avg. (%)	Stan. Dev. (%)	Max. (%)	Min. (%)
DNF	06	3017	38.1	gravel (mix)	3900	CTB	Agg.	85	14	98	46
	06	3021	38.1	gravel (mafic)	5250	CTB	Agg.	37	13	59	14
	06	7456	38.1	gravel (mix)	16000	CTB	Agg.	84	NA	NA	NA
	06	CS1	38.1	gravel (mix)	16000	CTB	Agg.	43	15	82	27
	06	CS3	38.1	Gravel mix incl. dol.	16000	CTB	Agg.	56	13	79	39
	06	I-10	50-62	gravel (mix)	>16000[2]	CTB	Agg.	88	6	95	78
DF	53	3019	38.1	gravel (mafic)	6200	Granular	Agg.	46	23	83	23
WF	19	3006	25.4	dol. limestone	3975	CTB	Dowels	80	2	82	77
	19	3055	25.4	dol. limestone	4265	Granular	Agg.	85	1	86	83
	27	4054	25.4	dol. limestone	10700	Granular	Dowels	73	17	94	48
	39	3801	19.1	Grav.+dol. Limestone	4685	CTB	Dowels	67	12	100	58
	55	3008	38.1	dol. limestone	15220	Granular	Agg.	NA	NA	NA	NA
WNF	53	3011	25.4	gravel (mix)	8935	Granular	Agg.	34	20	73	12
	53	3812	38.1	gravel (mix)	12765	Granular	Agg.	NA	NA	NA	NA
	13	GA1-5	38.1	Granite/granodiorite	23025	CTB/ATB	Dowels	78	17	90	37

[1] Based on sieve analysis of thermally decomposed cores.

[2] Estimate

4.3 Transverse Cracking

4.3.1 Effect of Higher Cement Content on Transverse Cracking

Early transverse cracking occurred in the higher cement content section (06-CS3) of the experimental test project near Tracy, California. Caltrans distress surveys (Wells and Nokes, 1991) showed, that 42 percent of the slabs in the higher cement content (06-CS3) section were cracked within the first year after construction, while none of the other sections had developed cracking. Within this time period the project had carried a total of 2.34 million ESAL's. They suggested that slab cracking was due to factors such as thermal shrinkage and drying shrinkage combined with base restraint and/or late joint sawing. This is supported by findings of this study, where this concrete was found to have about 40 percent higher CTE, and estimated to have about 20 percent higher drying shrinkage as compared to the control concrete. This is because the relative volume of shrinking paste increased from 25 percent in the control section 06-CS1 to about 28 percent in section 06-CS3 due to 40 percent higher cement content. At the time of this investigation section 06-CS3 had developed 23 transverse cracks (72 percent) whereas 06-CS1 had developed only 7 cracks (21 percent) as seen from table 4.1.2. See section 5.8 for further discussion on drying shrinkage and CTE values.

4.3.2 Transverse Cracking of JPCP on CTB due to Pumping-Erosion

Upward curled/warped slabs and pumping erosion at joints lead to faulting, and result in uneven slab support. This in turn can cause transverse cracking (Wells and Noke, 1991). This has occurred for some of the test sections on the California experimental project, sections 06-CS1 and 06-CS3, mainly in the longer slabs (i.e. > 5.5 to 5.8 m (18 to 19 ft)). The exception is the thickened section 06-7456, which at the time of this investigation had not developed the associated transverse slab cracking despite the high amount of joint faulting. This is probably due to the greater bending resistance of this thicker section compared to the thinner control section. Figure 4.3.1 shows an overview site photo of the thickened test section, 06-7456. See also table 4.1.2.

Figure 4.3.1 *Overview of the experimental test road at Tracy. Thickened test section 06-7456 with low distress levels.*

4.3.3 Location of Transverse Cracking

For the experimental test road near Tracy, the transverse cracks develop closer to the leave side of the joint than to the approach side of the joint. The same crack pattern had developed in the Ohio test section 19-3006, which had an average joint spacing of 6.1 m. Figures 4.3.2 through 4.3.4 each show the distance to the transverse crack from the approach and leave joint for test sections 06-CS3, 06-I-10, and 19-3006, respectively. The cracks are closer to the leave joint consistent with a greater loss of support near the leave joint. Cracks are typically about 2 to 2.5 m from the leave joint. Figure 4.3.5 shows a typical example of the location of transverse crack for section 19-3006.

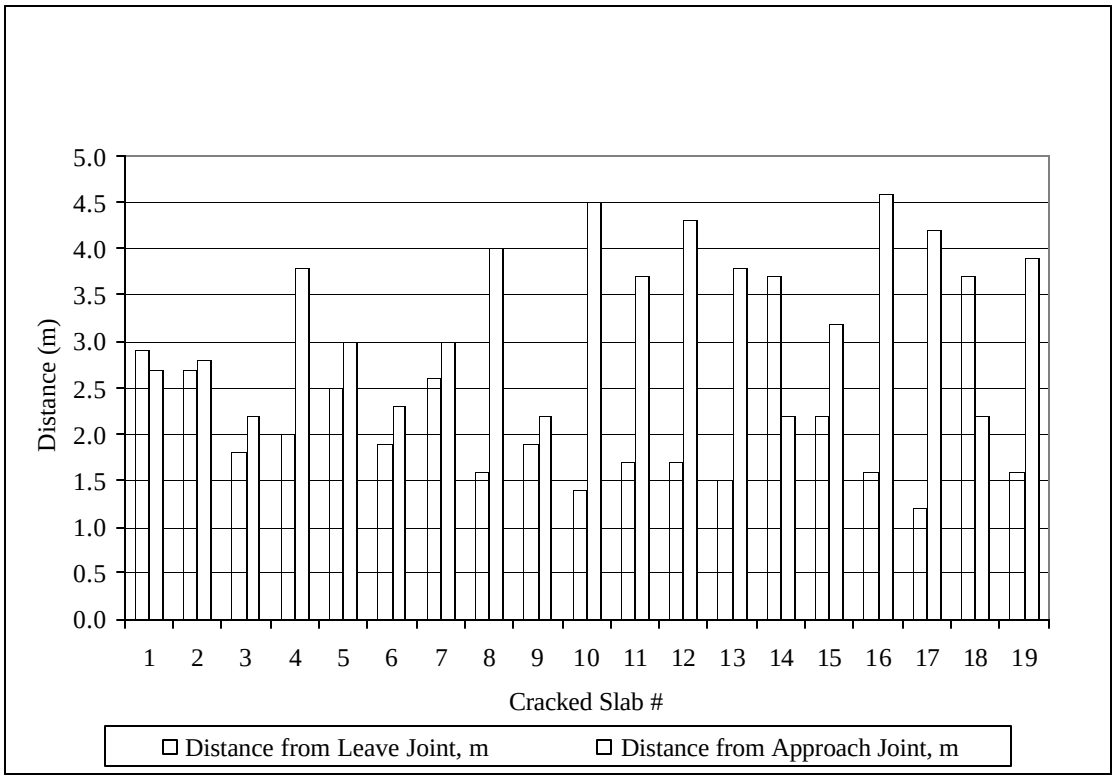

Figure 4.3.2 *Location of transverse cracks from joints for section 06-CS3.*

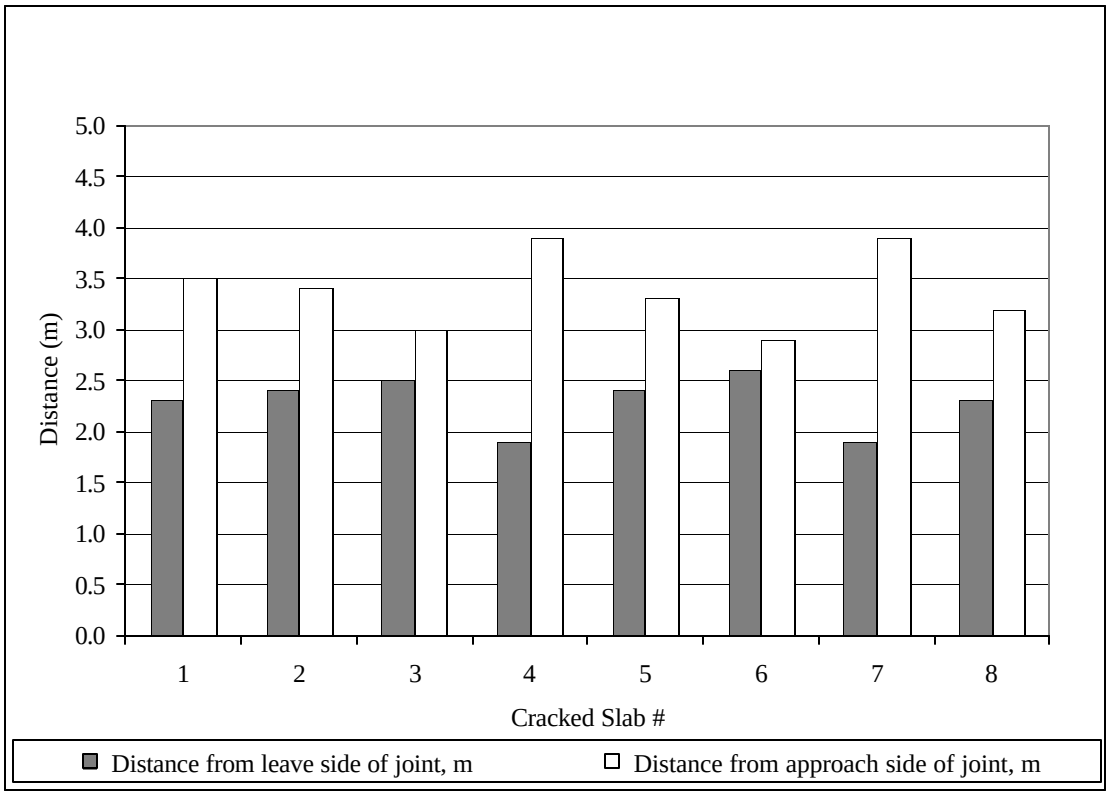

Figure 4.3.3 *Location of transverse cracks from joints for section 06-I10.*

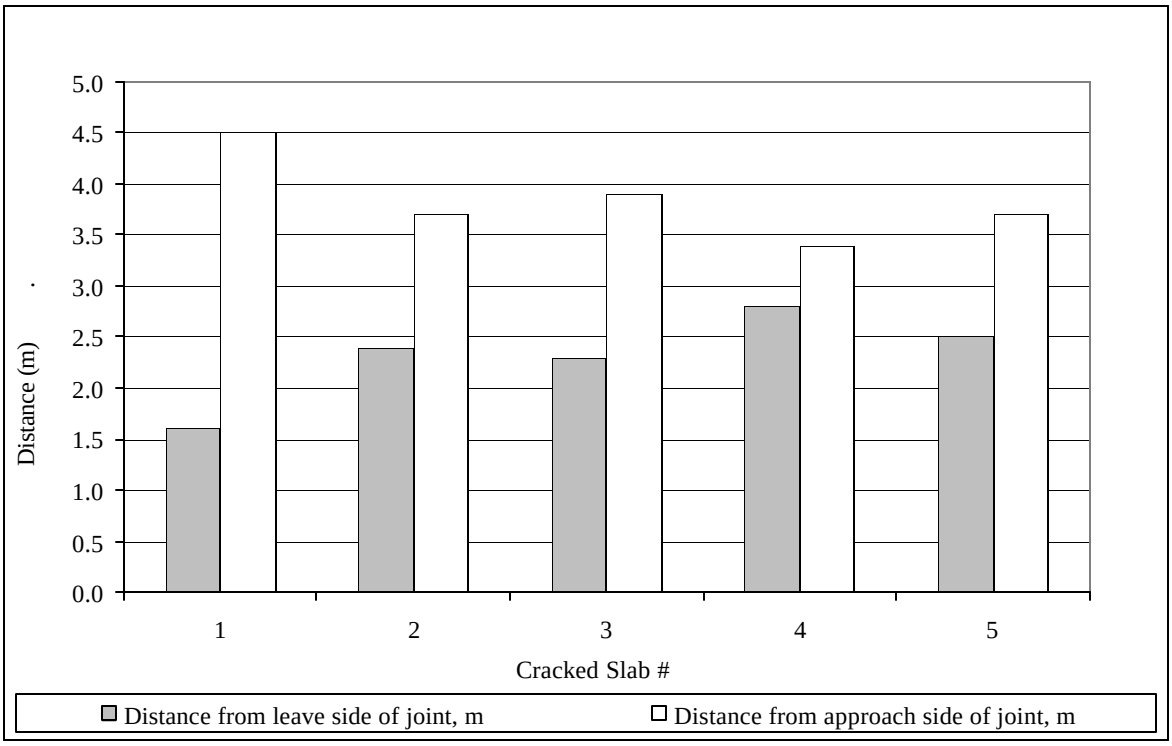

Figure 4.3.4 *Location of transverse cracks from joints for section 19-3006.*

Figure 4.3.5 *Transverse cracking closer to the leave joint for the Iowa section 19-3006.*

4.3.4 Extent of Loss of Joint Support in JPCP on CTB from FWD Testing.

Data obtained from falling weight deflectometer (FWD) testing can illustrate permanent loss of joint support. This is demonstrated in figures 4.3.6 through 4.3.8 for the California experimental test sections. The slab deflection profile was obtained for 40 kN

loading at 0.6 m (2 ft) intervals along the outer wheel path in the direction of traffic for two consecutive slabs.

The effect of intermittent loss of support on joint deflection from daily curling appear to be small, as surface heating of slabs did not change the joint deflection significantly. This is based on the fact that a wide range in surface temperatures occurred during FWD slab testing as seen from the recorded slab surface temperature data in figure 4.3.9.

Permanent loss of joint support increases joint deflection, causing a significant bending stress at the slab surface about 1.5 m to 2.0 m from the joint. This is in addition to the internal tensile stress from curling that will occur in the slab. The observed location of transverse cracking, as discussed, is consistent with these FWD slab deflection profiles. Large (200-250 µm) joint deflections were found in the three sections from the Tracy Test Road in California, consistent with loss of support. See figures 4.3.6-4.3.8.

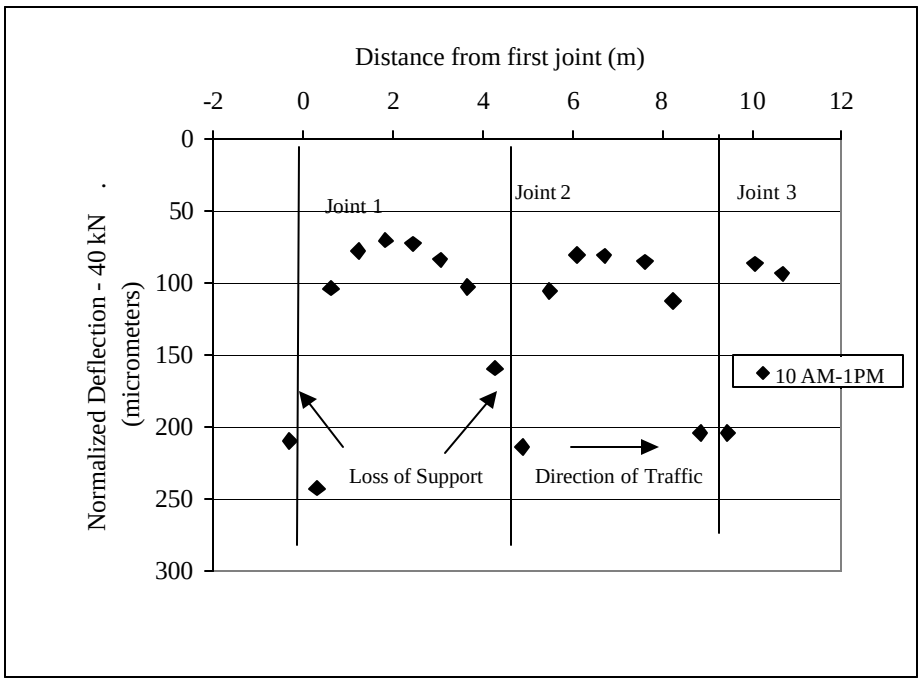

Figure 4.3.6 *FWD slab profile for two slabs on 06-7456 near Tracy (thickened slabs). (Increased edge deflections indicate loss of support.)*

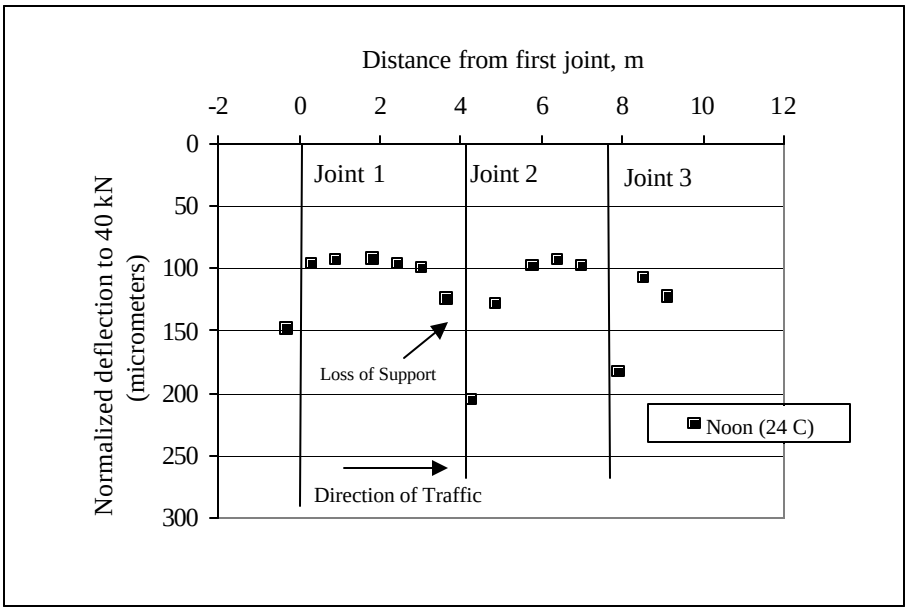

Figure 4.3.7 *FWD slab profile for two slabs on 06-CS1 near Tracy. (Increased edge deflections indicate loss of support.)*

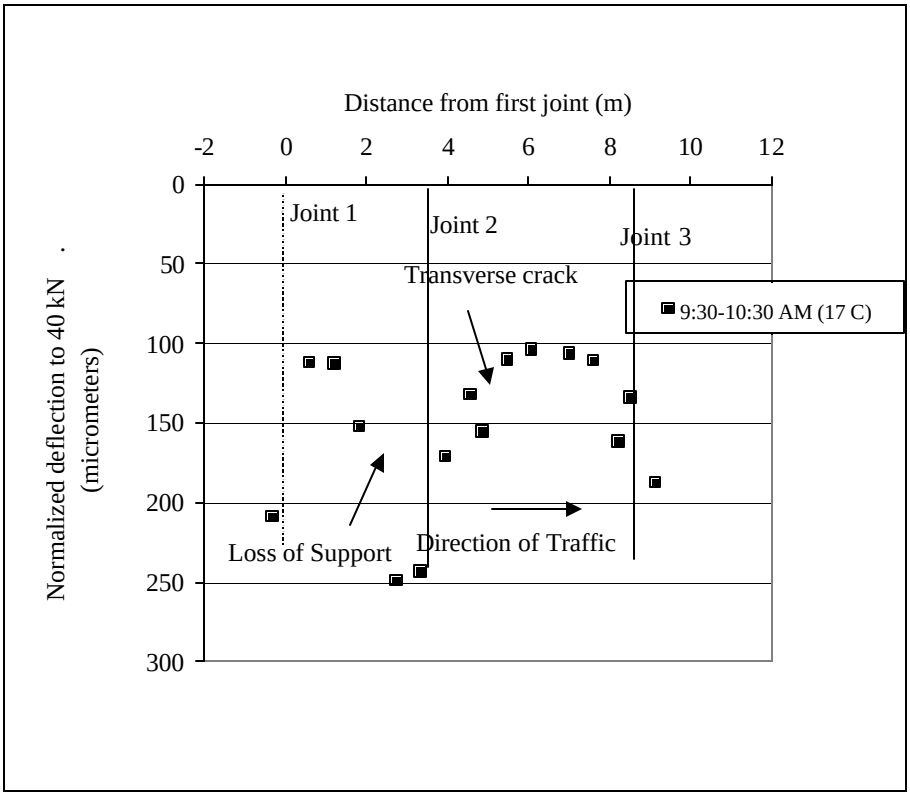

Figure 4.3.8 *FWD slab profile for two slabs on 06-CS3 near Tracy (higher cement content). (Increased edge deflections indicate loss of support.)*

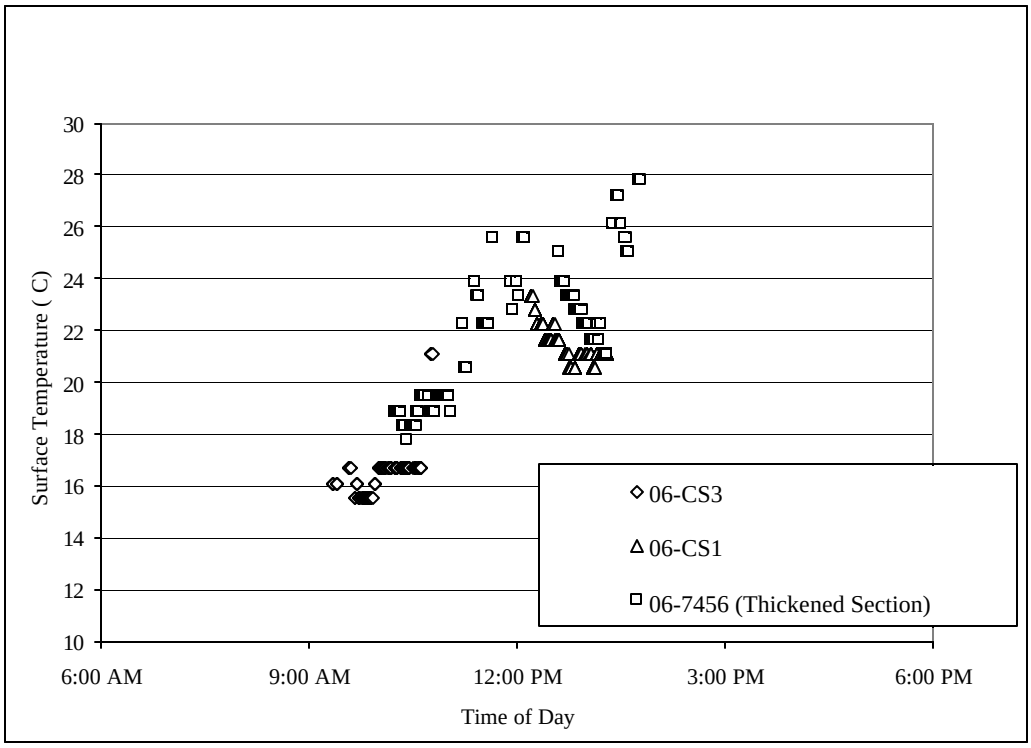

Figure 4.3.9 *Slab surface temperatures during FWD testing.*

4.3.5 When Pumping Erosion Does Not Develop

The relatively long 6.1 m (20 ft) normal strength JPCP slab design in Georgia supported on CTB/ATB has not developed appreciable faulting or any transverse cracking. Figure 4.3.10 shows an overview of the Georgia site.

Figure 4.3.10 *Overview of the Georgia test section, 13-GA 1-5.*

Surface profile measurements showed the slabs were not curved upward, and this is shown in figure 4.3.11. In this case the longer slab length of 6.1 m has performed well.

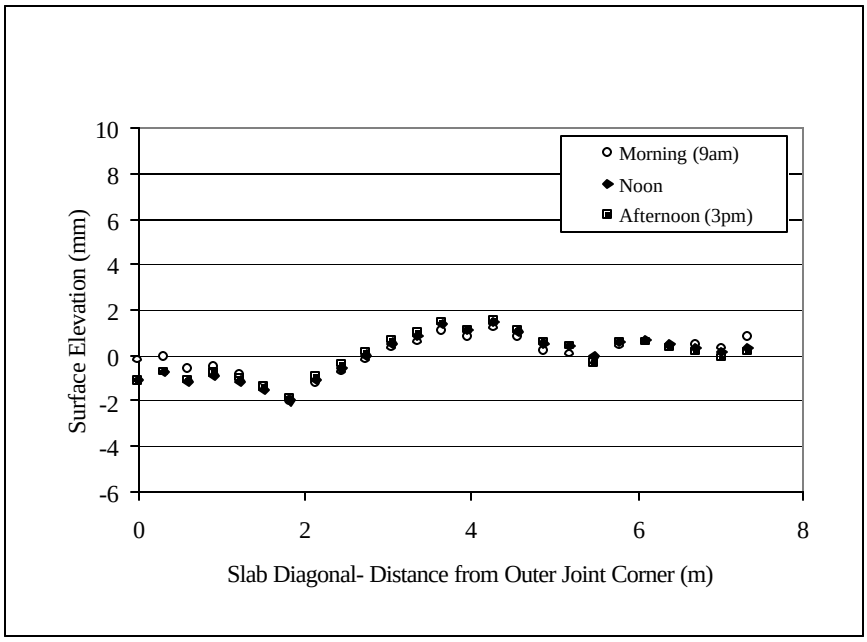

Figure 4.3.11 *Surface elevation profile for 13-GA1-5.*

The Iowa project 19-3055 and the Wisconsin section 55-3008 have overall the same foundation and joint characteristics. Yet, 19-3055 has not nearly developed the same amount of faulting. This is likely due to the much lower traffic volume. Furthermore, section 19-3055 is resting on a granular base with good subsurface drainage. Thus, pumping of fines is not expected. The section has gradually developed a slight permanent downward curvature at the joints as illustrated in figure 4.3.12. The figure shows Dipstick profiles for two 30-m sections for both outer and inner wheel paths. The PCC adapts to this shape without permanent loss of support or cracking. Figure 4.3.13 shows an overview of this test section.

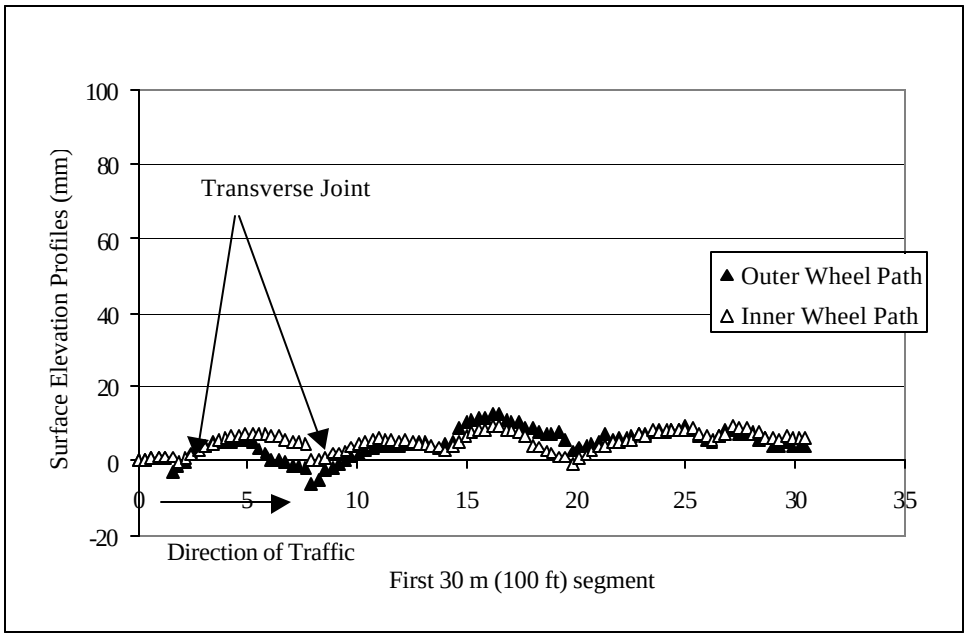

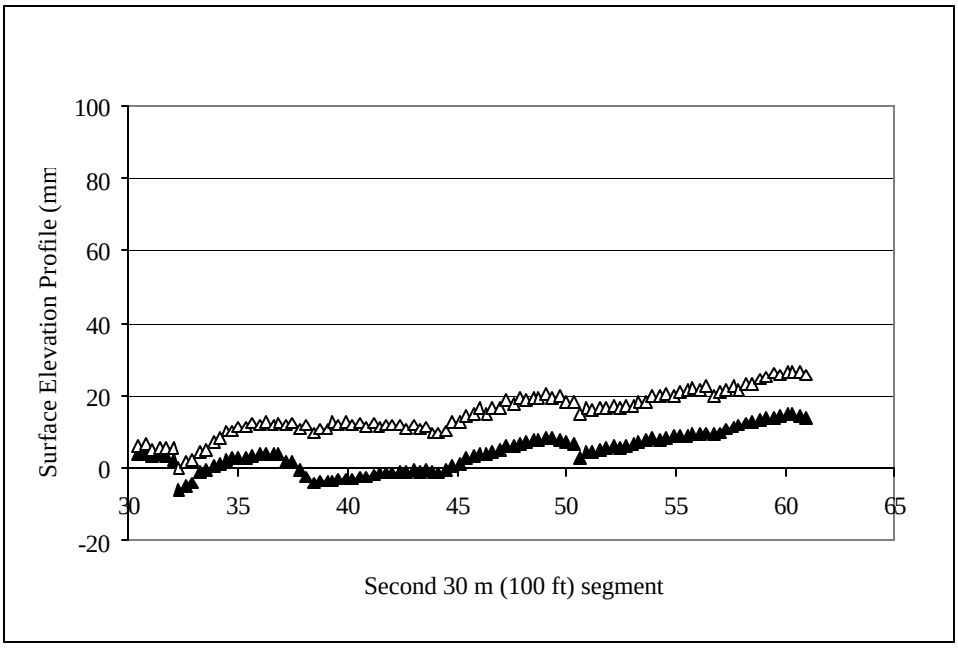

Figure 4.3.12 *Surface profiles for test section 19-3055.*

Figure 4.3.13 *Overview of test section 19-3055.*

4.4 Factors Affecting Joint Spalling

One test section was chosen for investigation because of its spalling deterioration. Section 19-3006 in Iowa has developed high severity joint spalling and is the highest spalling pavement in the LTPP GPS-3 database. It is also the most severely spalled of the pavement sections investigated in this study, as is illustrated in figure 4.4.1. It has also experienced transverse cracking from loss of slab support.

The type of distress observed in this test section is not typical. It is reminiscent of "D" cracking, but without the conventional surface patterns near the edges. Full depth and lane width cracking is observed running about 0.3 m (1 ft) parallel to each transverse joint on either side of the joint. This is illustrated in figure 4.4.2. Core sampling around the deteriorated joint areas, as seen in figure 4.4.3, shows that PCC deterioration started at the bottom of the slab, where high moisture conditions are prevalent.

The concrete itself has been exposed to a severe micro-environment near the joints (i.e. combined effects from prolonged high moisture content, deicing salts, freeze-thaw cycles and about 4 million ESAL's of traffic loading). The cores have a macroscopic crack pattern parallel to the surface as seen in figure 4.4.3.

The combined effects of pumping erosion from truck traffic, high moisture content at the joints due to poor drainage, and moisture warping over time have resulted in a permanently upward curved slab. The warping is especially pronounced at the approach joints. A detailed discussion of the mechanisms causing this type of joint distress is found in section 5.7.

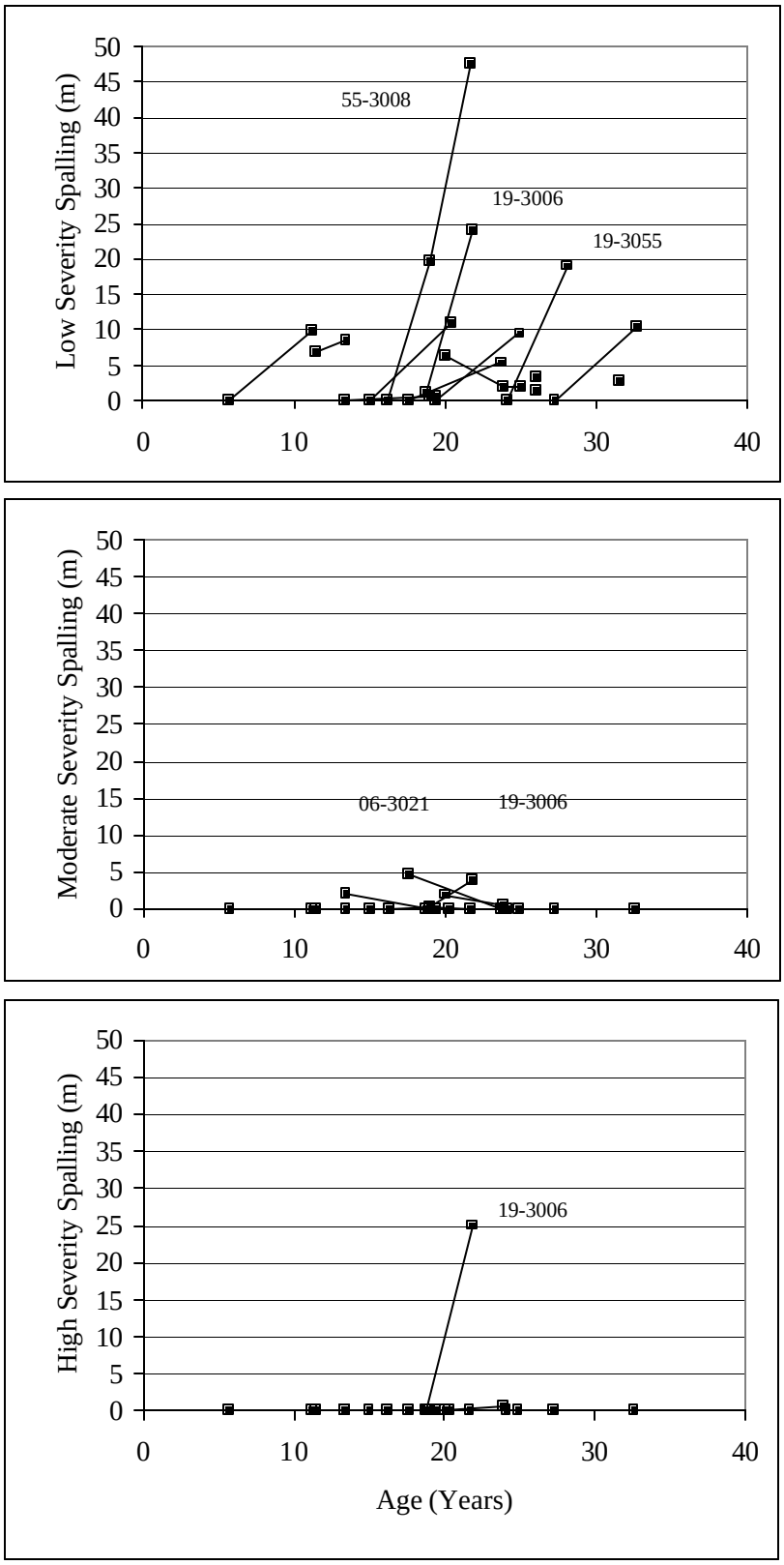

Figure 4.4.1 *Development of spalling over time for the investigated test sections. (Spalling is categorized as low, medium, and high severity.)*

Figure 4.4.2 *Spalling crack running parallel with the joint in a distance of about 0.3 m.*

Figures 4.4.3 *Close-up photos of joint deterioration from test section 19-3006.*

CHAPTER 5. CONCRETE PROPERTIES

5.1 Investigated Strength Range

As seen from figure 5.1.1 the LTPP sections in this study cover nearly the entire flexure and compressive strength range of JPCP's found in the LTPP database (GPS-3 in DataPave 97). The majority of the LTPP test sections have field compressive strength values between 30 and 70 MPa with a few exceptions, and flexural strength values between 4.5 and 7.0 MPa. It should be noted that the field flexural strength values have been estimated from the field splitting tensile strength values using the approximation used by Mahoney et. al. (1991).

$$f_m = 1.02 \cdot f_{sp} + 1.45 \qquad (5.1.1)$$

where f_m = flexural strength (MPa), and
f_{sp} = splitting tensile strength (MPa).

Of the 15 test sections, 11 are found in the LTPP database, of which 9 have strength values listed. Four of these projects were from the lower strength range around 5 MPa. Two projects were from the mid-range of 5.5 MPa, and three projects were selected from the upper strength range of 6.3 MPa.

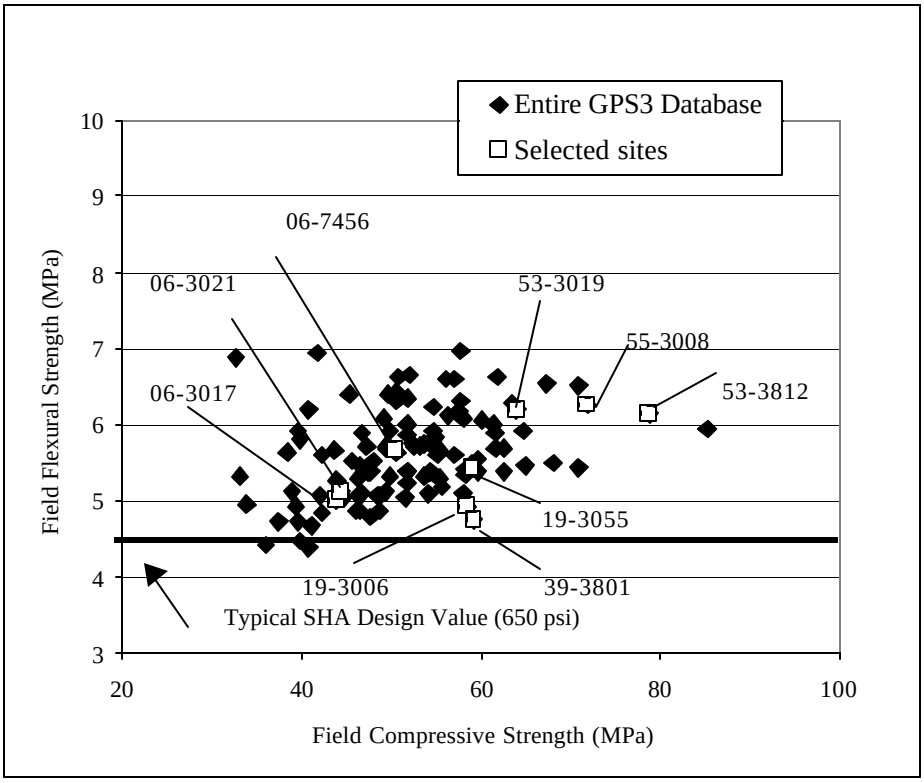

Figure 5.1.1 *Field flexural strength versus compressive strength for the test sections available in the LTPP database.*

5.1.1 Field and LTPP Comparison of PCC Mechanical Properties

In chapter 3, table 3.3.3 lists the average mechanical properties obtained in this study for the field concrete with respect to compressive strength, f_c; elastic modulus, E; and splitting tensile strength, f_{sp}. The LTPP database values are also listed. Overall, the test results for mechanical properties from this study and LTPP are in good agreement. However, the LTPP database does in general show higher f_c and f_{sp} values compared to the values obtained in this laboratory study, see chapter 3. This is likely related in part to the fact that the LTPP uses smaller specimen sizes of 100- by 200-mm cylinders. This study used 150- by 200- to 250-mm cylinders. According to the well-known Weibull effect, this difference in specimen size can account for a difference of 6 percent or higher.

For this laboratory study the average field concretes were about 25 years of age at time of testing. The test matrix ranges from 11 to 51 years old. The average compressive strength is 49 MPa, and ranges from 33 MPa for California section 06-3021, to 75 MPa for Washington section 53-3812. The average elastic modulus is 32,638 MPa, and ranges from 23,714 to 46,931 MPa (same sections as mentioned above). The average splitting tensile strength is 3.7 MPa and ranges from 2.8 to 4.5 MPa.

Figures 5.1.2a, b, and c show graphically the values for compressive strength, flexural strength, and elastic modulus obtained in this study compared to the values available in the LTPP database. As stated above, it is seen that there is overall good agreement with the LTPP database values.

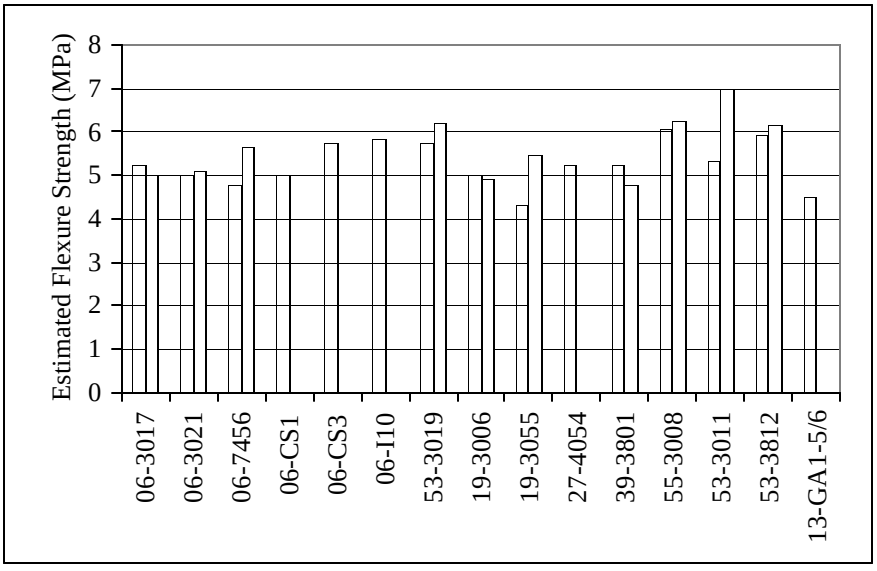

Figure 5.1.2a *Field flexural strength for this study and the LTPP database. (Shaded data bars are from this study, and the clear bars are from the LTPP database.)*

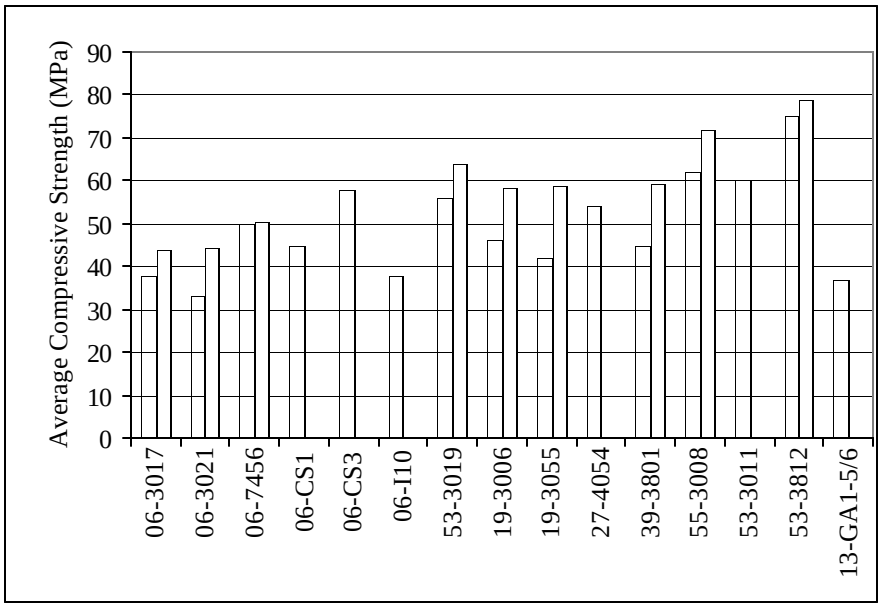

Figure 5.1.2b *Field compressive strengths for this study and the LTPP database (Shaded data bars are from this study, and the clear bars are from the LTPP database.)*

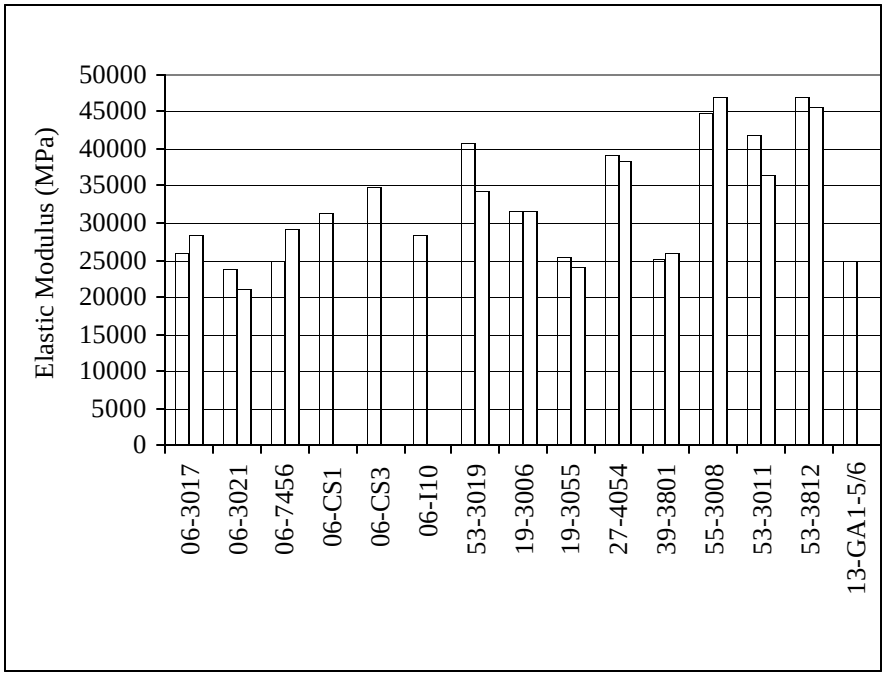

Figure 5.1.2c *Field elastic modulus for this study and the LTPP database. (Shaded data bars are from this study, and the clear bars are from the LTPP database.)*

5.1.2 Estimated Flexural Strength versus Compressive Strength for This Study

Most SHA's use compressive strength and flexural strength as their main PCC design requirements. Therefore, it is important to identify the relation between these two PCC parameters. Figure 5.1.3 shows the estimated flexural strength versus compressive

strength as obtained in this study. Six pavement projects were in the lower strength range with insitu flexural strength ranging between 4.3 MPa and 5.0 MPa. Four projects were close to the average strength of 5.26 MPa. Five projects were in the high-end range of 5.5 MPa to 6 MPa.

The compressive strength range varied between 33 MPa and 75 MPa. From these results it is apparent that the practical range for tensile strength used in fatigue-based design for plain concrete (i.e. without steel or fibers) is relatively narrow, spanning between 4.0 and 6.5 MPa. It is noteworthy that the investigated strength ranges for flexure as well as for compressive strength fall in the expected average range for these values when considering the ACI upper and lower-bound limits. A few exceptions were observed in the lower compressive strength range. In the lower range, a few sections were found to have very high flexure strength. In the upper strength range, when the field compressive strength increases above 60 MPa, it appears that the flexure strength has reached a threshold of approximately 6.5 MPa.

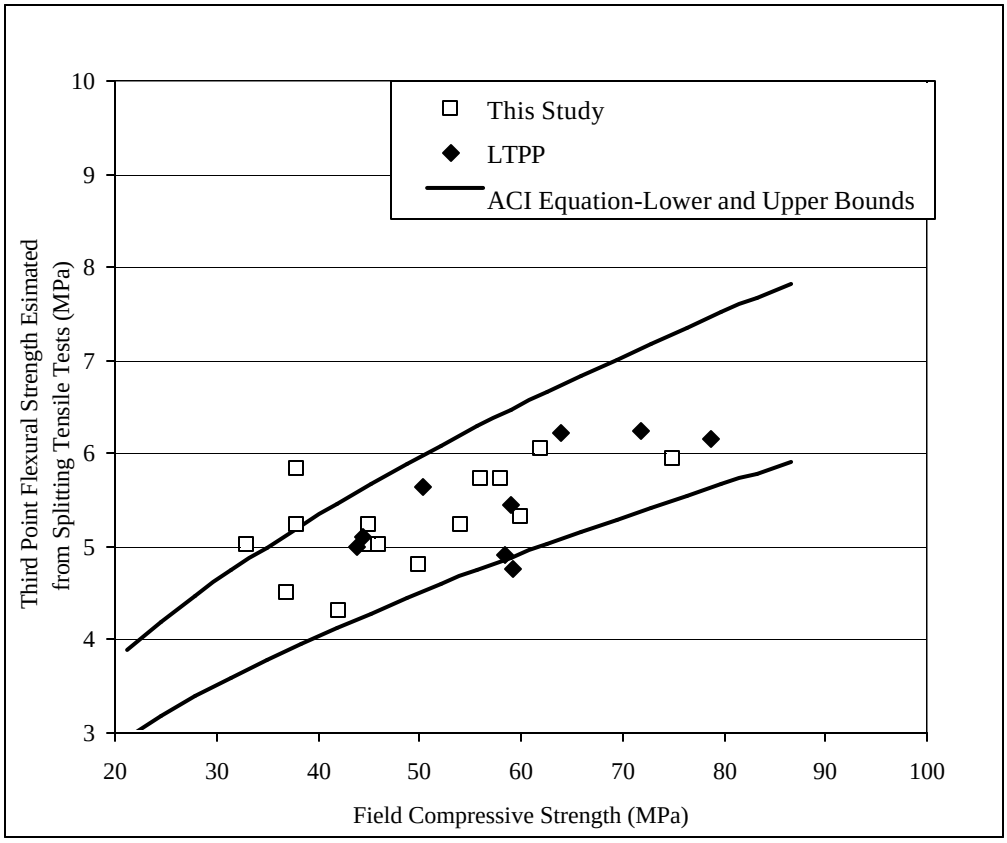

Figure 5.1.3 *Estimated field flexural strength versus field compressive strength for the 15 test sections in this study.*

The 15 different test sections have an average value of 5.26 MPa for their ultimate flexure strength. This corresponds to an estimated 28-day flexure strength of approximately 4.7 MPa, which is based on a well established rule of thumb that long-term tensile strength is about 10 percent higher than the 28-day strength. The average 28-

day flexure strength value agrees well with the 28-day flexure strength of 4.5 MPa used by most SHA's in the United States for pavement design. As discussed in chapter 4, this is an adequate limit for ensuring good long-term pavement performance.

5.1.3 Ultimate versus 28-day Design Compressive Strength

In order to evaluate the overall effect of increasing compressive strength on pavement performance it is necessary to have an estimate of the 28-day design value. The LTPP database does not contain these values for all test sections. Instead the 28-day strength value is evaluated using overall strength gain.

In order to make this estimation, the LTPP GPS-3 database was used to evaluate the increase in compressive strength of field concrete over the 28-day strength. A total of 37 of the LTPP GPS-3 sections had been in service for 10 years or longer, and had 28-day field as well as long-term data available. These results are shown as a density function in figure 5.1.4. The data fall into two normal distribution curves. The lower peak represents 12 concrete sections from climates other than the WF climatic zone. Their average strength gain was estimated to be 28 percent. The major peak shows an average of long-term strength gain of 68 percent. This peak represents 25 pavement sections from the WF climatic zone.

Using these averages, the 28-day compressive strength values can be estimated for the test sections in this study. The 28-day strengths of the two Washington State sections in the WNF climate were also estimated based on a 68-percent long-term strength gain because the curing environment in that region is nearly ideal. Based on the field compressive strength data, listed in tables 3.3.1 and 3.3.2, the estimated 28-day values for the test sections in this study range from about 24 MPa to 45 MPa. The JPCP's located in the dry regions fall in the lower end of the scale and the JPCP's in the wet regions fall in the higher end of the scale. These estimates indicate that the concretes used in these JPCP's all fall in the category of normal strength concrete using the definition of the American Concrete Institute (ACI). Based on figure 5.1.4, the concretes in WF and WNF regions have probably gained more compressive strength over time than the concrete pavements in the DNF climate such as in California.

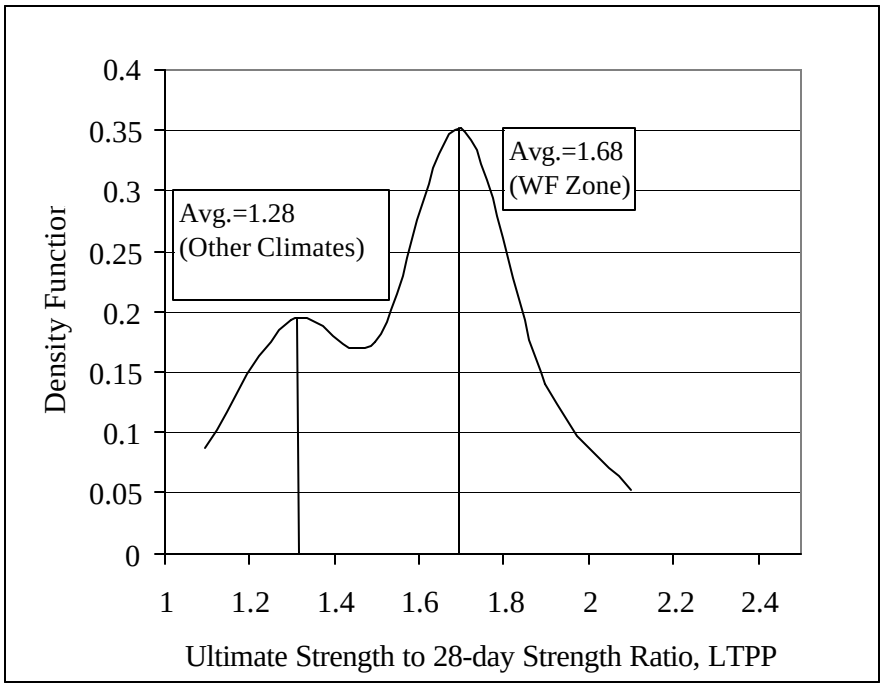

Figure 5.1.4 *Density function of the ultimate strength to 28-day strength ratio for data available in GPS-3 in the LTPP database. (DataPave 97.)*

5.2 Compressive Strength

Although compressive failure is extremely rare in the pavement structures, the compressive strength of concrete is perhaps the most comprehensive measure of concrete quality (Ahmad, 1994). Compressive strength is strongly related to the hydrated paste porosity. This is the reason behind considering the compressive strength to specify, control and evaluate the concrete quality. Although the mode of failure of concrete specimens under other loading schemes is quite different, many of these properties can be correlated to compressive strength.

Table 1.5.1 listed the PCC mix characteristics that were found to significantly affect the PCC compressive strength. They were w/c ratio, coarse aggregate characteristics, cement type and content, mineral additives, and air entrainment.

The results from this study confirm the influence of w/c ratio and the cement content on the PCC compressive strength. However, no correlation with coarse aggregate characteristics or air entrainment could be established. Because the studied pavements predate the common use of mineral additives, all contained only ordinary portland cement (OPC). Thus, it was not possible to evaluate the effect of mineral additives from the field study. The role of mix characteristics on concrete properties is discussed in detail in chapter 6.

5.3. Effect of Increasing Compressive Strength on the Splitting Tensile Strength

Tensile strength represents one of the most important mechanical properties of concrete as it relates to PCC's resistance to crack initiation. As discussed in chapters 1 and 4, the fatigue transverse cracking and corner breaks are directly related to the PCC tensile properties (e.g. flexural strength). If tensile stresses induced by wheel loading, environmental effects, or both, exceed the concrete tensile strength, cracks will form. PCC flexural strength is typically 25 percent higher than the PCC splitting tensile strength. The flexural strength and splitting tensile strength can be considered to be proportional with an initial offset of about 1.50 MPa as was described in section 5.1. This section discusses only splitting tensile strength as determined from the field cores in this study.

The relation between the compressive strength and the splitting tensile strength from this study is shown in figure 5.3.1. A good correlation is obtained between the field splitting tensile strength and the compressive strength, irrespective of air void characteristics. Note that a scatter band of 1 MPa is not uncommon even for field compressive strength values around 35 to 40 MPa. From this figure it is observed that the increase in the concrete compressive strength is not associated with an equal percentage increase in the splitting tensile strength. This is in agreement with the literature on this subject. As the compressive strength increases from 30 to 75 MPa (125-percent increase), the increase in tensile strength is limited to 2.8 to 4.4 MPa, which is only a 56-percent increase.

The fact that there is not an equal percentage increase in tensile strength with increasing compressive strength suggests that increasing the compressive strength for pavement applications beyond the conventional 28-day strength range of 24-28 MPa has limited benefit on increasing the splitting tensile strength. Figure 5.3.2 shows the ratio between the splitting tensile strength and the compressive strength versus the compressive strength. The strength ratio decreases as compressive strength increases and follows a power curve behavior. As is illustrated in the figure, the R^2 value is high at about 0.85. For compressive strengths of about 30 MPa the tensile strengths reach about 10 percent of the compressive strength value. However, for compressive strengths around 60 MPa the tensile strengths only reach about 7 percent of the compressive strength.

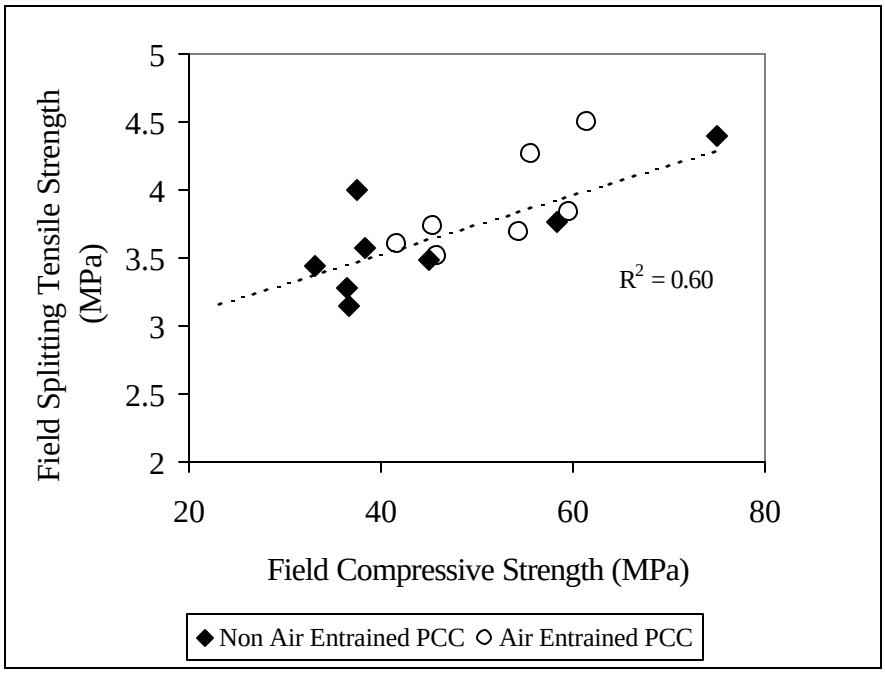

Figure 5.3.1 *Ultimate splitting tensile strength versus ultimate compressive strength for field specimens.*

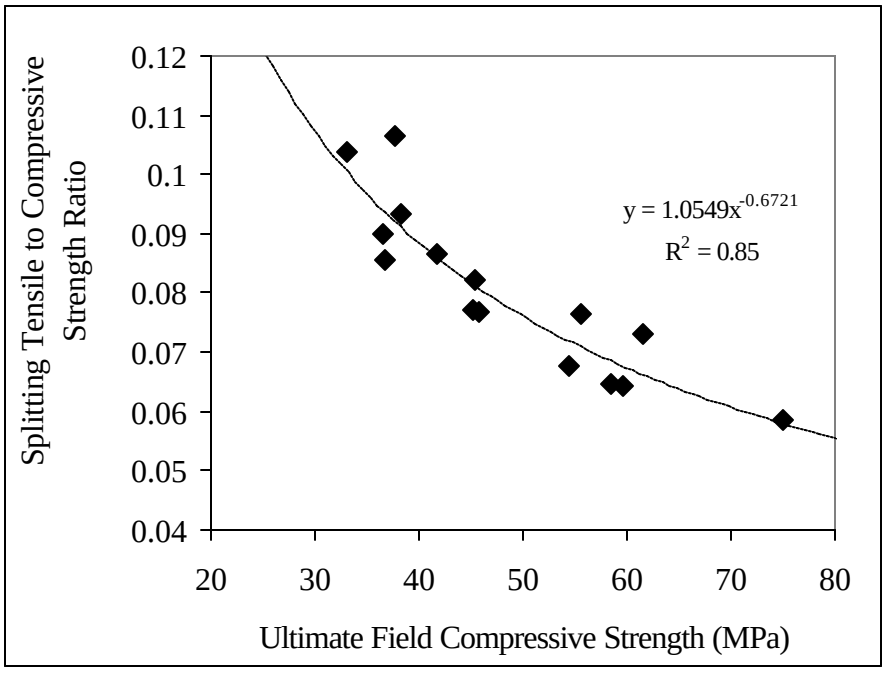

Figure 5.3.2 *Ratio of the splitting tensile strength and compressive strength versus the ultimate compressive strength.*

When compared to the results from this study, the LTPP database shows a much higher degree of scatter between splitting tensile and compressive strength for the same field concretes. This is illustrated in figure 5.3.3. The reasons are not clear, but may be

associated with the use of very different test specimen sizes. The LTPP database shows use of 100-mm by 75- to 200-mm samples according to DataPave 97. This study used 150-mm by 200- to 250-mm depending on the slab thickness. See also section 3.3.

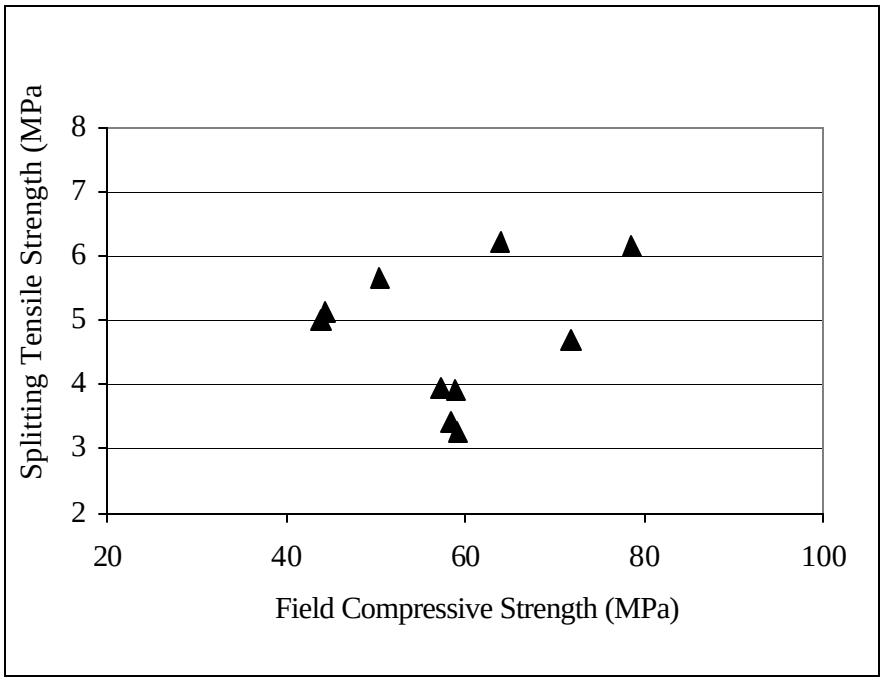

Figure 5.3.3 *LTPP database values for splitting tensile strength versus compressive strength for sections in this study.*

5.3.1 Prediction of Splitting Tensile Strength From Compressive Strength

The commonly used ACI equation for predicting the tensile strength, f_{sp}, as a function of the compressive strength, f'_c (ACI Committee 363, 1984), was found to slightly overestimate the splitting tensile strength of the field concretes from this study. This equation reads

$$f_{sp} = 0.59\sqrt{f'_c}\,. \qquad (5.3.1)$$

This indicates that the pavement designer should use such an equation with caution. As was indicated earlier, splitting tensile strength cannot fully be predicted by compressive strength, and general equations will only provide rough strength estimates. Actual laboratory tests should be conducted during the mix design process to ensure that desired tensile strength is obtained.

5.4. Effect of Increasing Strength on Elastic Modulus

Elastic modulus, E, of concrete has a pronounced effect on the pavement deformation and curling stress. As E increases, the pavement slab deformation due to wheel loading will

decrease. However, as discussed in chapter 4 the potential for increased curling stresses can not be ignored.

A strong correlation was obtained between long-term f_c and E as seen from figure 5.4.1. The same trend was obtained using the LTPP data for these same pavements, but again, as seen for f_{sp}, with a higher degree of scatter. See figure 5.4.2. The laboratory data from this study increases the confidence in the observed trend.

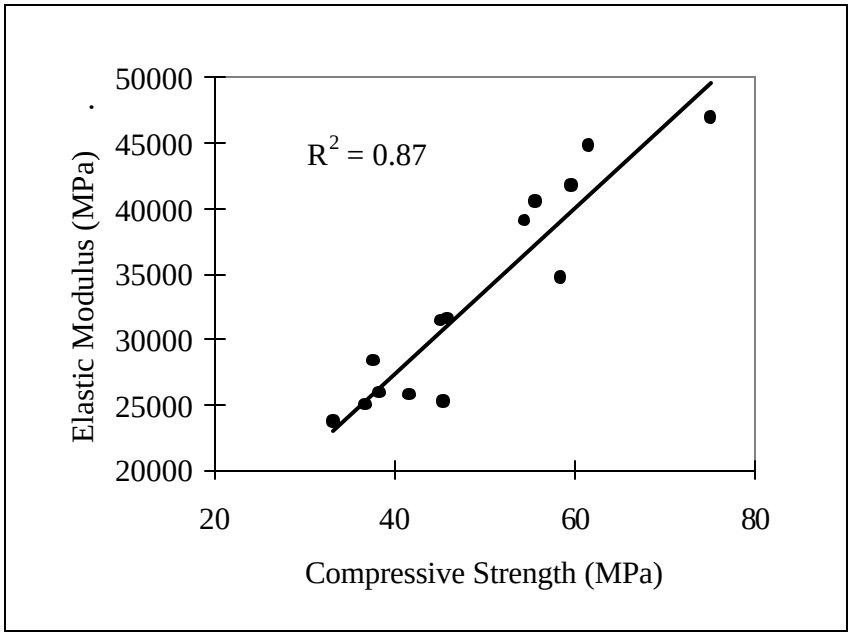

Figure 5.4.1 *Elastic modulus versus compressive strength for field samples.*

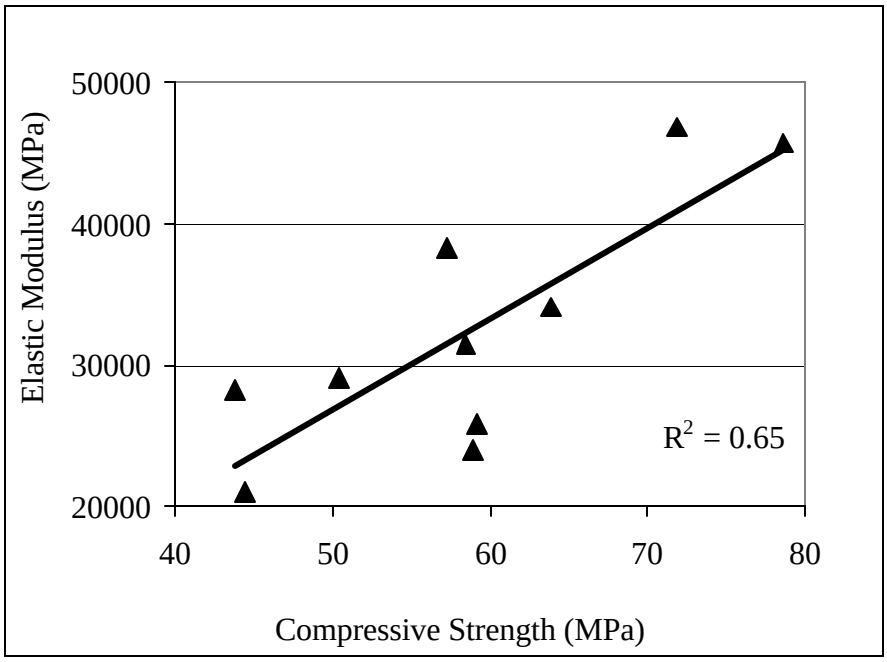

Figure 5.4.2 *Elastic modulus versus compressive strength. LTPP results on field concrete.*

5.4.1 Prediction of Elastic Modulus from Compressive Strength

If the E is predicted based on the ACI equation for normal strength concrete (ACI Committee 363, 1984), the elastic modulus is greatly underestimated for compressive strengths higher than 50 MPa. The ACI equation is written as:

$$E = 4733.6 \cdot f'_c \qquad (5.4.1)$$

It should be noted that this equation is based on 28-day data, which can be a part of the reason why the values are underestimated. It should also be noted the equation was developed based on a large database and there was a significant amount of scatter. As with tensile strength, it appears that E cannot be fully predicted from f'_c, and that the relationship is at least in part mix specific. This suggests that it is preferable to measure E on the design concrete, rather than predict it from a generalized equation.

5.4.2 Increasing Elastic Modulus and Splitting Tensile Strength

The expected relation was obtained between f_{sp} and E. Figure 5.4.3 shows that increasing tensile strength is related to increasing elastic modulus. As elastic modulus increases about 80 percent from 25,000 to 45,000 MPa, the splitting tensile strength only increases about 50 percent from 3.0 to 4.5 MPa.

For pavement applications this indicates that increasing the PCC resistance to fatigue crack initiation by increasing tensile strength significantly increases the PCC elastic modulus. This has a positive and a potentially negative effect on pavement performance as related to slab deformations and slab curling, respectively. This complex relation is discussed in chapter 4.

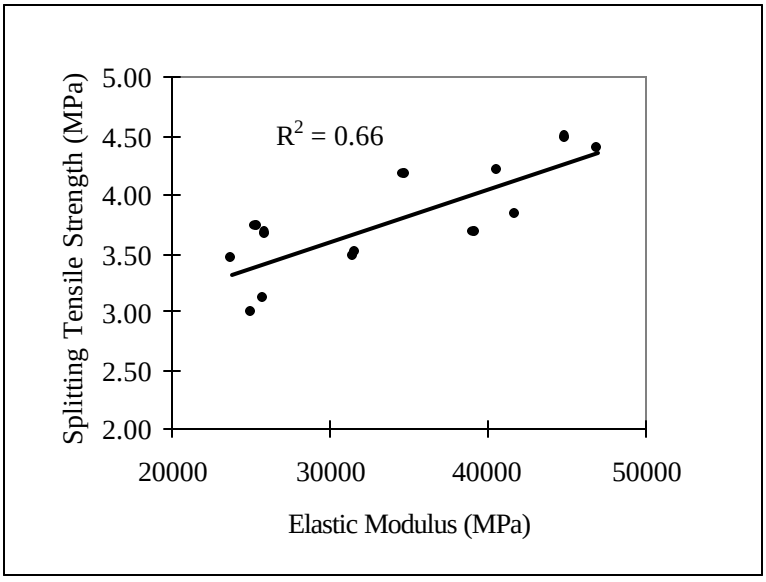

Figure 5.4.3 *Splitting tensile strength versus elastic modulus for field specimens.*

5.5 PCC Fracture Resistance

The PCC fracture behavior is another important characteristic to evaluate when investigating the effect of increasing PCC strength on pavement performance. Increasing the concrete flexure strength increases the concrete's resistance to crack initiation. However, the increased strength can also be detrimental for plain concrete as it may result in increased brittleness during fracture.

Evaluation of PCC brittleness requires measurements of the PCC fracture energy (G_F). Fracture energy was obtained from four California test sections. With help from Caltrans, large beams were obtained from the California test sections 06-3017, 06-3021, 06-I10, and 06-CS3. The tests were performed as described in chapter 2. Fracture energy cannot be determined for the other 11 sites in this study, for which field beams could not be obtained.

The ultimate PCC fracture properties obtained for the four California test sites are valuable. However, these properties alone cannot clarify what mix characteristics control fracture energy or what the effect of increasing strength is on the PCC fracture behavior. These gaps are addressed using results from an ongoing study at the University of Michigan, performed for the Michigan Department of Transportation, MDOT (Hansen and Jensen, 2000, and Jensen and Hansen, 2001). The ongoing study evaluates the effect of coarse aggregates on the PCC fracture behavior for typical pavement mixes.

5.5.1 Resistance to Crack Initiation

The most apparent improvement from increased PCC strength is the increased resistance to crack initiation. The resistance to crack initiation can be estimated for a given material using the linear elastic fracture mechanics concept of fracture toughness, K_I. Fracture toughness is determined from the peak load, and the specimen and load configuration. For a center-notched beam subjected to three-point bending, K_I can be calculated as:

$$K_I = \frac{2}{3} g(a) \cdot P \cdot l \cdot \frac{\sqrt{a}}{W \cdot h^2} \qquad (5.5.1)$$

where P = maximum load (N).
l = beam span (mm).
a = crack length (mm).
h = beam height outside the notch (mm).
W = beam width (mm).
$g(\alpha)$ = geometric factor depending on span-to-depth and notch-to-depth ratio. Expressions for $g(\alpha)$ can be found in fracture mechanics handbooks.

Figure 5.5.1 shows the effect of concrete matrix strengthening in terms of fracture toughness versus compressive strength. Generally, the fracture toughness increases about 50 percent when the compressive strength increases 100 percent. This is the same order of magnitude as observed for splitting tensile strength as discussed in section 5.3. The data shown here represents a large range of compressive strengths (20 to 60 MPa) from the field concretes in this study and normal strength concretes at different ages (7, 28 and

91 days) from the ongoing MDOT study. Note that the concrete from the Tracy experimental test road (test section 06-CS3) with higher cement content (418 kg cement per m^3) follows the same trend as the other concretes that contain 280 to 335 kg cement per m^3.

As the concrete matures, the matrix becomes stronger and the strength increases, resulting in increased resistance to crack initiation. This trend is observed for concretes containing rounded as well as crushed coarse aggregate. The only difference between the concretes is that the ones containing crushed aggregates tend to develop higher 7-day strength than the ones containing rounded aggregates. The improved early strength is likely due to the fact that crushed aggregates in general have improved matrix-to-aggregate bond over rounded aggregates. Thus, concretes containing crushed aggregates will typically have improved resistance to crack initiation at early age.

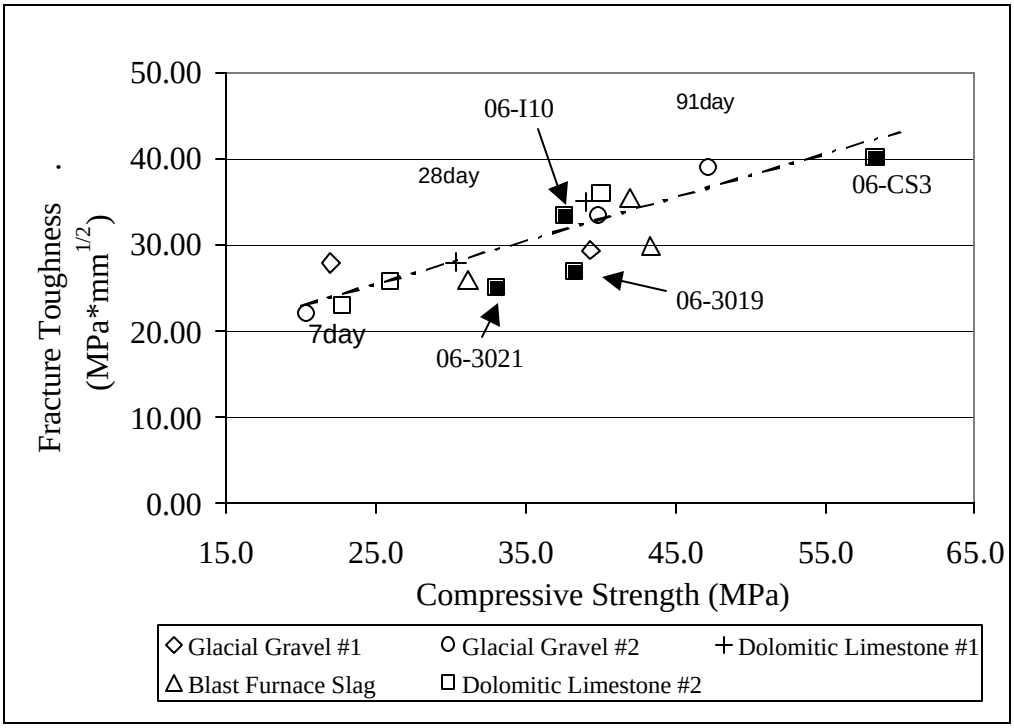

Figure 5.5.1 *Fracture toughness versus compressive strength based on data from this study and the Michigan study (965-mm span,204-mm height, 102-mm width, 102-mm notch).*

The concrete strength (compressive or flexure) depends largely on the strength of the mortar and on the interface bond between the mortar and aggregate. The PCC strength is also affected by the strength of the aggregate, but most normal weight aggregates have strengths much higher than the strength of the mortar with which they are used (e.g. normal strength concretes). However, considering the ACI committee report on high strength concrete, the PCC strength is limited by the strength of the coarse aggregates, as the bond between the matrix and the aggregates reaches an upper limit above which additional matrix strength would not increase the concrete strength (ACI 363R-7).

The coarse aggregate gradation also affects the PCC strength. It should be emphasized that in high strength concrete the maximum aggregate size is recommended to be kept at a minimum to obtain the optimum bond between the aggregates and the matrix. This makes it potentially more difficult to justify high strength concrete for highway pavements, as decreasing the maximum aggregate size tends to increase the PCC brittleness and the potential for low aggregate interlock at joints and cracks. However, if high quality aggregates are used (e.g. hard aggregates) the increased brittleness may be avoided. These aspects are discussed in the following sections. Of course aggregate durability to environmental attacks must also be considered, as will be discussed in chapter 6.

5.5.2 PCC Brittleness Models

Hillerborg (1983) defined a brittleness number, B, that considered the ratio of fracture energy over the elastic energy stored in a specimen at peak load. The brittleness number is based on the behavior of PCC subjected to uniaxial tension, and B is defined as

$$B = \frac{l_{ch}}{D} = \frac{EG_F}{f_t^2 D} \tag{5.5.2}$$

where l_{ch} = characteristic length (mm).
D = critical structural dimension (mm).
E = elastic modulus (MPa).
G_F = fracture energy (N/m).
f_t = tensile strength.

Carpinteri (1986) simplified the Hillerborg brittleness number to the energy brittleness number, s_e, defined as

$$s_e = \frac{G_F}{f_t D} \tag{5.5.3}$$

The consideration is that the PCC elastic modulus and the tensile strength increase at similar rates for increasing PCC strength. Based on these equations, it is of key importance to optimize a higher strength mix for maximum fracture energy.

5.5.3 Fracture Energy from Field Concretes

As mentioned earlier, fracture energy was obtained for four California test sections. Table 5.5.1 lists the key PCC properties representing the four sites. As discussed in chapter 3, the concretes were designed as normal strength concrete. However, due to their ages (20 years or older), they have matured and their in situ compressive strengths range from 33-58 MPa. The dominant coarse aggregate type for the four sections is gravel. The average fracture energy values range from 200 to 285 N/m for the four sections. Section 06-CS3 yields the highest value and section 06-3021 yields the lowest value. It is to be expected that the G_F value is highest for 06-CS3, when considering that the coarse aggregate type,

content, and maximum size are similar for the four California sections, and that this section has the highest compressive strength and the lowest w/c ratio.

The fracture energy values obtained in this study ranged in the high end of what is typically reported for concrete in the literature. This can be due to the larger size aggregates and well-developed bond between the coarse aggregate and the matrix (and for 06-CS3 due to high strength and lower w/c ratio).

Table 5.5.1 *Key ultimate PCC properties for the four investigated sections in California.*

LTPP Section ID	Age (Yrs)	Compressive Strength (MPa)	Splitting Tensile Strength (MPa)	Elastic Modulus (MPa)	Fracture Energy (N/m)
06-3017	19	38.3	3.68	25868	224
06-3021	24	33.1	3.46	23714	201
06-CS3	26	58.4	4.18	34679	284
06-I10	51	37.6	4.30	28321	230

5.5.4 PCC Brittleness and Fracture Energy

Recall from chapter 2 that the fracture energy is the work-of-fracture and is equal to the area under a complete load-deflection curve. It was stated above that the fracture energies from these field concretes were significantly higher than expected from results reported in the literature. Figure 5.5.2 shows the load-deflection curve from the California test section at Tracy that contains very large gravel-like aggregates (maximum aggregate size about 38 mm) and two concretes from the ongoing laboratory study containing glacial gravels and dolomitic limestone, respectively. The laboratory beams are 28 days old at testing. The field concrete yields the highest fracture energy and splitting tensile strength. However, considering equation 5.5.3, the field concrete is less brittle than the laboratory concrete containing dolomitic limestone, but only slightly more brittle than the laboratory beam containing glacial gravel.

This can also be illustrated by plotting the fracture energy versus splitting tensile strength. Figure 5.5.3 shows this for the four field concretes and for several laboratory concretes. The mixes are all normal strength concrete pavements where the main difference is the coarse aggregate type.

The straight line in the plot represents an equilibrium brittleness line. The line was generated based on the laboratory concretes containing glacial gravel using equation 5.5.3. Using this equilibrium line, it is clear that the old field concretes exhibit excellent fracture behavior not only in terms of fracture energy, but also in terms of relative brittleness.

Fracture energy plotted versus the compressive strength does not show a similar clear picture of brittleness. The reason is that the fracture energy is related to a PCC tensile failure and not a compressive failure. The excellent fracture behavior of these old field

concretes is due to the use of very hard gravel-like coarse aggregate that over time have developed excellent bond to the concrete matrix. The aggregates serve as crack obstacles, where the crack either will penetrate the aggregate at a given load or will be forced to propagate around the aggregate.

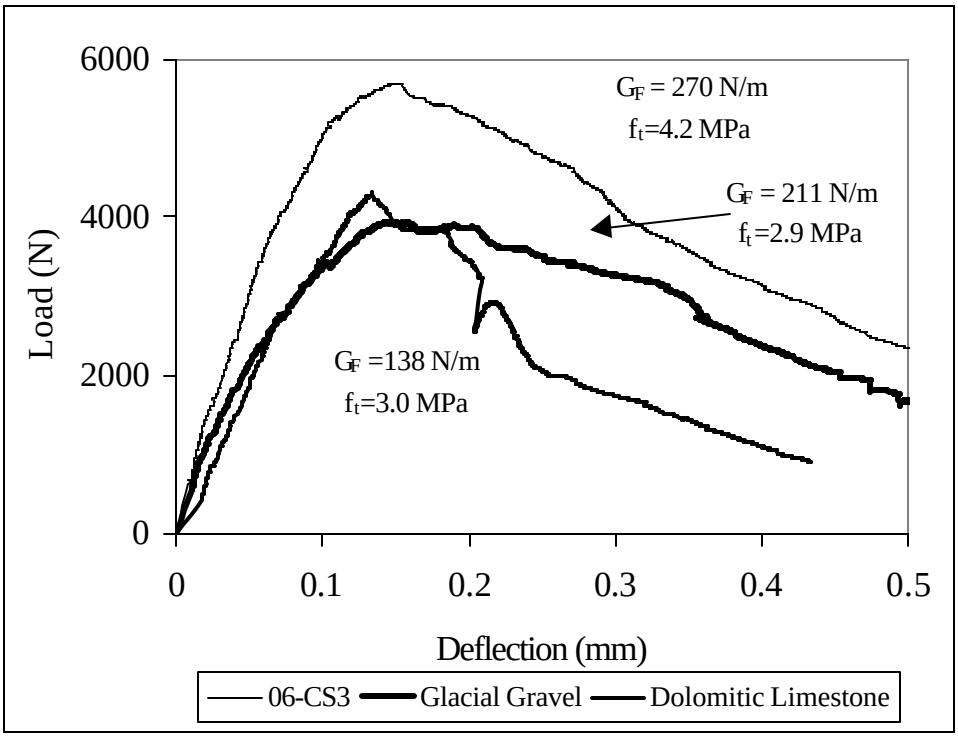

Figure 5.5.2 *Load versus deflection for laboratory and field concretes of same dimensions.*

It is commonly believed that cracks penetrate the coarse aggregate in cases where the properties at the interface, the zone between the coarse aggregate and the matrix, are close to the matrix properties, as in high strength concrete (ACI 363R-7). However, experimental and numerical results reported in the literature show that the phenomenon of crack patterns through or around the aggregates is more complex (e.g. Vervuurt, 1997; and Mohamed and Hansen, 1999). Results show that for increasing interface-to-matrix strength ratio (approaching 1) the specimen peak tensile capacity increases, keeping all aggregate and matrix properties the same. At the same time, it was shown for interface-to-matrix strength ratios approaching 1, that the crack penetrates the coarse aggregates when the aggregate tensile strength is lower than that of the matrix. This occurs irrespective of the fracture energy ratio between the aggregate and the matrix. Yet, the overall specimen 'toughness' increases when aggregate-to-matrix fracture energy ratio increases. Furthermore, in the cases where the tensile strength of the aggregate equals the strength of the matrix, the fracture energy ratio between the aggregate and the matrix is the dominating factor for whether or not the crack penetrates the aggregates. For ratios lower than 1, cracks will penetrate the aggregates, and for ratios higher than 1 the crack will not penetrate the aggregates.

This discussion magnifies the importance of selecting high quality aggregates if higher strength concrete is used in pavement design.

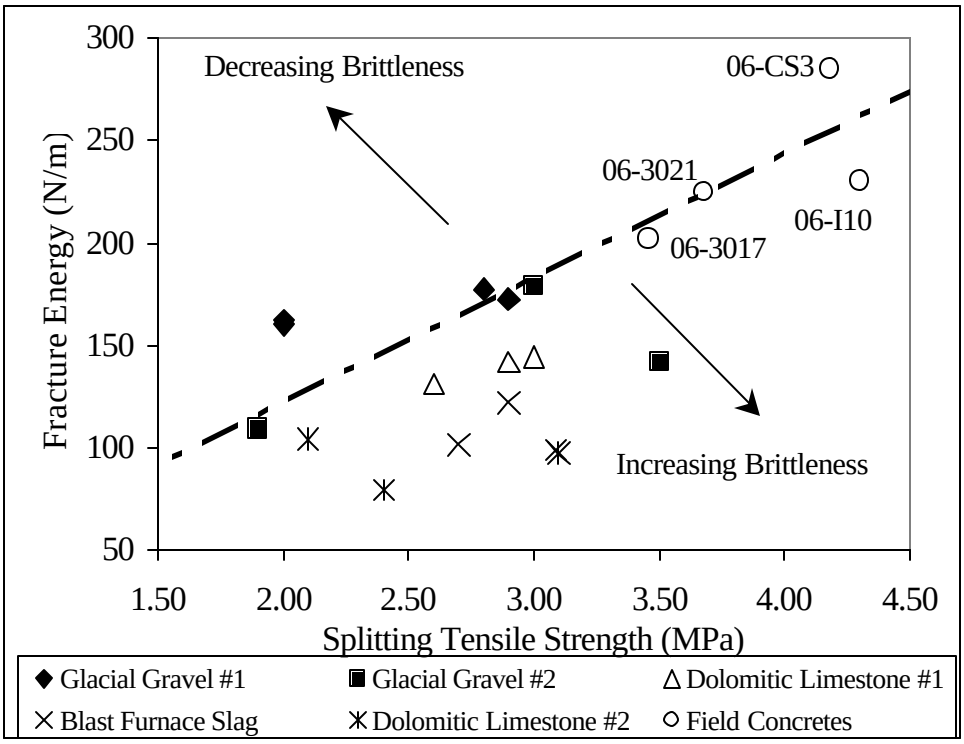

Figure 5.5.3 *Fracture energy versus splitting tensile strength.*

Figure 5.5.3 also shows that the resistance to cracking described by G_F varies greatly, which is related to the coarse aggregate fracture properties. The five aggregates used in the laboratory study yielded 28-day G_F values ranging from 80-170 N/mm, which is an increase of 100 percent from the "softest" aggregate sources to the "hardest" sources. It is also important to emphasize that f_c, E, and f_{sp} were very similar for these mixes. The average bulk properties at 28 days were: f_c = 39 MPa, f_{sp} = 2.9 MPa, and E = 31,000 MPa. In the ongoing study it was found that aggregates' Los Angeles abrasion values were inversely related to G_F for the same strength mixes.

In addition, it appears that fracture energy is in general independent of the PCC's strength level in the age range of 7, 28, and 91 days. However, for increased PCC tensile strength, as seen for the field concretes, it appears that the fracture energy does increase with strength. This suggests that the PCC tensile strength reaches a level where the bond between the aggregates and the matrix becomes increasingly important to the absolute fracture energy.

This shows that for normal strength concrete as designed for highway pavements, the fracture energy property is controlled by the coarse aggregate at early ages, and that as the concrete matures, the effect of the aggregate-to-matrix bond becomes increasingly important. This is in part due to the very high coarse aggregate content in highway mixes

compared to regular structural concrete mixes. Hence, G_F is an important concrete property and it is a quantitative measure of the energy absorbed during crack propagation.

In the Michigan study it was observed that increasing the maximum aggregate size from 25 mm to 38 mm for a glacial gravel and a dolomitic limestone introduced a 10- to 15-percent increase in G_F (at 28 days). It is apparent that increasing the coarse aggregate size improves the concrete resistance to crack propagation. However, the effect is less significant compared to the improvement achievable from selecting another aggregate source. This is in agreement with literature as discussed in chapter 1.

Visual evaluation of the fractured beams clarifies why a concrete containing one type of coarse aggregate yields a higher G_F value than another type. A qualitative relation was observed between the crack path roughness and G_F for the laboratory beams. The crack path for concrete containing glacial gravel is very rough and the majority of the coarse aggregates remain intact. This type of crack path generates large G_F values. The crack path for concrete with the dolomitic limestone or blast furnace slag showed smooth and straight-line crack path with a high percentage of fractured aggregates. For a same strength mix, this type of crack path generates low G_F values.

5.6 Effect of Higher Strength on Concrete Transport Properties

The purpose of determining the transport properties in this study is to investigate relationships between the higher strength and its added resistance to physical and chemical deterioration as measured by a variety of transport property tests. These results will be used to develop recommendations for the desired transport property levels needed for good performance, by either direct measurement or by association with a typically measured property such as compressive strength.

Permeability is generally considered the property which best characterizes the resistance of concrete to deterioration (Schonlin and Hilsdorf, 1988). Thus permeability can be an indicator of long-term durability (i.e. performance) of the concrete at joints, cracks and free edges, where exposure conditions to moisture and deicers are more severe. The literature review and evaluation of the LTPP database also indicate that concrete transport properties like permeability and diffusivity play important roles in spalling.

Permeability and diffusivity are distinguished in that the former measures of the movement of a fluid through the concrete, while the latter measures the diffusion of chemical ions through the concrete. These properties are similar enough in mechanism that they are often (though incorrectly) used interchangeably, such as the Rapid Chloride Permeability Test (RCPT), which is actually an index test relating to chloride ion diffusion. In this report the distinction will be drawn where it is critical to understanding the experimental results.

In view of the varied transport properties governing the durability of concrete with regard to chemical and physical deterioration (Bentz, et al. 1999) different permeability tests were used in this study. They include the RCPT, which is a measure of the concrete's resistance to ionic diffusion of chlorides. Water permeability was determined using the Florida Field Permeability Test. Air permeability was determined using the Torrent Air Permeability Test. The resistance of PCC to water uptake from capillary forces was investigated from the water absorptivity test method. These test methods are described in greater detail in section 2.4.3.

Most deterioration mechanisms are associated with prolonged exposure to high moisture levels, which exist primarily at joints and cracks. Therefore climatic factors, such as annual precipitation, number of freeze-thaw cycles, and subsurface drainage conditions are important, as they control the severity of exposure and the exposure duration. Consequently PCC in the WF climate would be expected to benefit the most from lower permeability. However, irrespective of climate, resistance to ASR or ACR as an example, would be improved with lower permeability as well.

In this investigation, the 15 studied pavements span a wide range in strength and permeability. All have typical mix designs for pavements, and none contain mineral additives. While these studied pavements represent only a minute fraction of in service pavements, they do provide significant clues to permeability's importance.

5.6.1 Effect of Higher Strength on PCC Transport Properties

Concrete compressive strength and elastic modulus were the only two PCC properties found to correlate well with permeability. Both of these mechanical properties correlate to the pore characteristics of the hardened paste (i.e. capillary porosity, pore size, and the pore connectivity) (Hearn et al., 1994; Garboczi, 1990). Shown below in figures 5.6.1-5.6.4 are the results and best fit curves with compressive strength for the different transport property test methods. Other researchers have reported similar relations using the RCPT method (Armaghani, et al., 1992).

It can be seen from these results that the resistance to physical and chemical deterioration improves dramatically with increasing strength and that the strength range from lower strength (33 MPa) to high strength (75 MPa) covers three to four permeability classes ranging from high to very low. These classes are commonly accepted for the rapid chloride, water and air permeability methods. Thus for highway concrete the compressive strength is a good indicator of permeability level. This is significant as PCC mixes can be designed for a permeability level based on compressive strength versus w/c ratio relations at different times. This is illustrated in figure 6.2.1. for results of long-term compressive strength versus w/c ratio from the test sections in this study.

RCPT

In figure 5.6.1, the chloride penetration resistance (RCPT result) vs. compressive strength relation is plotted for the field specimens. In this figure the average compressive strength for each test section is plotted against average RCPT results for each section.

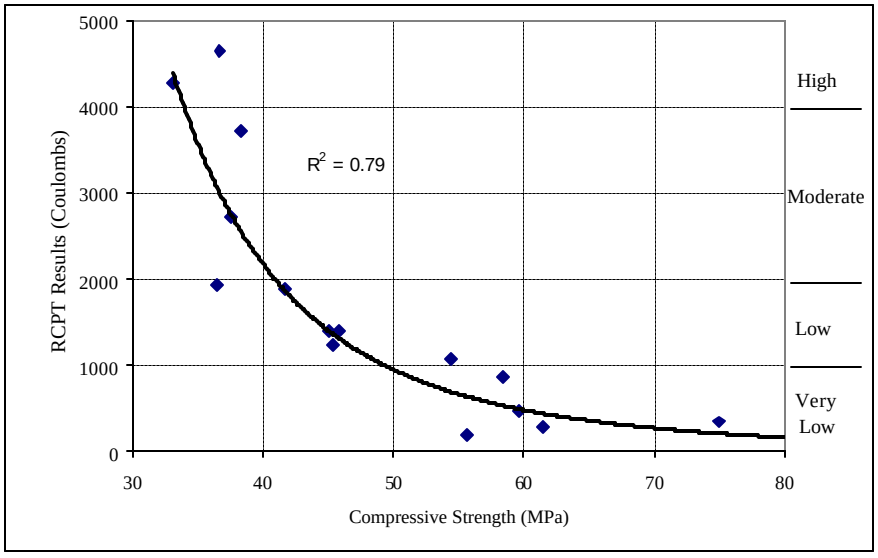

Figure 5.6.1. *Long term RCPT results versus compressive strength relation for pavement concretes from field study.*

A power law regression fit of the data yields a strong correlation (R^2 = 0.79). The RCPT results suggest that compressive strength can be used as a predictive measure for chloride diffusivity or permeability of OPC pavement concretes. Specifically, it is seen that

RCPT results can be greatly reduced with moderate increases in strength. By moving from 35 to 45 MPa compressive strength, the RCPT results can be expected to decrease from over 4000 to under 2000 coulombs (a drop of two RCPT classes). At high strength, however, the benefits to chloride penetration resistance are less pronounced. The RCPT result decrease above 60 MPa is minor. This is important in several ways, primarily for economic reasons, as increased strength is usually associated with increased cost. In addition, these high strength levels can lead to negative effects on other concrete properties, such as increased brittleness, high early (autogeneous) shrinkage and greater thermal deformations at early ages.

A similar permeability trend was found by Armaghani et al. (1992). They also noted the tight relation at higher strength and lower RCPT results, with increasing scatter at the lower strength end of the relation. Shilstone et al. (1992) also found a strong relation between strength and permeability, indicating that both high strength and low permeability were needed to ensure good performance.

The RCPT is criticized for the fact that high chloride penetration samples tend to heat up during the 6-h test duration. High RCPT samples such as the Georgia and some of the California sections were found to heat up by as much as 30^{o}C or more during the test. That heating is believed by some scientists to alter the testing conditions, causing an overestimation of the amount of charge that would be passed if the temperature had remained constant. Recently, however, researchers have been suggesting the use of initial current measurements can accurately predict the charge passed after 6 hours. Indeed, when the initial current data from this study's samples is plotted against the 6-h charge values, a straight line correlation with an R^2 value of 0.98 is observed, as seen in figure 5.6.2. Similar correlations have been shown by other researchers for both normal and high strength concretes (eg. Aldea et al., 1999). This indicates that the heating of the samples during the test does not significantly change the results. Furthermore, the use of initial current readings as opposed to measuring 6-h charge passing appears to be a credible modification to the RCPT method

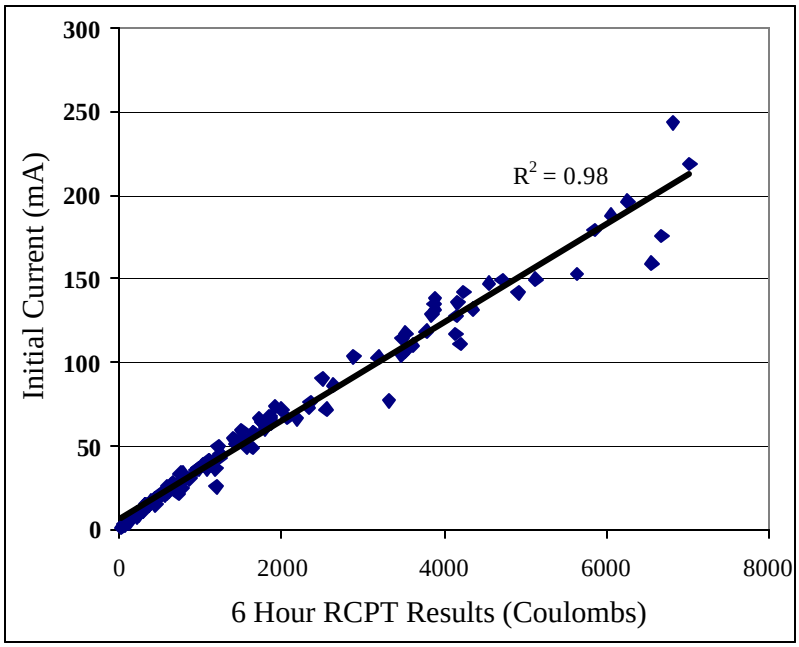

Figure 5.6.2 *Initial current values versus 6-h charge passed using the RCPT method.*

Water Permeability

Water permeability is measured at two depths in the concrete, once near the top surface, and once closer to the bottom surface, as has been described earlier. As with air permeability and chloride penetration resistance, a good correlation is seen with field compressive strength ($R^2 = 0.73$). In figure 5.6.3, water permeability at the top of the concrete is shown versus compressive strength. As before, the compressive strength is averaged over the entire concrete thickness. All values plotted are averages for each pavement section.

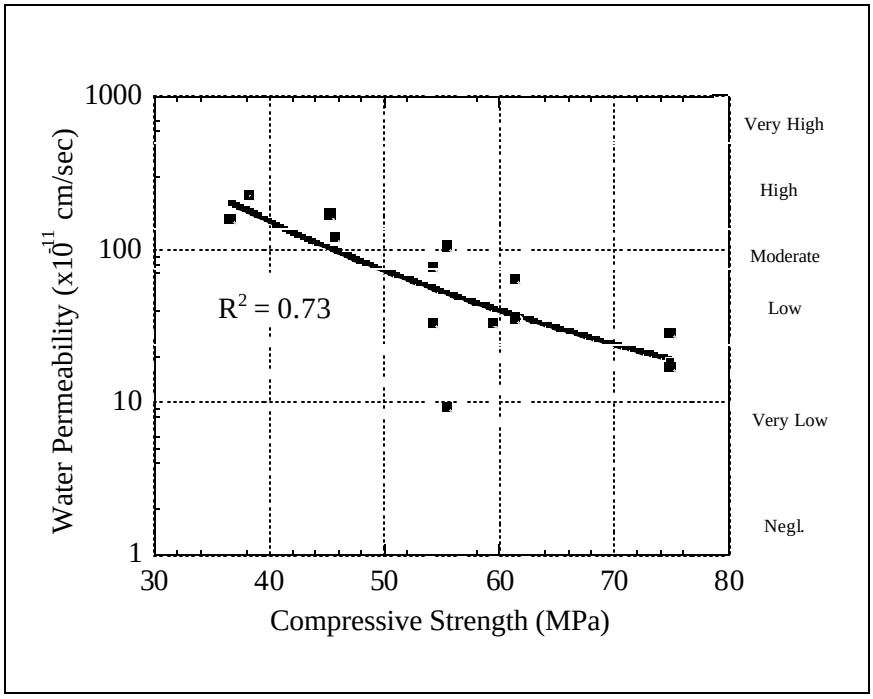

Figure 5.6.3. *Water permeability versus compressive strength for the pavement specimens near the top of the sample.*

The permeability data is plotted on a log scale to cover the several orders of magnitude in readings, and a logarithmic function is used in the regression analysis. Considerably higher scatter in the water permeability data is observed as compared to the RCPT results. This is likely due to the configuration of the test setup, which measures only a small test area (1.25 cm high circular area, 2.2 cm in diameter) as seen in figure 5.6.4. This leads to higher variability in the data because of inhomogeneity in the concrete samples. Figure 5.6.4 demonstrates how the positioning of large aggregate piece can influence the results.

As with the RCPT and Torrent air permeability tests, the results of the water permeability method also span four permeability classes. In this case, the moderate-low boundary appears to be slightly higher at 50 MPa.

It should be noted that there are several different water permeability test methods. The results of each method are dependent on the test configuration and theoretical assumptions (Armaghani and Bloomquist, 1994). The water permeability results therefore should be used as relative values for classification purposes, and not as intrinsic material property measurements.

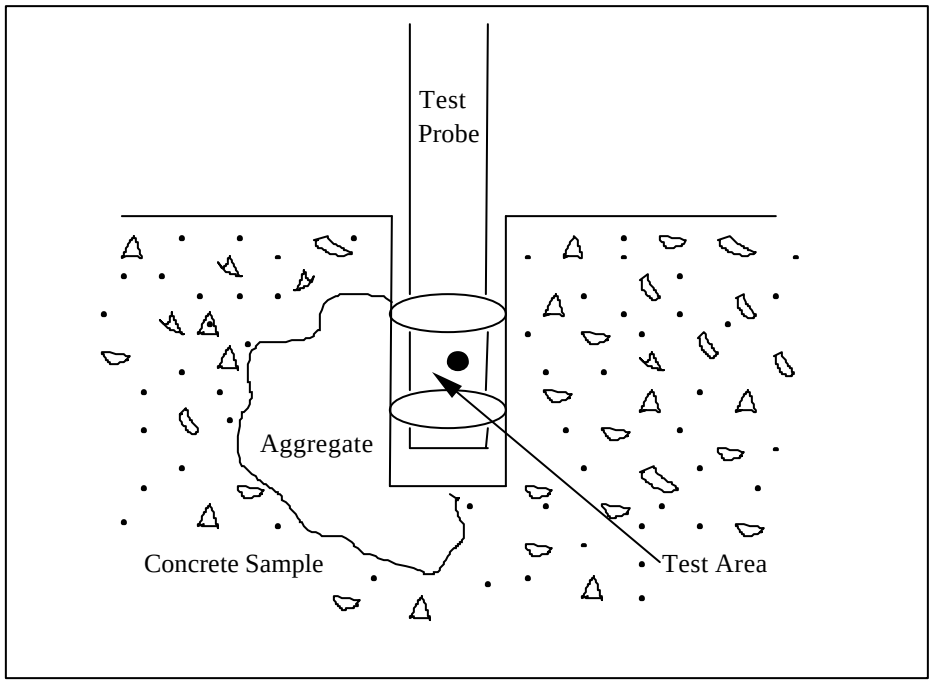

Figure 5.6.4. *Schematic of the potential influence of a large aggregate piece on the water permeability test.*

Air Permeability

The Torrent air permeability test results support the RCPT and water permeability-strength correlation as seen in figure 5.6.5. Air permeability, similar to water, is plotted on a log scale because the technique spans five orders of magnitudes in its results. An excellent strength correlation is achieved using this method ($R^2 = 0.83$). In both the RCPT and Torrent tests, the transition from moderate to low permeability levels occurs at approximately 45 MPa. The fact that RCPT, water and air permeability tests all require similar strengths to reach low permeability levels adds confidence to the strength versus permeability relations.

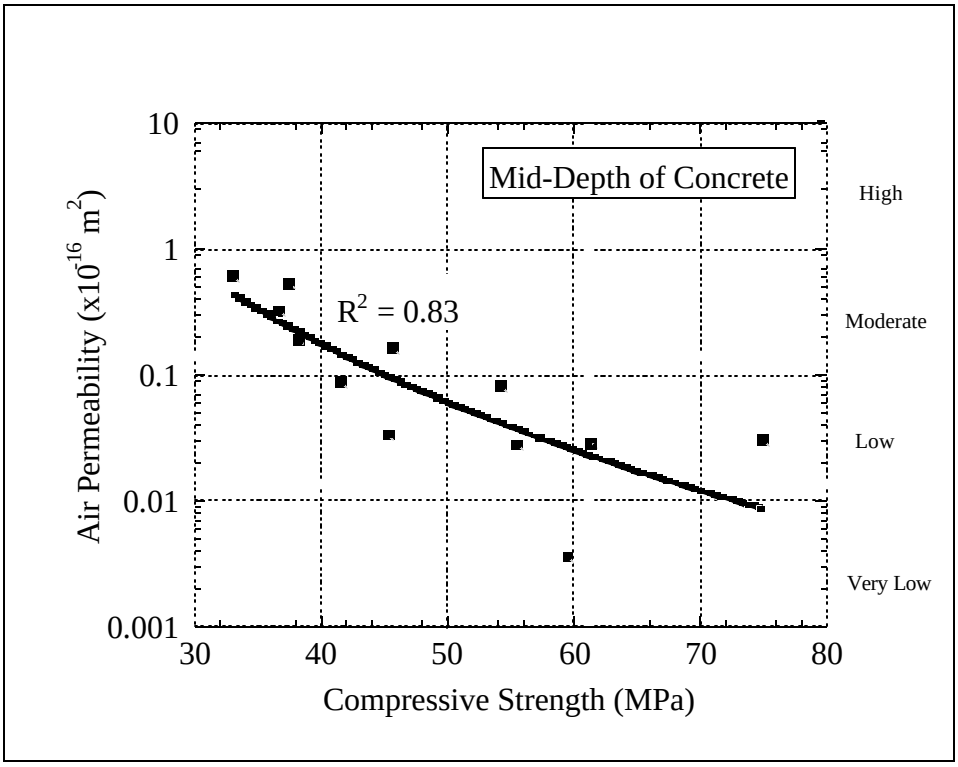

Figure 5.6.5 *Long-term air permeability at the mid-depth of the concrete versus long-term compressive strength for the pavement specimens.*

Water Absorptivity Test

The water absorptivity test was used as it provides important insight into the moisture transport properties during non-steady state conditions, which often exist when dried concrete is in contact with water. Water filling in the micropores (i.e. gel and capillary pores) occurs through capillary suction forces followed by a much slower macropore filling of the much larger air voids.

In this case 150 mm diameter field cores were used. Specimen thickness of 38.1 mm (1.5 in.) was selected to account for the large aggregate size of these concretes. To minimize cracking during heat drying the specimens were dried at 60 to 65^{o}C from both sides until constant weight was reached. This was achieved after 7 days of drying. The specimen sides were then coated with epoxy to ensure one-directional water uptake. Figure 5.6.6 illustrates the test setup in the closed container during the water absorption test.

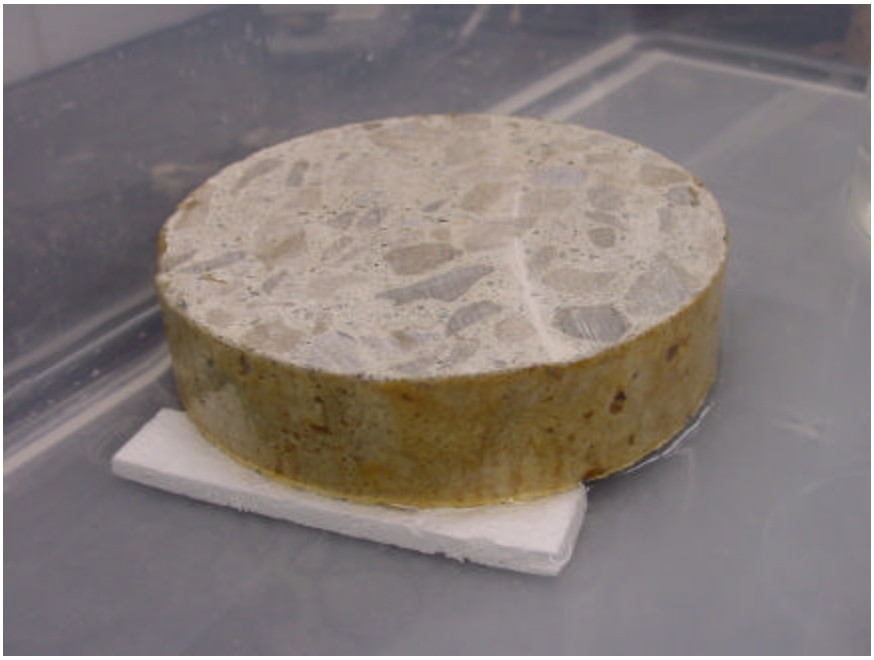

Figure 5.6.6 *Close-up of water absorptivity test.*

The water absorption rate obtained from the initial linear part of the water absorption test of water uptake versus square root time is a measure of concrete permeability and it follows the same trend with compressive strength as the other permeability tests. To illustrate this, the results for the WNF region concretes are shown in figure 5.6.7. The slope of the initial linear part of the water uptake curve (to 3.5 $h^{0.5}$) is plotted versus compressive strength in figure 5.6.8.

The other major features of this test are that it can be used to accurately determine the total air content and the w/c ratio of the sample. This is shown in Chapter 6. It can also be used to determine the exposure time for critical saturation level, which is important for freeze-thaw resistance and for drainage considerations. The latter is discussed in the following section.

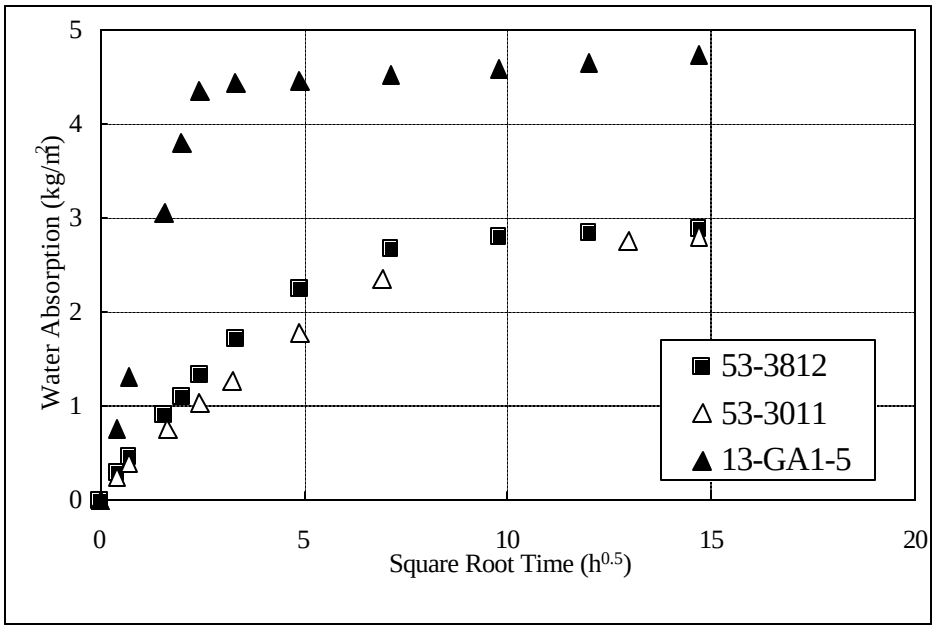

Figure 5.6.7 *Water uptake versus square root time during the water absorptivity test for the WNF region concretes.*

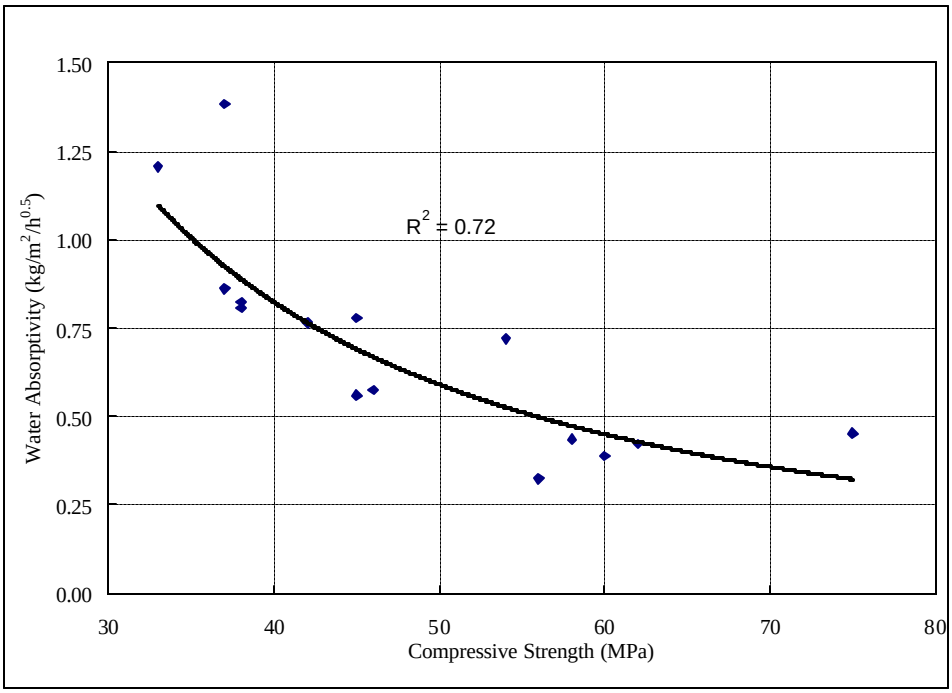

Figure 5.6.8 *Water absorptivity test results versus compressive strength for the studied test sections.*

5.6.2 Effect of Climate and Drainage

The LTPP database was used to determine the effect of long-term field curing on compressive strength. A bi-modal normal density function was obtained showing a substantial increase (68 percent) in compressive strength for the WF region over the 28-

day field compressive strength. In other climates the average increase was much less (28 percent). Consequently, concrete pavements in the WF region have probably reached the low permeability level, associated with a compressive strength of about 45 MPa, within 1 to 2 years after construction. The estimated average 28-day field compressive strength is about 35 MPa. This corresponds to a moderate to high permeability class at the age of 28 days. These concretes were found to have a w/c ratio range of about 0.42 to 0.46 as will be illustrated in table 6.2.1

Moderate to high permeability level is typical for older concrete pavements in California, as they generally have higher w/c ratio (0.47 to 0.56) based on the LTPP database and a lower strength gain over time, as they are located in the DNF climate region. Thus in DNF region concretes containing non-deleterious aggregates, permeability is not as critical as for concrete in the WF zone. Permeability, however may become a factor when mix components favor ASR or ACR as high moisture levels in the PCC trigger these reactions. Petrographic evaluation of the California concretes showed that the aggregates were non-deleterious. The Georgia concrete section located in the WNF region was also lower strength and high permeability, without any signs of durability related distress.

Higher strength concrete such as the three Washington State pavements located in the WNF and the DF regions and the Wisconsin pavement in the WF region were found to have low to very low permeability levels, and thus high internal resistance to physical and chemical deterioration. These pavements had no durability related distresses.

However, in the WF zone very low permeability is not sufficient to guarantee good long-term durability. It appears that adequate subsurface drainage is a prerequisite. This can be inferred from the two Iowa sections (19-3006 and 19-3055). Section 19-3055 was 28 years old at time of this investigation and was found to be distress free, whereas section 19-3006 had deteriorated rapidly during the last 5-6 years, as seen from figure 4.4.1. At the time of the field investigation for this project the section was 22 years old and had developed the highest level of high severity joint spalling in the LTPP database. This section was found to have poor subsurface drainage associated with a CTB and no longitudinal edge drains.

Water absorptivity measurements show that if this concrete is subjected to saturated conditions, which is believed to be the case, high internal moisture levels will develop within 3-4 months due to slow filling of air voids. This can be seen from figure 5.6.9. Initially the smaller capillaries are filled rapidly from capillary suction. Continued exposure to water will gradually fill the air voids, although at a much lower rate. When a critical saturation level corresponding to about 88 percent or higher (Neville, 1997) is reached the PCC loses its frost protection. In other words the air void system is rendered ineffective.

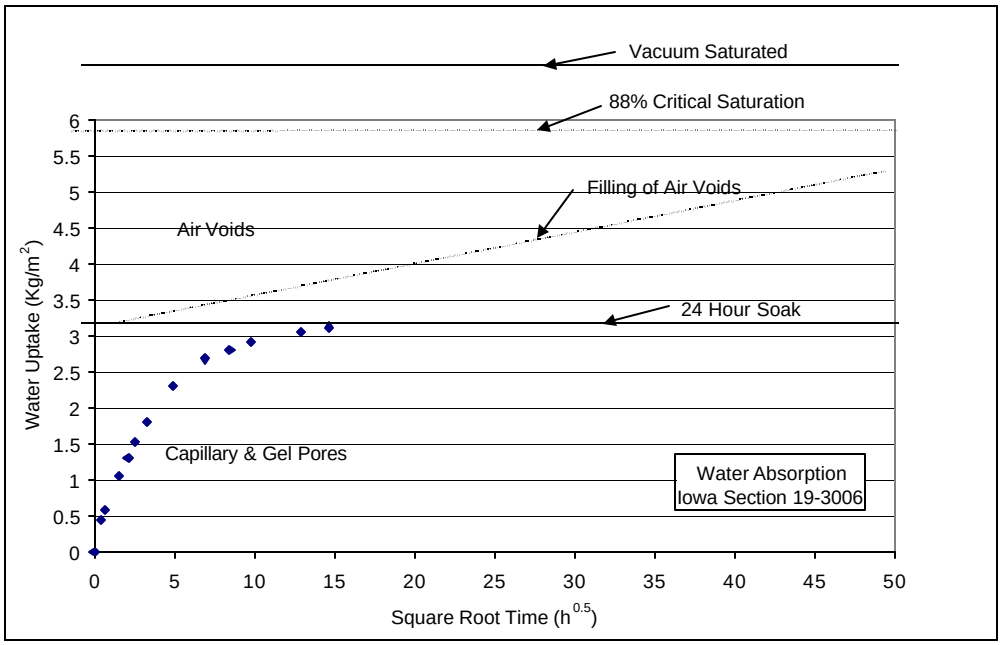

Figure 5.6.9 *Pore filling of test section 19-3006 in saturated conditions from water absorptivity test results.*

As discussed in section 5.7 the Iowa concrete, section 19-3006, has excellent air void characteristics (i.e. air content, spacing factor and specific surface). However, petrographic evaluation of joint cores showed that the air-voids were rendered ineffective as they contained substantial amounts of precipitated material. No visible signs of "D-cracking" patterns were observed on the surface, and petrographic evaluation of the distressed PCC did not implicate the coarse aggregate as the source of deterioration.

For same WF climate conditions, the older Iowa pavement section, 19-3055, has no durability related distress. This concrete was also low in permeability. The combination of a well draining base (e.g. granular base) and low permeability concrete has been effective in avoiding prolonged exposure to high moisture levels. When poor drainage conditions exist, low permeability can at best delay the onset of rapid joint deterioration.

5.6.3 Variation in Permeability with Depth Below the Slab Surface

Several of the test sections were found to have decreasing permeability within the first 100 mm (4 in) from the surface. This is seen from figure 5.6.10 a-e for RCPT results of selected test sections. Similar trends are seen in the Torrent air permeability data. This phenomenon was especially pronounced in the higher w/c ratio concretes from California and Georgia, as seen in figure 5.6.10 a and b. Shrinkage cracking, surface moisture loss, and poor finishing can all contribute to permeability gradients. However, differences in w/c ratio between the top and bottom of a slab are likely the greatest contributing factor to the permeability gradient. In a high w/c ratio concrete some consolidation of the paste can be expected. This results in a denser concrete near the base, and a more porous microstructure near the surface. Mercury intrusion porosimetry results for the Georgia

(13-GA1-5) and California (06-3017) concretes confirm that total pore volume decreases with increasing distance from the concrete surface, as seen in table 5.6.1.

The higher strength, lower w/c ratio concretes were more uniform and did not exhibit permeability gradients through their thicknesses, as illustrated in figure 5.6.10 c and d for Washington State section 53-3812, and Wisconsin section 55-3008. Low w/c ratio concretes are less susceptible to variability in w/c ratio, and thus have more uniform properties through their depth.

Table 5.6.1 *Total porosities and RCPT values at different depths of selected test sections from mercury intrusion porosimetry.*

Depth in Slab	06-3017		53-3812		13-GA1-5	
	Avg RCPT	Avg. Total Porosity %	Avg RCPT	Avg. Total Porosity %	Avg RCPT	Avg. Total Porosity %
Top	5555	8.40	427	5.86	6928	10.38
Middle	3647	7.26	334	5.86	4309	8.60
Bottom	1996	6.18	268	4.85	2951	7.38

As is seen here, within a cross section permeability can vary by as much as two permeability classes. This is significant for the deteriorated Iowa section 19-3006, as this concrete has achieved very low permeability (i.e. <1000 Coulombs) at its base. See figure 5.6.10 e. Nonetheless, bottom-up freeze-thaw deterioration has occurred anyway. Thus, in WF climate concretes, good drainage is a prerequisite for good long-term PCC durability at joints.

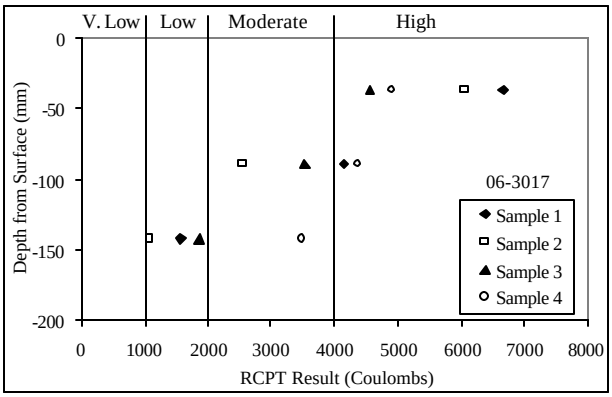

a. Test section 06-3017, California.

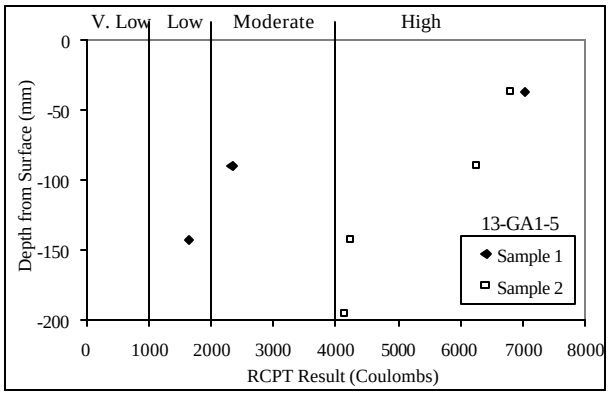

b. Test section 13-GA1-5, Georgia.

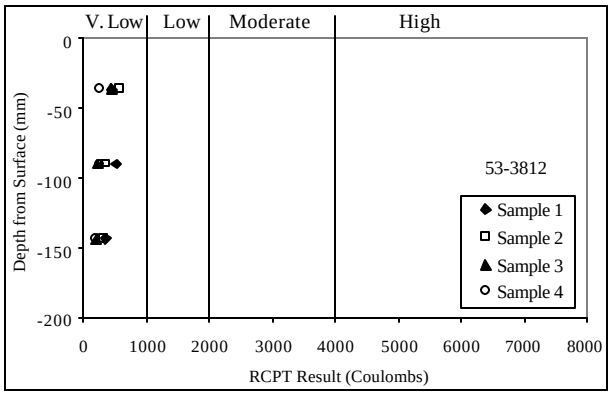

c. Test section 53-3812, Washington.

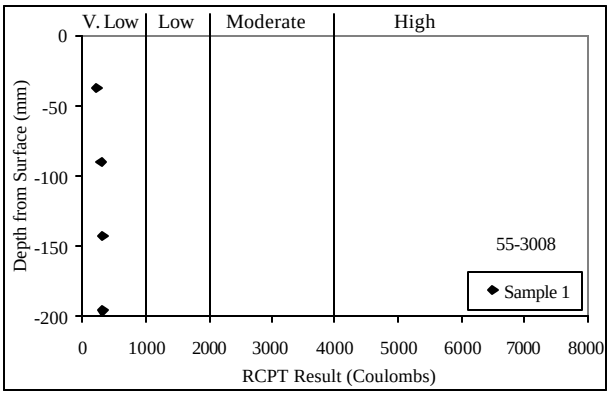

d. Test section 55-3008, Wisconsin.

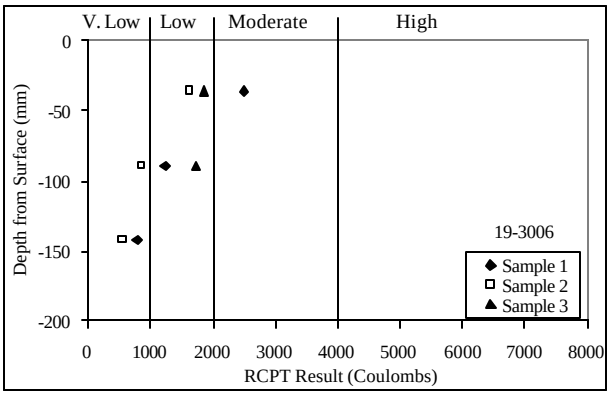

e. Test section 19-3006, Iowa.

Figure 5.6.10 *Through-thickness RCPT gradients in selected test sections.*

5.7 Air Void System and Freeze-Thaw Resistance

Freeze-thaw deterioration in concrete is due to the 9 percent volume expansion of water when it solidifies during freezing. The vulnerability of mature and conventional strength PCC (i.e. 28-day design strength of 24 MPa (3500 psi)) to freezing, in the context of durable aggregates, is a function of the pore structure of the cement-paste, and the moisture condition of the PCC when it is exposed to freezing (Philleo, 1986).

During freezing the entrained air voids, consisting of discontinuous air filled macro-pores, provide a reservoir and pressure relief for the expanding water in the micro-pores of the hardened cement paste. Several studies have shown that the degree of saturation, determined as the ratio of micro-pores to total available pore volume, including the air voids, is a measure of frost protection (Neville, 1997). The critical degree of saturation is reached when the degree of saturation reaches about 88 percent and above, provided that the aggregate are freeze-thaw durable.

Factors affecting the freeze-thaw durability of a concrete pavement are the paste pore system, entrained air, and freeze-thaw resistance of aggregates. D-cracking is a freeze-thaw problem directly related to the coarse aggregate, characterized by the aggregate's internal pore structure and maximum aggregate size. It was beyond the scope of this project to investigate D-Cracking.

Assuming non-deleterious aggregates are used, the freeze-thaw durability of normal strength concrete can be estimated from a spacing factor, which indicates the distribution of air voids. A spacing factor less than 0.2 mm is often required for freeze-thaw resistance (Powers, 1945 and 1949). For higher strength concrete the requirement is not clear, but ACI allows a 1-percent reduction in recommended air content for compressive strength higher than 34.5 MPa (5,000 lbf/in^2). It is not fully understood how the air content affects the freeze-thaw durability for higher strength concrete (ACI 318-95, 1994).

5.7.1 Air Void System of Higher Strength Concrete in the WF Region

The concretes investigated in the WF region are regular strength highway mixes with an average water-cement ratio of about 0.42 to 0.46 based on the LTPP database and this study. Therefore, the average air content is typical of normal strength concrete (6.2 percent based on water absorption test and 6.9 percent from ASTM C 457).

Table 5.7.1 *Summary of air-void analysis from ASTM C457-90.*

Climate Region	LTPP State ID	LTPP Section ID	Air (%)	Spacing Factor (Microns)	Specific Surface (mm^2/mm^3)
DNF	06	3017	7.4	127	14.1
	06	3021	3.1	305	18.5
	06	CS1	4.0	330	16.4
	06	CS3	4.5	279	17.2
	06	I-10	3.9	305	16.9
DF	53	3019	9.4	76	22.1
WF	19	3006	8.3	102	22.4
	19	3055	7.5	152	26.7
	27	4054	6.2	127	24.4
	39	3801	6.3	178	22.4
	55	3008	6.2	51	40.6
WNF	53	3011	8.6	76	31.0
	53	3812	3.4	229	24.3
	13	GA1-5	7.9	127	23.9

The five concretes in the WF region all have good air void characteristics (spacing factor, air content and specific surface area) based on ASTM C 457 as seen from table 5.7.1. Total air ranged between 6.2 and 8.3. The spacing factor varied between 51 microns and 178 microns, and specific surface of the entrained air varied between 22.4 and 40.6 mm^2/mm^3. Only two test sections fell slightly below the minimum recommended specific surface of 24 mm^2/mm^3. These measurements were conducted by the Michigan Department of Transportation (MDOT).

Table 5.7.2 lists total air content obtained three ways. Generally good agreement is obtained between results from the water absorption test on hardened concrete and the LTPP results on fresh concrete. The ASTM C 457 values are generally higher. Based on the water absorptivity test results and LTPP it appears that the California concretes are not air entrained. The same appears to be the case for the Washington State LTPP section 53-3812 and the Georgia concrete. These concretes have total air less than 4 percent.

Table 5.7.2 *Air void contents from the LTPP database, ASTM C457, and water absorptivity test.*

Climate Region	State	Section	Average Air Content		
			Absorptivity Test (%)	LTPP Database (%)	ASTM C-457 (%)
DNF	6	3017	2.9	-	7.4
	6	3021	2.6	-	3.1
	6	7456	3.7	3.9	5.1
	6	CS1	2.9	3.0	4.0
	6	CS3	2.3	2.5	4.5
	6	I10	2.5	-	3.9
DF	53	3019	4.8	4.3	9.4
WF	19	3006	7.5	6.4	8.3
	19	3055	5.9	5.9	7.5
	27	4054	5.8	-	6.2
	39	3801	6.9	-	6.3
	55	3008	4.9	6.5	6.2
WNF	53	3011	4.2	6.2	8.6
	53	3812	2.4	3.4	3.4
	13	GA15	1.8	-	7.9

5.7.2 When the Air Void Structure is Rendered Ineffective

The Iowa concrete, LTPP section 19-3006, has excellent air void characteristics. Therefore this concrete should have adequate freeze-thaw resistance. However, petrographic examination of the upper half of a 150-mm diameter core taken from the deteriorated joint area shows that the smaller air voids (< 75 microns) are lined with a white clear crystalline deposit, which has rendered the voids ineffective. The air void spacing in this area is deficient based on a threshold value of 200 microns as recommended by ACI for freeze-thaw durability. A value of 221 microns is obtained for the spacing factor, as measured by linear traverse according to ASTM C457. The specific surface area of air voids is 17.6 mm^2/mm^3, which is less than the 24 mm^2/mm^3 recommended by ACI. Although the sample has a total air content of 7.2 percent, the spacing factor is high because of high paste content (27.9 percent).

A core sample from the mid-slab region away from the distressed area was found to have total air content of 8.3 percent, and an estimated spacing factor of 102 microns, well below the ACI threshold value. The specific surface area of air voids is 22.4 mm^2/mm^3, which is slightly below ACI recommendations. Thus it appears that freeze-thaw resistance has been compromised in the joint area due to prolonged exposure to water and deicing salts at the slab bottom.

In addition to the filling of air voids with precipitates, reaction rims have formed near the surfaces of several of the coarse aggregates. These rims are likely caused by partial de-dolomitization of the dolomite aggregates and are associated with highly carbonated paste at the aggregate-paste interface. Some associated cracking is observed in some of these large aggregates. Some of the larger cracks run through the large aggregates, but

deflect around the fine aggregates in the paste. Gan et al. (1996) observed this same de-dolomitization mechanism in dolomite aggregates in several other Iowa pavements.

The distresses in section 19-3006 near the joint are shown in figure 5.7.1 a-d using low power stereomicroscopy and thin section microscopy in plane polarized light.

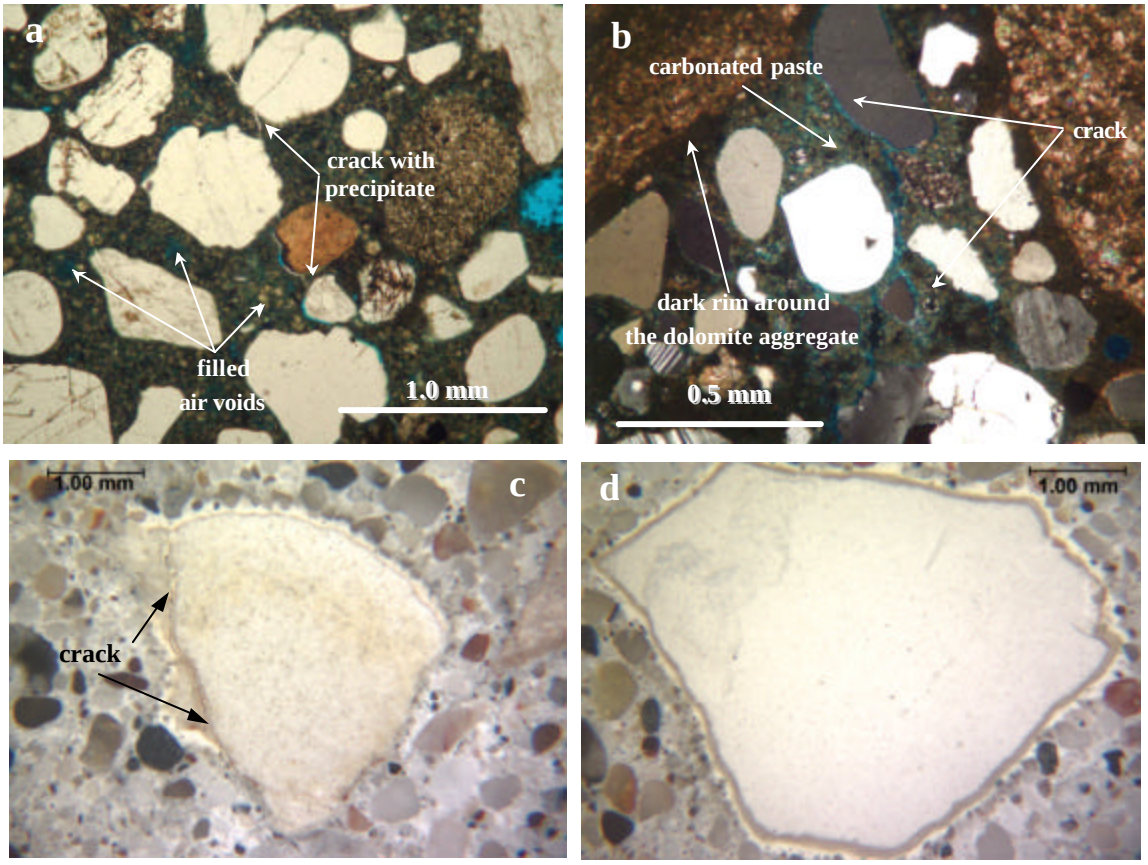

Figure 5.7.1 a, b, c, and d) *Distresses shown in section 19-3006 near the joint using low power stereomicroscopy and thin section microscopy in plane polarized light.*

Based on the condition survey of section 19-3006 performed 3 years earlier in August of 1994, the site conditions have deteriorated rapidly since that time. It appears that joint deterioration and spalling started out as corner spalls rated as corner breaks with some low severity spalls along the joints.

Away from the deteriorated areas this concrete is found to have low permeability (<2000 coulomb). This may have played a role in delaying deterioration, but the severe microenvironment near the joints has prevailed. In view of this, it is doubtful that the use of higher strength concrete for this pavement would have eliminated joint distress.

Joint deterioration and spalling in the WF climate should also consider whether the large aggregates in the slab are susceptible to freeze-thaw damage and D-cracking. The more

water there is available to saturate the slab over long periods of time, the greater the extent of D-cracking. (Peshkin et al., 1994). Pavement sections in Michigan on impermeable bases (i.e. asphalt treated bases and full-depth asphalt concrete shoulders) result in bathtub-type designs, from which water does not readily drain. The Clare test road in Michigan is an example of sudden deterioration of the concrete at the joint starting from the bottom up. This section was found to have no distress after 17 years in service based on the LTPP database, but deteriorated rapidly since then and has now been decommissioned.

Such joint deterioration in WF climates starting at the slab base without the traditional "D" cracking pattern has been reported in several States.

5.8 Concrete Shrinkage and Coefficient of Thermal Expansion

In pavement design, shortening of a slab on grade associated with drying and cooling is of primary interest, as it over time controls joint movement and cracking tendency. Concrete drying shrinkage is a dimensional change due to loss of water, whereas the coefficient of thermal expansion (CTE) is used to determine the dimensional change from temperature effects.

Maintaining small crack and joint opening is critical for long-term pavement performance as it affects the performance in terms of load transfer, faulting, and spalling. A tight joint/crack width (<0.6 mm) maintains high load transfer capacity of the pavement. Joint movements are controlled by the PCC drying shrinkage characteristics and the coefficient of thermal expansion.

Resistance to transverse slab cracking from restrained slab movement is also strongly controlled by thermal and drying shrinkage and the elastic modulus of the concrete. The tensile stress associated with temperature and drying is produced by internal and external restraints. The general thermal and shrinkage stress analysis of pavement slabs is very complex. However, lowering the drying shrinkage and CTE of concrete could minimize the risk of cracking and problems related to exposed cracks.

In this study the CTE property was directly measured on 150-mm diameter field specimens using a modified FHWA procedure (FHWA, 1996) presented in detail in chapter 2. In general, the CTE was found to be very similar for the investigated concretes despite the range of investigated aggregate types. One section, Tracy test section 06-CS3, stands out because of its high cement content.

Drying shrinkage is an irreversible property, which has already taken place for the field concretes of this study. Thus it could not be obtained from laboratory testing. However, the drying shrinkage is estimated based on an approximate relationship between shrinkage and the splitting tensile strength.

5.8.1 Drying Shrinkage

Shrinkage occurs mainly in the cement paste, and is highly related to the w/c ratio and the cement content. For decreasing w/c, the shrinkage will decrease. However, for increasing cement content, the shrinkage will increase. The coarse aggregate counteracts the shrinkage of the cement paste. Increasing stiffness of the aggregate leads to reduced shrinkage. For higher strength concrete with high cement content and/or low coarse aggregate volume it is therefore increasingly important to minimize the shrinkage effects.

Table 5.8.1 lists the estimated relative shrinkage of the different sites based on their estimated 28-day splitting tensile strength (AASHTO, 1993). The 28-day splitting tensile strength is assumed to be 90 percent of the ultimate strength. See also section 5.3. The concrete used in the Tracy test section with increased cement content had 20 percent higher paste content than

the control section. The relative shrinkage has been adjusted accordingly. See chapter 7 for a detailed discussion.

The typical 28-day shrinkage values for JPCP's range within 400 to 800x10^{-6} mm/mm. In table 5.8.1 the shrinkage is given relative to the conservative shrinkage value of 800x10^{-6} mm/mm. Despite the inaccuracy of the estimate, it appears that the drying shrinkage have been in the expected range for JPCP's. However, it should be pointed out that the relative shrinkage in the dry regions is likely being underestimated.

Table 5.8.1 *Estimated relative shrinkage based on the estimated 28-day PCC splitting tensile strength.*

Climate Region	State ID	Section ID	Estimated 28-day Splitting Tensile Strength Mpa	Estimated Shrinkage Relative to 800x10^{-6} mm/mm
DNF	06	3017	3.37	0.57
	06	3021	3.18	0.62
	06	7456	2.98	0.68
	06	CS1	3.18	0.62
	06	CS3	3.82	0.82[1]
	06	I-10	3.91	0.42
DF	53	3019	3.82	0.45
WF	19	3006	3.18	0.62
	19	3055	2.55	0.82
	27	4054	3.37	0.57
	39	3801	3.37	0.57
	55	3008	4.09	0.38
WNF	53	3011	3.45	0.54
	53	3812	4.00	0.40
	13	GA1-5	2.73	0.76

[1]Adjusted for high cement content (paste content)

5.8.2 CTE Test Results and Ranges for the Pavements Investigated

The cement paste and the aggregate have different CTE (Neville, 1997). The coefficient of thermal expansion of the hydrated cement paste varies between 11 to 20E-06 /^{0}C which can be substantially higher than the CTE of the coarse aggregate (Forster, 1997). Typical CTE values of different rock types, as reported by Lane (1994), are shown in table 5.8.2.

The concrete's CTE is a resultant of the two values, but is very sensitive to the cement paste content as the hydrated paste is, despite the smaller volume fraction (about 25 percent) the continuous matrix in which the aggregates are embedded. Thus, for most cases the PCC CTE value are controlled by the cement paste.

Table 5.8.2 *Typical CTE values of different rock types. [after Lane (1994)]*

Rock	CTE value ($x10^{-6}/^oC$)
Quartzite, silica shale, chert	11.0-12.5
Sandstones	10.5-12.0
Quartz sands and pebbles	10.0-12.5
Argillaceous shales	9.5-11.0
Dolomite, magnesite	7.0-10.0
Granite, gneiss	6.5-8.5
Syenite, andesite, diorite, phonolite, gabbro, diabase, basalt	5.5-8.0
Marble	4.0-7.0
Dense, crystalline, porous limestone	3.5-6.0

In this study no strong correlation was detected between aggregate types and PCC CTE. However, the Tracy test section with higher cement content, 06-CS3, containing 40 percent more cement than the control section, 06-CS1, had a 40 percent higher thermal expansion. All CTE values obtained by the procedure described above are shown in table 3.3.11. The average value for each climate region is:

- DNF: 9.93E-06/^{0}C
- DF: 8.9E-06/^{0}C
- WF: 9.49E-06/^{0}C
- WNF: 9.10E-06/^{0}C

These results show that the coefficients of thermal expansion of concrete in different climate regions do not differ significantly from each other. Compared to values obtained from the literature on normal strength concrete, these results can be considered in the range of low to normal.

For sections tested, the average CTE values vary from 8.83 to 10.27 E-06 /^{0}C except for two sections. The variation of CTE of sections tested can be considered quite narrow and close to the expected median CTE value (Neville, 1997). The same finding has also been reported Alungbe et al. (1990). However, the key similarity of these concretes is that the aggregate volume contents were very close at about 75 percent.

Higher CTE values have been identified for two sections from different climatic regions. The highest CTE was determined for section 06-CS3 in the DNF region (13.64E-06 /^{0}C) followed by 39-3801 in the WF region (11.27E-06 /^{0}C). The high CTE in test section 06-CS3 can be attributed to its high cement content (418 kg per m^3 compared to 307 kg per m^3 for the control section 06-CS1). The higher CTE of the Ohio section, 39-3801, compared to the other

PCC's containing dolomitic limestone is likely due to the fact that 50 percent of the coarse aggregate is sandstone and quartz which both have about twice the CTE of limestone.

CHAPTER 6. CONCRETE MIX CHARACTERISTICS

6.1 Introduction

It was shown in the interim report and in chapter 1 that the mix characteristics (such as w/c ratio, cement content, aggregate size and gradation, aggregate content and type) have a varied influence on several of the key mechanical and durability properties of concrete. These properties, in turn, were found to affect pavement performance. This section presents the relations between the mix characteristics and concrete properties obtained from laboratory testing of field cores.

Extensive laboratory evaluation of the concretes cored from the 15 pavement test sections in this study was undertaken to determine the role of mix proportions on the strength level, associated properties, and pavement performance. The data gleaned from petrographic studies, LTPP database values, and historical information available on these test sections confirm that no special mix designs were used, even for the very high strength pavements studied. The high strength and performance levels were achieved not through special mixes, but primarily through careful attention to selection of high quality materials, proper design, and fortuitous placement and environmental conditions.

The concrete mix composition for each of the field projects is shown in table 6.1.1. In general, the mix designs are typical pavement mixes.

Table 6.1.1 *Mix designs for the investigated test sections.*
(Values reported are from the LTPP database except where otherwise indicated.)

Climate Region	State	Section	Cement (kg)	Cement Type	Water (kg)	W/C Ratio	Air Content (%)	Coarse Aggregate (kg)	Fine Aggregate (kg)	C/F Ratio
DNF	6	3017	282	Type II	160[1]	0.57[1]	2.9[2]	1195	703	1.7
	6	3021	335	Type II	188	0.56	2.6[2]	1186	648	1.8
	6	7456	307	Type II	144	0.47	3.9	1208	699	1.7
	6	CS1	307	Type II	144	0.47	3.0	1208	699	1.7
	6	CS3	418	Type II	140[3]	0.35[3]	2.5			
	6	I10	252[3]	--	121[3]	0.48[3]	2.5[2]	1218[3]	681[3]	1.8
DF	53	3019	335	Type II	114	0.34	4.3	1222	730	1.7
WF	19	3006	335	Type I	141	0.42	6.4	1001	832	1.2
	19	3055	358	Type I	154	0.43	5.9	943	806	1.2
	27	4054	320	Type I	147	0.46	5.8[2]	1280	564	2.3
	39	3801	356	Type IA	135	0.38	6.9[2]	1005	683	1.5
	55	3008	335	Type I	134	0.40	6.5	1201	646	1.9
WNF	53	3011	335	Type II	134	0.40	6.2	1222	729	1.7
	53	3812	335	Type IIA	131	0.39	3.4	1222[4]	729[4]	1.7
	13	GA1-5	310[4]	--	152[4]	0.50	4.0[4]	1180[4]	662[4]	1.8

[1] Water content estimated from LTPP database

[2] Air content from water absorptivity test

[3] Water-cement ratio estimated from water absorptivity test (assuming 90% hydration)

[4] Mix design estimated from other test sections in the same state. (Data entry error for LTPP section, 53-3812, Washington State.

From table 6.1.1 it is noteworthy that the mix designs vary with climate region and locally available materials. These variations represent shifts in emphasis to different areas of the mix design to reflect the exposure conditions.

For example, the wet freeze region concretes tend to have smaller coarse aggregate sizes (generally up to 25.4 mm nominal max. size) consistent with the need to avoid durability related aggregate distresses such as freeze-thaw deterioration and D-cracking. In the other climates, larger aggregates (about 38 mm nominal max. size) are used. Large high quality aggregates tend to improve concrete fracture properties and load transfer efficiency after cracking.

Similarly, w/c ratios are generally lower in the wet freeze climate concretes than in those from other climate regions. Low w/c ratio helps to densify the microstructure and reduce permeability and transport properties. This in turn protects the concrete from the ingress of water and salts that can lead to durability related distresses in freeze-thaw susceptible climates. In the other climate regions, higher w/c ratios are observed. It is believed that the workability of the concrete at time of construction in these hot climates is likely the overriding consideration for these pavements.

In general cement contents are held to typical ranges in these mixes, irrespective of climate region. It is noteworthy that one site in California used increased cement content to increase compressive strength. However, this was an experimental section that is atypical of California mix designs. Very high strength can be achieved using normal cement contents on the order of 335 kg/m^3.

6.2 Water-Cement Ratio

Sellevold (1986) has pioneered the w/c ratio prediction in hardened concrete using the capillary sorption method and the Powers-Brownyard equation shown below. The water absorption technique was used in this project to evaluate the transport properties, air content, and the water-cement ratio as well.

In table 6.2.1, the w/c ratio values are shown for each test section based on the LTPP database, the ASTM C1084 maleic acid method, and as predicted using the Powers-Brownyard (1948) equation below, and using the absorptivity results for micro-pore volumes:

$$W/C = (0.317 \cdot P + 0.172 \cdot \alpha) / (1-P) \qquad (6.2.1)$$

where P = normalized micro pore volume (i.e. relative ratio on a paste content basis)
α = degree of hydration (relative amount from 0 to 1).

On average, the binder content by volume from the LTPP database was estimated at 25 percent. This value was then used to normalize micropore volume from absorption tests on the concrete to paste (i.e. binder) porosity.

The estimated w/c ratio was calculated for three different hydration values, 80, 90 and 95 percent. This results in a range of predicted w/c ratios typically within 0.05 from 80 to 95 percent hydration. Overall, good agreement was obtained with the LTPP database values and the maleic acid method, with only a few exceptions. Using the Powers-Brownyard equation, the w/c ratio values for the sections not included in the LTPP database were estimated as well based on the assumption of a 25 percent binder volume. These results appear to be appropriate based on the compressive strength versus w/c ratio curve shown in figure 6.2.1. This curve follows the expected Abram's relation well.

The maleic acid method is based on ASTM C1084, "Standard Test Method for Portland-Cement Content of Hardened Hydraulic-Cement Concrete." The method uses a solution of maleic acid in methanol to dissolve the cement paste from a concrete specimen. The approach involves accurately weighing a sample of ground concrete, dissolving the concrete in the methanol-maleic acid solution, and filtering the mixture after allowing time for settling. The solid residue resulting after dissolution is weighed, and the weight loss is taken as the cement paste content of the concrete. To get cement content, the bound water must be determined and subtracted from the cement paste content. While the method gives generally good approximations of cement content and w/c ratio, it is known that the maleic acid solution also attacks some carbonate aggregates while not dissolving carbonated cement pastes. This may account for differences in cement contents and w/c ratios observed in table 6.2.1. The methanol-maleic acid test was conducted by MTU.

Table 6.2.1 *Water-Cement Ratios of the studied test sections from the LTPP database, maleic acid test, and water absorptivity test.*

Climate Region	LTPP		w/c Ratio				
	State ID	Section ID	LTPP Database	Maleic Acid	Absorptivity Test		
					80% Hyd	90% Hyd	95% Hyd
DNF	06	3017	0.57	0.46	0.43	0.46	0.48
	06	3021	0.56	0.50	0.63	0.67	0.69
	06	7456	0.47	--	0.49	0.52	0.54
	06	CS1	0.47	0.47	0.43	0.46	0.47
	06	CS3	--	0.37	0.33	0.35	0.37
	06	I-10	--	0.45	0.45	0.48	0.50
DF	53	3019	0.34	0.43	0.43	0.46	0.49
WF	19	3006	0.42	0.32	0.40	0.43	0.44
	19	3055	0.43	0.26	0.51	0.54	0.55
	27	4054	0.46	0.49	0.39	0.41	0.43
	39	3801	0.38	0.48	0.46	0.49	0.50
	55	3008	0.40	0.67	0.33	0.35	0.37
WNF	53	3011	0.40	0.38	0.37	0.39	0.41
	53	3812	0.39	0.38	0.32	0.35	0.36
	13	GA15	--	0.49	0.53	0.56	0.57

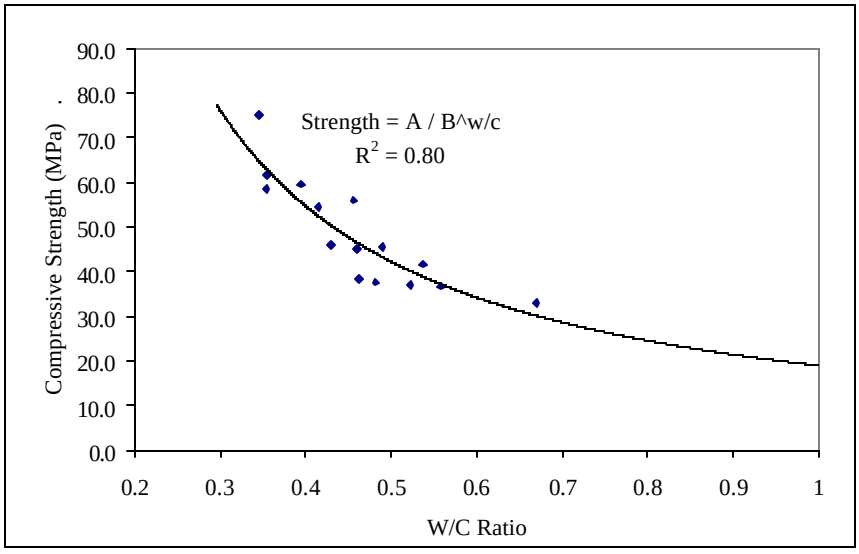

Figure 6.2.1 *Ultimate compressive strength versus w/c ratio from absorptivity test results.*

6.3 Cement Type and Content

The cement types and contents were obtained from the LTPP database and using the maleic acid method. It is significant that although various strength levels were achieved in the field, all of these concretes contain ordinary portland cements (type I and II). In addition, it is noteworthy that none of these concretes contain mineral additives such as fly ash or slag. From the LTPP database, it is seen that for most of the sections, cement contents fall within a relatively narrow range of 307 kg/m^3 to 358 kg/m^3 (517 lb/yd^3 to 604 lb/yd^3). The exceptions are test sections 06-CS3, 06-3017, and 06-I-10. As can be derived from table 6.3.1, the average cement content for all sections is 331 kg/m^3 (557 lb/yd^3). The average within each climatic zone is 332 kg/m^3 (559 lb/yd^3) for DNF, 341 kg/m^3 (573 lb/yd^3) for WF, and 313 kg/m^3 (528 lb/yd^3) for WNF. It can be seen that these average cement contents do not vary significantly from the overall average.

Section 06-CS3 at Tracy, California was an experimental section designed to test the effect of higher cement content on performance. The cement content is 418 kg/m^3 (705 lb/yd^3), and is not typical of the mixes studied. As seen earlier, the higher cement content of the 06-CS3 concrete has produced an increase in compressive strength to 58.4 MPa (8,471 lbf/in^2), as compared to the control mix in section 06-CS1 at the Tracy site. That section has a cement content of 306 kg/m^3 (517 lb/yd^3) and field compressive strength of 45 MPa (6,535 lbf/in^2). However, the increase in cement content has only increased the tensile strength by about 8 percent, from 3.48 MPa (505 lbf/in^2) for the 06-CS1 to 3.77 MPa (547 lbf/in^2) for the 06-CS3. The moderate increase in tensile strength has not been able to counteract the effect of increased shrinkage and CTE on pavement performance. See chapter 4 and section 5.8.

Table 6.3.1 *Cement Types and Contents for the studied sections based on LTPP database and mix design data.*

Climate Region	LTPP		Cement	
	State ID	Section ID	Type	Content Kg/m^3
DNF	06	3017	Type II	282
	06	3021	Type II	335
	06	7456	Type II	307
	06	CS1	Type II	307
	06	CS3	Type II	418
	06	I-10	-	252[1]
DF	53	3019	Type II	335
WF	19	3006	Type I	335
	19	3055	Type I	358
	27	4054	Type I	320
	39	3801	Type IA	356
	55	3008	Type I	335
WNF	53	3011	Type II	335
	53	3812	Type IIA	335
	13	GA1-5	-	326[1]

[1] calculated from volume distribution of coarse and fine aggregates and paste as determined by ASTM C-457.

In addition to strength observations, cement content can also affect thermal expansion in the concrete. Test section 06-CS3, has a high value of CTE at 13.64E-06 /^{0}C. This high CTE is thought to be caused by higher cement content used in the mix. As has been reported (Neville, 1997), a mix having higher paste content tends to give a higher CTE value. Although having almost the same mix composition as 06-CS3 except for cement content, 06-CS1 gives a moderate CTE of 9.79E-06 /^{0}C. This suggests that the cement content significantly influences the thermal expansion of concrete.

An important finding when comparing tables 6.2.1 and 6.3.1 is that the higher strength concretes from Washington and Wisconsin, sections 53-3812, 53-3011, 53-3019, and 55-3008, do not contain high cement contents. Their cement contents are all 334 kg/m^3 (564 lb/yd^3). The high strengths were instead obtained by using low w/c ratio (0.4 or lower).

Figure 6.3.1 shows the cement content as a weight percentage of the concrete mix for each pavement as determined from the LTPP database and the maleic acid method. It is noteworthy that the maleic acid method yields slightly higher cement contents for almost all test sections. This is likely because some dissolution of the aggregates has occurred using the maleic acid method.

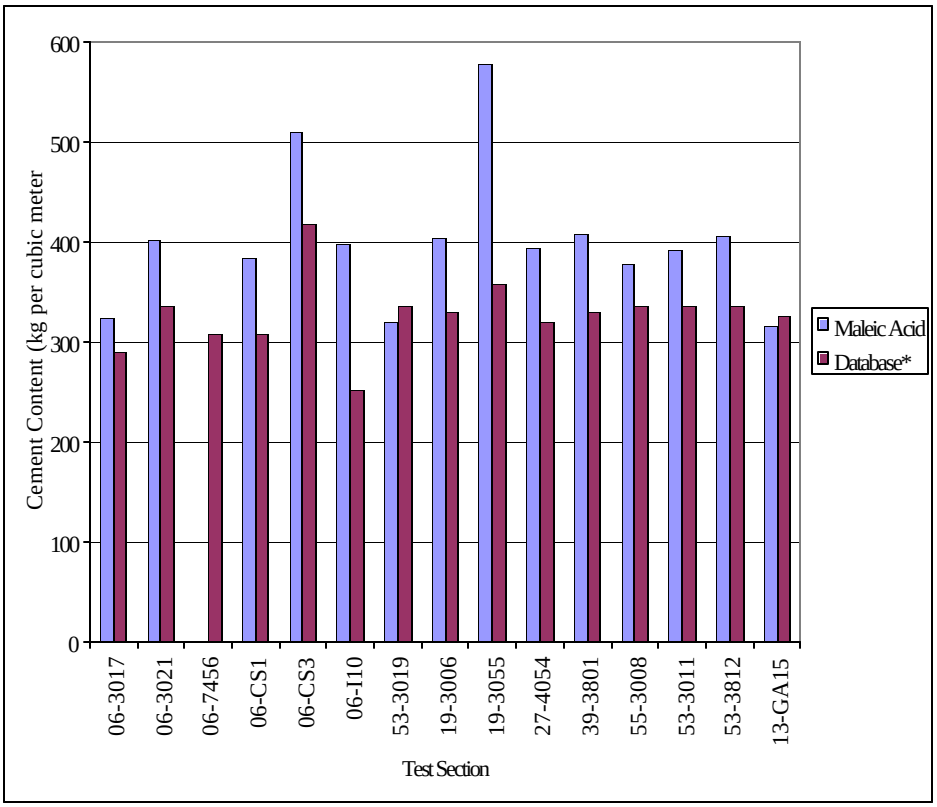

*As determined from the LTPP database and mix design data

Figure 6.3.1 *Cement content as a weight percentage of the concrete mix for each pavement as determined from the LTPP database and the maleic acid method.*

6.4 Aggregates

Coarse and fine aggregate types were determined from petrographic analysis. These results for the coarse aggregates are shown in table 6.4.1. Principally, three different coarse aggregate types were used in the studied concretes: silicate rock gravel, dolomite/limestone, and crushed silicate rocks. The dolomite/limestone aggregates were exclusively used in concretes for the WF zone (19-3006, 19-3055, 27-4054, 39-3801, and 55-3008). The Ohio section 39-3801 also contained a significant amount of sandstone and quartzite. Section 13-GA1-5 contained crushed granitic to granodioritic aggregates while the other concretes (06-3017, 06-3021, 06-7456, 06-CS1, 06-CS3, 06-I-10, 53-3019, 53-3011, and 53-3812) contained gravel of silicate rocks.

The 06-I-10 (in San Bernadino County, California) concrete is composed of a natural silicate gravel mix (gneiss, quartz, and minor basalt) (see section 3.2). These aggregate types are well-known for their high strength and durability. Similar aggregate types were found in other California concretes including, 06-3017, 06-3021, 06-7456, and the other experimental sections investigated on I-5 at Tracy (control section 06-CS1 and higher cement content section 06-CS3). The maximum nominal aggregate size in most of these pavements was 38.1 mm (1.5 in). Silicate gravel was also found in sections 53-3019, 53-

3812, and 53-3011. The Georgia section (on I-85, test section 13-GA1-5) had crushed granite-granodiorite rock in the coarse and the fine fraction. This aggregate contains numerous microcracks. Because these cracks are only present within the aggregate they must have formed during processing.

In the WF region dolomitic limestone was associated with excellent concrete quality. It appears that this is related to the use of high quality limestone with low microporosity. These aggregates generally had smaller nominal aggregate sizes (19.1-38.1 mm). The smaller maximum aggregate size found in the WF region is probably due to general consideration of the effects of coarse aggregate size on concrete D-cracking susceptibility.

At this point there is no clear evidence as to whether a dolomite or a silicate gravel would have a different durability in different climates. However, the durability of an aggregate is highly dependent on its particular source, and cannot be generalized to aggregate type.

Table 6.4.1 *Coarse aggregate characteristics obtained from laboratory analysis.*

Climate Region	LTPP		Coarse Aggregate			
	State ID	Section ID	Shape	Type	Max Nominal Aggregate Size[1] mm	Max Aggregate Dimension [2] Mm
DNF	06	3017	Rounded	gravel (mix)	38.1	46
	06	3021	Rounded	gravel (mafic)	38.1	46
	06	7456	Rounded	gravel (mix)	38.1	75
	06	CS1	Rounded	gravel (mix)	38.1	76
	06	CS3	Rounded	gravel mix incl. dol.	38.1	45
	06	I-10	Rounded	gravel (mix)	50-62	44
DF	53	3019	Rounded	gravel (mafic)	38.1	47
WF	19	3006	Angular	dol. Limestone	25.4	31
	19	3055	sub-rounded	dol. Limestone	25.4	42
	27	4054	sub-rounded	dol. Limestone	25.4	40
	39	3801	Rounded	grav.+dol. Limestone	19.1	27
	55	3008	Rounded	dol. Limestone	38.1	43
WNF	53	3011	Rounded	gravel (mix)	25.4	38
	53	3812	Rounded	gravel (mix)	38.1	32
	13	GA1-5	Angular	syenite/granodiorite	38.1	36

[1] Based on sieve analysis of dissolved cores
[2] Based on petrographic analysis

6.4.1 Coarse Aggregate Characteristics

Coarse Aggregate Fracture in Higher Strength PCC

High fracture energy values were obtained for the four California test sections 06-3017, 06-3021, 06-I-10, and 06-CS3. The values ranged from 200 to 280 N/m. These sections all had high content of strong coarse aggregate of a gravel mix, and a significant amount of the coarse aggregate exceeded 25.4 mm (1 in). From the literature review it was found

that the coarse aggregate type and the aggregate-to-paste bond have significant impact on the PCC fracture energy. Field beams from these few sites gave insight into the level of fracture energy that can be achieved over time. These concretes contained very tough large-size coarse aggregates, which improved the PCC fracture behavior.

Coarse Aggregate Gradations

The aggregate gradations for coarse and fine aggregate were determined on the field cores by thermal decomposition of the concretes and manual separation of the aggregate from the paste. The nominal maximum aggregate size used in these pavements ranges from 25.4 mm for the WF zone to 50 mm for the DNF zone. These values are greater than those typically used today for PCC pavements. Over the years there has been a trend toward using smaller maximum aggregate size.

The coarse aggregate size has also a significant effect on the deterioration of cracks. In a field study, discussed by Yu et al. (1998) it was shown that decreasing the maximum aggregate size from 38.1 to 25.4 mm increased the deterioration of cracks by 15 percent. Further decrease in aggregate size to 12.7 mm increased the deterioration another 100 percent. This indicates that the coarse aggregate sizes above 12.7 mm are the main contributors to aggregate interlock and load transfer.

Figure 6.4.1 shows the coarse aggregate gradation curves for the investigated sections. The gradation curve for 06-7456 was not determined, but is assumed similar to 06-CS1. The gradation curve for test section 06-I-10 was not available due to a limited number of core samples available from the site.

The California gradations were very coarse with 30 to 40 percent retained on the 25.4 mm sieve, and only 15 to 20 percent passing the 12.7 mm sieve. Also, the gradation curves between the projects were very similar. In the WF region the gradation curves are significantly finer than in the DNF region. Typically the maximum aggregate size in the WF zone is 25.4 mm as observed for the Iowa (19-3006, 19-3055), Minnesota (27-4054), and Ohio (39-3801) concretes. At the same time, these concretes had a higher percent passing the 12.7 mm sieve (on the order of 35 to 55 percent). It is worth noting that the Wisconsin concrete has a coarser gradation, with about 20 percent retained on the 25.4 mm sieve. The coarse aggregate here was a dolomitic limestone, and the concrete was in excellent conditions with no trace of freeze-thaw damage. The Wisconsin coarse aggregate gradation is very similar to the gradations used in Washington State (53-3011, -3019, and –3812) and in Georgia (13-GA1-5/6). These sections in the WNF and DF region had typically 20 percent retained on the 25.4 mm sieve and about 25 to 40 percent retained on the 12.7 mm sieve.

a)

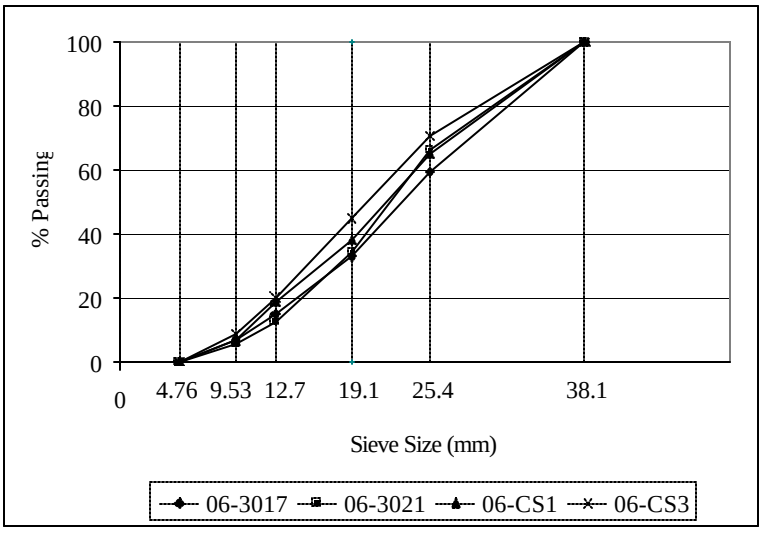

b)

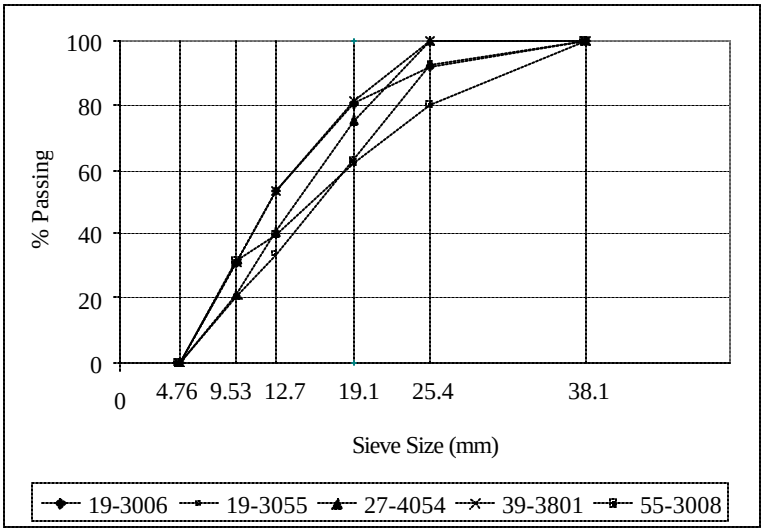

c)

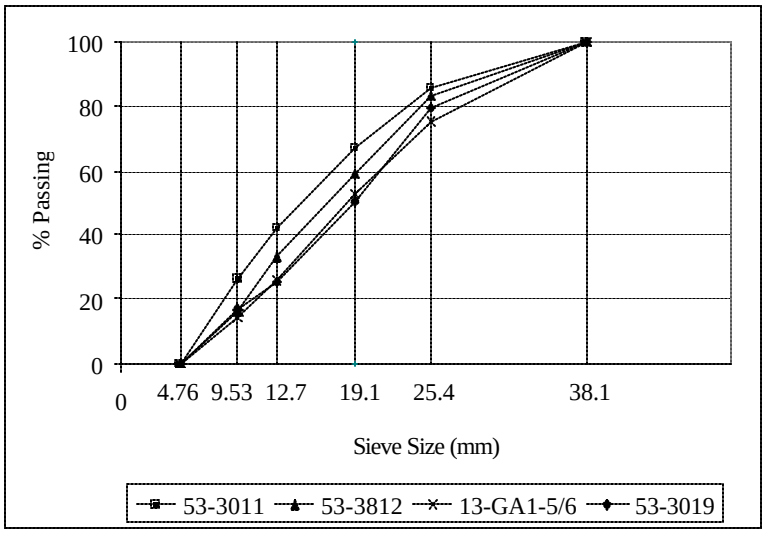

Figure 6.4.1a-c. *Coarse aggregate gradation curves. a)DNF zone, b)WF zone, and c)WNF and DF zones.*

6.4.2 Combined Fine and Coarse Aggregate Gradations

The coarse and fine aggregate gradation results as determined from the field cores are plotted in figure 6.4.1 as percent retained of combined aggregate gradations. They have been separated by climatic zone as the gradations appear to be related to regionally available sources of materials and climate zone requirements. These results show that the samples from the DNF and DF zones contain relatively high aggregate contents (46.3 to 53.2 percent by weight) in the size range of 12.7 to 25 mm (1/2 to 1 in). A higher content is also observed for aggregate size below 2.5 mm. This is particularly evident for the California sections 06-3017 and 06-3021 that contain very little material (2.88 to 4.74 percent by weight) in the intermediate size ranges (3.2 to 9.5 mm).

As compared with the specimens from the dry zones, the pavement sections from the WF and WNF zones generally have smaller grain sizes and less material retained on the larger sieves. Moreover, the aggregate distribution in the samples from the WF and the WNF zones generally plot within typical boundaries of the combined aggregate gradation curves.

In general, combined aggregate gradations in the WF zone are well graded. However, the aggregate distribution in one of the WF sections, 19-3055, is different from the others in that most of its aggregates (54 percent by weight) are between 6.1 mm (0.25 in) and 0.5 mm (0.02 in) in size. The highest aggregate contents in the other WF zone samples were observed on the 6.1-mm (0.25-in) sieve for sections 19-3006, 39-3801, and 55-3008, and on the 12.7-mm (0.5-in) sieve for section 27-4054. In the WF zone, very little aggregate is retained on the 25.4-mm (1-in) sieve (less than 4.1 percent by weight) for most sections. In one section, 55-3008, aggregate retained in this sieve is 12.4 percent by weight.

In the samples from the WNF sections, the maximum aggregate contents are retained on the 12.7-mm (0.5-in) sieve in sections 53-3812 and 13-GA1-5, and on the 6.1-mm (0.25-in) sieve for section 53-3011. Section 53-3011 contains less coarse material than 53-3812 and 13-GA1-5, but all three sections contain less material with aggregate sizes below 9.5 mm (0.375 in) than the WF sections.

a)

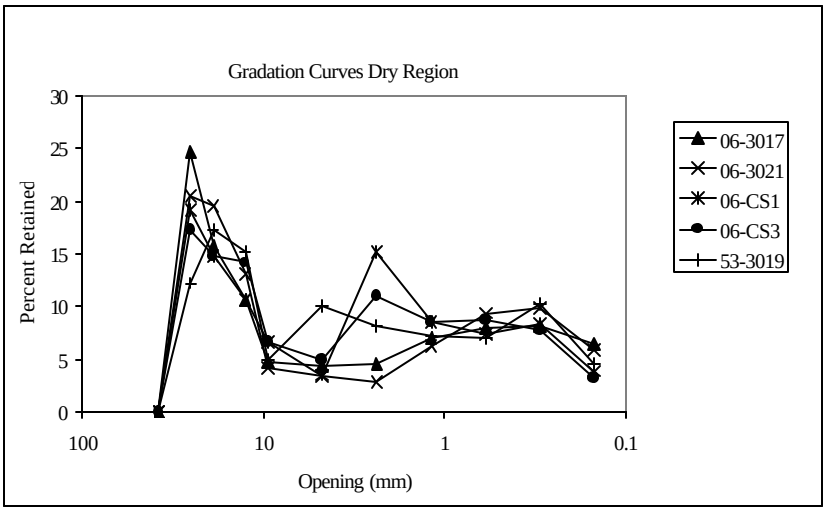

b)

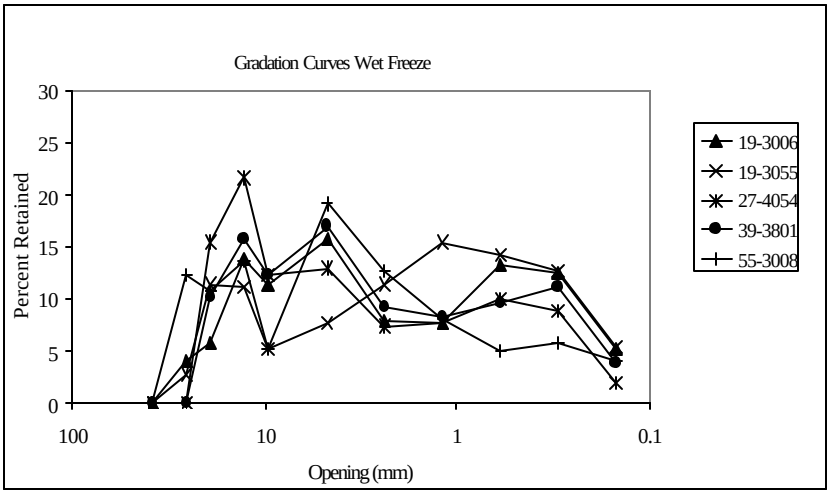

c)

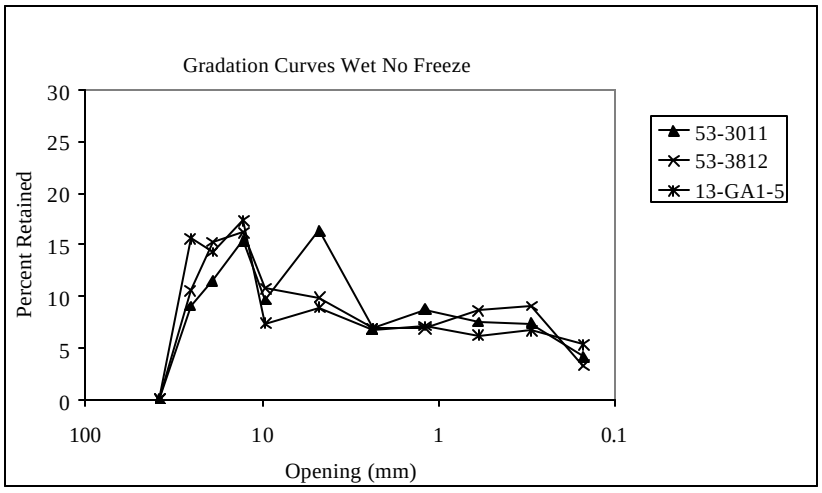

Figure 6.4.2 *Gradation curves for a) the DNF and DF zones, b) the WF zone, and c) WNF zone plotted in terms of percent weight retained.*

CHAPTER 7. DEVELOPMENT OF RECOMMENDATIONS

Project Background

In concrete applications other than pavements (e.g. bridges, columns for high rise buildings, off shore structures, etc.) there is a trend toward using higher strength. The advantages of higher compressive strength for structural applications are well understood. In pavement applications, high early strength concrete is used in special projects where it is convenient to minimize the interruption of traffic flow through congested areas. However, lacking good evidence of long-term performance benefits to be derived from additional strength, pavement engineers have been more reluctant to consider using higher than normal (28 MPa) strength PCC in typical pavement applications. Long-term pavement performance is affected by over 30 primary factors (table 1.4.1) in addition to concrete compressive strength.

It appears that the major benefit in using higher strength concrete is its improved resistance to chemical and physical deterioration as determined from fluid transport properties such as rapid chloride permeability and water permeability. Permeability is known to decrease several fold with increasing compressive strength. Thus, higher strength concrete would be expected to improve concrete spalling resistance at joints. This property is of major interest to SHA's in the wet-freeze regions, where spalling often is the major distress type, and repair and rehabilitation of the joint areas is expensive.

Project Objectives

In order to develop performance based specifications for the use of higher strength concrete in pavement applications, a materials study was undertaken to:

1. Determine the key concrete properties of Portland cement concrete (PCC) found in excellent performing, in-service, pavements (especially at joints.)

2. Determine the key PCC mix and materials characteristics and their proportions, responsible for the levels of the PCC properties.

3. Develop revised mix design procedures in order to provide concrete with the desired properties.

4. Develop prototype concrete mix designs, which will result in the production of concrete for use in pavements that possess these properties.

5. Identify test methods to measure these properties, which can be used for direct or indirect measure of key properties and mix features, needed to monitor the PCC quality level.

Project Tasks

Task A: This phase consisted of identifying the key PCC properties and materials characteristics known to play a role in PCC pavement performance. A synthesis report was developed based on literature review and preliminary analysis of PCC properties and pavement performance obtained primarily from the LTPP database. Based on these findings a select number of pavements were identified for detailed field and laboratory study in order to verify expected trends and/or develop new relations. The literature review is found in the interim report and is summarized in chapter 1.

The LTPP database and other available pavement project information were used to select pavements for detailed field and laboratory data collection and analysis in order to verify and further improve previously established trends. Further, gaps in current knowledge will be addressed. Several primary selection criteria were used such that a range of variables was investigated. These variables were PCC age (primarily PCC pavements older than 20 years), climate, traffic levels, distress levels and types, and strength levels. It was decided to concentrate the efforts on JPCP's.

Fifteen in-service concrete pavements ranging in age between 11 and 51 years, with traffic levels ranging between 3.9 million to over 23 million ESAL's were selected for detailed investigation. The selected fifteen test sections ranged from good to poor performing pavements, where the performance was determined from distress measurements of faulting, transverse cracking, and spalling according to the SHRP methods. The distress development over time was obtained from the LTPP database.

Six of these test sections from the DNF region were located California. These pavements were undowelled JPCP's, and they were all constructed on CTB and had variable joint spacings typical of California pavements. The California test sections were older pavements that at the time of investigation varied in age between 20 and 51 years. Three sections on the experimental test road, near Tracy, which had carried substantial traffic (16 million ESAL's), were selected to investigate the effects of strength and slab thickness on transverse cracking.

Five PCC pavements (four JPCP and one JRCP) were investigated in the WF climate ranging in age from 13 to 28 years. They were all LTPP test sites located in Ohio, Iowa, Wisconsin, and Minnesota. Three had doweled joints, and two were undoweled.

Three LTPP sections were selected from Washington as they had high field compressive strengths ranging from 57 to 79 MPa and had developed low levels of distress. Two sections were in the WNF climate, and one was in the DF climate (53-3019). A low strength and older JPCP in Georgia, located in the WNF climate, was selected, as it was almost distress-free despite its high age (25 years) and its high cumulative traffic (23 million ESAL's).

Task B: This was the data collection phase of the study. Field studies of the 15 pavements were conducted, and samples were tested in the laboratory for various properties. The field and laboratory test procedures are described in chapter 2. Results from the field and laboratory testing are presented in chapter 3 and the appendixes.

Task C: The field and laboratory results were analyzed in Chapters 4 through 6. The PCC properties (and their required levels) were determined, which are responsible for the good performance in JCP's of higher strength. Considering the key PCC properties, materials characteristics and mix design features were identified which produce these property levels.

Work carried out in Tasks A and B provides the basis for development of recommendations. Section 7.1 and 7.2, respectively, present major findings for PCC properties materials characteristics, and trends found with increasing strength. Mix design features and recommended additional design considerations are presented in section 7.3. In section 7.4 the effects of changing concrete properties and material characteristics on prototype mixes are discussed. Section 7.5 discusses additional PCC tests for improved quality and acceptance control.

7.1 Concrete Properties Necessary for Good Long-Term Performance

A major objective of this study was to determine key concrete properties and their effect on pavement performance. The key concrete properties found to relate to pavement performance were transport properties, strength, elastic modulus, coefficient of thermal expansion, drying shrinkage, and entrained air void system.

7.1.1 Long-Term PCC Properties

It is important to realize that long-term PCC properties were investigated. The average pavement age at time of testing was about 25 years. A substantial strength gain has occurred since time of construction as seen from the LTPP database values in table 7.1.1.

Early strength results from eight out of fifteen pavements clearly illustrate that they are regular strength highway concretes at the age of 28 days. As most of these concrete are good long-term performers it is clear that it is not necessary to achieve the long-term mechanical property levels at 28-days. However, it is important that substantial strength gain occurs in the field. This will vary for each cement type and environmental exposure conditions. Typically a Type II cement has higher later age strength gain as compared to a Type I. The environmental exposure conditions causing lower initial curing temperature is beneficial with respect to later age strength, and conditions associated with WF and WNF climates are beneficial in achieving substantial long-term strength gain based on analysis of the LTPP database. See section 5.1.

Table 7.1.1 *Field results of strength and elastic modulus from the LTPP database*

Climate	SHRP ID	State	Age at Testing (Days)	Flexural Strength (MPa)	Age at Testing (days)	Compressive Strength (MPa)	LTPP SURVEY (date)	Compressive Strength (MPa)	Tensile[1] Strength (MPa)	Elastic Modulus (MPa)
DNF	06-3017	CA					11/25/1991	44	5.0	28276
	06-3021	CA	14	3.79	14	25	11/18/1991	44	5.1	21034
	06-7456	CA	14	4.17	14	21	10/19/1995	50	5.7	29138
	CS1*	CA			28	27				
	CS3*	CA			28	31				
	I-10**	CA								
DF	53-3019	WA	14	5.60			4/21/1992	64	6.2	34138
WF	19-3006	IA	14	5.40	28	30		58	3.4	31552
	19-3055	IA	14	4.83	28	35	9/14/1993	59	3.9	23966
	27-4054	MN					2/28/1992	57	4.0	38276
	39-3801	OH	4	3.52	28	29		59	3.2	25862
	55-3008	WI			7	21	2/26/1992	72	4.7	46897
WNF	53-3011	WA	14	4.92			6/2/1992		7.0	36379
	53-3812	WA	14	3.39			6/1/1992		6.2	45690
	GA1-5/6**	GA								

* Data obtained from Caltrans field reports (sections not included in LTPP database)

** Section not included in LTPP database

[1] Most likely flexure strength

7.1.2 Long-Term Spalling Resistance in the WF climate

Spalling is the prevalent distress type in many older pavements in the WF climate region. Spalling is of major concern to SHA's as high severity joint deterioration often require expensive repair. Although, the spalling mechanisms are yet to be fully understood it is generally accepted that spalling is primarily related to durability and to a lesser extent to tensile strength (e.g. Sanadheera and Zollinger, 1995, and Titus-Glover et al., 1999).

A major finding of this study is that good drainage is a prerequisite for improved spalling resistance in the WF climate as drainage has a profound effect on the concrete pore saturation level at the slab base. Regardless of concrete permeability and the quality of entrained air void system, concrete cannot withstand prolonged continuous exposure to water as the capillary pores and air voids will become critically saturated. High saturation levels can initiate freeze-thaw damage. For cases of good drainage, long-term spalling at joints and free edges can be avoided by improving the resistance to water and salt transport using higher strength concrete. The major PCC properties needed for excellent long-term spalling resistance were found to be low permeability, entrained air (6 to 8.5 percent) and non-deleterious aggregates (i.e. F-T resistant, and not susceptible to AAR and sulfate attack).

Transport Properties Needed for Good Spalling Resistance

PCC transport properties such as permeability, chloride ion penetration resistance and water absorption can be critical to performance in freezing environments. In cases of poor drainage, increased PCC resistance to water transport helps avoid or delay critical saturation levels in the concrete and associated freeze-thaw deterioration of the paste. Other factors such as foundation drainage, aggregate soundness, and air void structure are also critical to spalling resistance.

In this study it was found that a PCC property, which was closely linked to transport properties, was compressive strength, irrespective of permeability test method. This is not surprising as both properties are closely tied to the porosity of the hydrated cement paste.

In order to achieve low permeability, a compressive strength level of 45 to 50 MPa is required. The field concretes with w/c ratios below about 0.45 were found to develop low permeability. (i.e. 2000 coulombs from RCPT method, 75×10^{-11} cm/sec using the Florida field water permeability test, and 0.1×10^{-16} m^2 using the Torrent air permeability technique). These levels were met for all of the test sections in the WF climate zone. In the remaining regions higher levels of permeability were observed. See discussions in sections 5.6 and 6.2.

Additional reduction in concrete permeability through increased compressive strength will occur. But for ultimate compressive strengths exceeding approximately 65 MPa the reduction in permeability is minor and would only provide slight improvements from a

durability point of view. A detailed discussion of the test results can be found in section 5.6 of this report.

In PCC's of higher w/c, such as the California, Georgia, and the Iowa PCC's, a through thickness permeability gradients were found. This was attributed to a higher local w/c ratio near the surface based on porosity measurements from mercury porosimetry.

The five concrete pavements investigated in the WF climate all had low permeability, suggesting that this property is important in long-term durability of concrete at exposed areas such as joints, cracks and free edges. One of these concretes, the Iowa LTPP section 19-3006, was selected since it out of all the LTPP test sections developed the highest amount of joint deterioration (i.e. spalling) despite having higher strength. The joint deterioration occurred from the bottom up and was found to be due to critical saturation of the air voids from long-term exposure to high moisture levels. This occurred due to poor drainage conditions creating a "bath-tub:" a slab on a poorly draining CTB and lacking longitudinal edge drains. This shows that low permeability is not sufficient in itself for good performance in a WF climate, and good drainage is of key importance in avoiding prolonged exposure to water.

The other Iowa concrete, LTPP section 19-3055, constructed on a granular base provided better drainage, and in this case its low permeability was sufficient. This pavement was distress free at joints and free edges despite its age (28 years). The Wisconsin pavement, also on a granular base and of an age of 22 years, was found to have higher strength (62 MPa) and very low permeability. Again, excellent PCC durability was found.

PCC Air Void Characteristics Needed for Good Spalling Resistance

Severe climatic exposure conditions such as freeze-thaw cycles combined with high moisture levels at the bottom of a concrete slab play a significant role with respect to PCC joint performance. As stated in ACI 201.2R, only good quality concrete with non-deleterious aggregates and appropriate amount of entrained air can survive freeze-thaw cycles. However, even good quality concrete may suffer freeze-thaw damage if the concrete is at a high level of saturation as observed for the Iowa test section, 19-3006. This study found that good to excellent freeze-thaw durability had been achieved when typical freeze-thaw requirements pertaining to the air void system and aggregate soundness were met. In most severe freeze-thaw climates (annual precipitation > 500 mm, annual freeze index > 150, and annual freeze-thaw cycles > 80), the characteristics of freeze-thaw durable PCC pavements were entrained air of 6 percent, spacing factor of less than 200 microns, specific surface area greater than 24 mm^2/mm^3, and non-deleterious reactive coarse aggregates. See section 5.7.

The five concrete pavements in the WF region are expected to be freeze-thaw durable, with the Ohio section, 39-3801, and the Iowa section, 19-3006, falling slightly below the recommended limit on minimum specific surface area. For the five concretes investigated the air content varies between 6.2 and 8.3 percent by volume. The calculated air void spacing factor varies between 51 and 178 microns, and the specific

surface area of air voids (a measure of the size of the air voids) varies between 22.4 and 40.6 mm^2/mm^3.

As discussed above the Iowa test section, 19-3006 has suffered from severe joint deterioration. Petrographic examination according to ASTM C 457 on the intact upper half of a core taken from a deteriorated joint showed that the smaller air voids (< 75 microns) were lined with a white crystalline deposit, which had rendered these voids ineffective. Thus, the minimum freeze-thaw requirements for both the spacing factor and the specific surface area were not met. The spacing factor was 221 microns and the specific surface area was 17.6 mm^2/mm^3. The concrete away from the joint had excellent air void characteristics with spacing factor of 102 microns, air content of 8.3 percent, and specific surface area of 22.4 mm^2/mm^3.

In climates outside the WF region, transport properties are not as critical as long as the aggregate are non-deleteriously reactive and the concrete is not subjected to prolonged exposure of high internal moisture levels activating deterioration mechanisms such as AAR. In this study concretes known to have AAR and other chemical distress were omitted from further investigation.

Mechanical related spalling distress may have been avoided due the associated increase in tensile strength with higher compressive strength PCC. However, this component of spalling is not fully understood, but in general higher long-term flexure strength is beneficial.

7.1.3 Improved Resistance to Fatigue Cracking

Transverse cracking in JPCP's can be the result of fatigue effects causing either bottom up or top-down cracking. Higher tensile strength is not required for excellent long-term performance in any climate because slab thickness is the effective parameter in controlling the fatigue resistance. The Iowa section 19-3055 located in the WF climate, and Georgia section 13-GA1-5 located in the WNF climate, had the lowest tensile strength in this study, yet they were found to have excellent long-term performance characteristics. These pavements were 28 and 26 years respectively at the time of this investigation, and the Georgia pavement had carried significant truck traffic (23 million ESAL's).

However, the concrete tensile strength affects the stress/strength ratio, which dictates the fatigue life. Therefore significant improvement in mid-panel transverse cracking resistance is expected by increasing the PCC's tensile strength. However, improved fatigue resistance can also be achieved by increasing slab thickness. It is estimated that a 25 mm (1 in.) increase in thickness from 225 mm (9 in.) to 250 mm (10 in.) will have the same effect as flexure strength increase of 0.70 MPa from 4.8 to 5.5 MPa (e.g. Yu et al, 1998). Each, of these alternatives may eliminate fatigue cracking as the failure mode provided that loss of support from pumping erosion does not occur. Other factors such as slab length and whether a stabilized base is bonded or unbonded have significant impact as well.

The high strength Washington JPCP, section 53-3812, on granular base fits the class of a high tensile strength (6 MPa in flexure) concrete, moderate slab thickness (225 mm), with significant traffic (12.8 million ESAL's) and no transverse cracking. The Wisconsin high strength JPCP section 55-3008, also on a granular base, has high tensile strength (6.1 MPa flexure) and consists of a 50 mm thicker slab (277 mm) and similar traffic (15.2 million ESAL's). Also, no transverse cracking has developed despite substantial slab settlement. It appears that higher tensile strength and greater thickness have played a major factor. Both these concretes were found to have lower w/c ratio (0.35 to 0.40) than is typically used for highway concrete.

Elastic modulus of concrete has a pronounced effect on the pavement deformation and curling/warping stresses. As elastic modulus increases the pavement slab deformation due to wheel loading decreases. However, curling/warping stresses increase proportional to concrete elastic modulus. A slightly increasing load-related stress occurs with increasing elastic modulus.

A strong correlation was found between elastic modulus and compressive strength based on field cores. The elastic modulus ranged from approximately 23,000 to 45,000 MPa while the compressive strength ranged from 33 to 75 MPa. See section 5.4. These results show that the elastic modulus increase is almost proportional to the increase in compressive strength, which was not expected based on the ACI-363 equation. Consequently, curling/warping stresses are more significant with increasing strength.

Top-Down Transverse Cracking Associated with Loss of Slab Support at Joints from Curling-Warping and Pumping Erosion

In the case of loss of support from curling-warping or pumping erosion, the critical slab loading position is at the transverse joint. In this case, axle loading near joint and corner of the slab causes maximum tensile stresses in the top of the slab at some distance away from the joint (Darter et al., 1995, and Khazanovich et al., 2000).

Over time, the loss of support due to pumping erosion combined with curling-warping phenomena creates large upward slab curvature and increased joint deflection during joint loading. In such event, greater slab thickness is an effective means of improving bending resistance and controlling transverse cracking (Darter et al., 1995).

Stress predictions by Khazanovich et al. (2000) based on finite element analysis show, that top-down transverse cracking can occur starting at the midslab outer edge for combinations of high axle loads at joints (i.e. tandem axle at a joint and a single axle at the other joint) and high built-in upward curvature. This loading condition locks both slab ends from rotating. This is especially a problem in cases where the axle spacing of a truck matches the joint spacing. This loading combination prevents slab rocking in short jointed slabs. The analysis showed that curling effects significantly influences top tensile stresses. For a given temperature gradient through the slab, the curling stress increases proportionally to the coefficient of thermal expansion and elastic modulus. Other factors, which have significant effect, include joint spacing and foundation stiffness.

When comparing a 75MPa concrete with a 33 MPa concrete, it was noted that the curling stresses predicted for the same temperature gradient was nearly 100 percent. This increase was attributed from the elastic modulus increasing from 24 to 47 GPa. Higher curling stresses would also arise from increased coefficient of thermal expansion (CTE). For the Tracy, California experimental project the high strength section had about a 40 percent increase in CTE as compared to the control concrete due to the increase in cement and paste content.

Figure 7.1.1 illustrates the permanent upward slab-base gap from curling-warping and pumping erosion effects for the Tracy experimental sections in California. The deflection profile from curling-warping is obtained from analysis of FWD slab deflection profile measurements in steps of 0.6 m (2 ft) in the traffic direction along the outer wheel-path (i.e. 0.6 to 0.9 m from outer edge). The profiles are shown for two consecutive slabs starting before the joint of the first slab and ending just after the second joint of the second slab. The analysis is based on the deflection profile shown in section 4.3 assuming that the midslab is in contact (i.e. reference point) and that the deflections at the joint, for a flat slab, would be similar at the deflections at midslab.

The upward curved slab shape is consistent with surface profile measurements as illustrated in chapter 4. The upward joint and crack deflection is similar for the three sections (CS 1, CS3 and 06-7456) varying between 50 and 150 microns. These results were obtained during a clear and sunny day October 29 and 30, 1998 between 9 AM and 1:30 PM. During that time the surface temperature increased from about 15 to about 28 °C while the deflection profiles remained nearly constant as seen for the thickened section, which was tested twice during this time period. This is evidence that a permanent gap exists between the slab and the base caused by combined curling-warping and base erosion. Base erosion was confirmed from cores taken at the joint and away from the joint as illustrated for the high strength section (CS3). See figure 7.1.2.

The results discussed in chapter 4 follow the expected trend from pumping effect on slab shape. It gradually curves upward towards each approach joint and falls off sharply on the leave joint side. This is consistent with buildup of fines on the approach joint side. At the same time, a sharp downward curvature on the leave side is consistent with expected effects from base erosion and with fault measurements. Further, these results suggest that slab cracking is predominantly expected at a distance of about 1.5 to 2.5 m (5 to 8 ft) from the leave joint, which is also in agreement with the observed crack location as discussed in section 4.3.

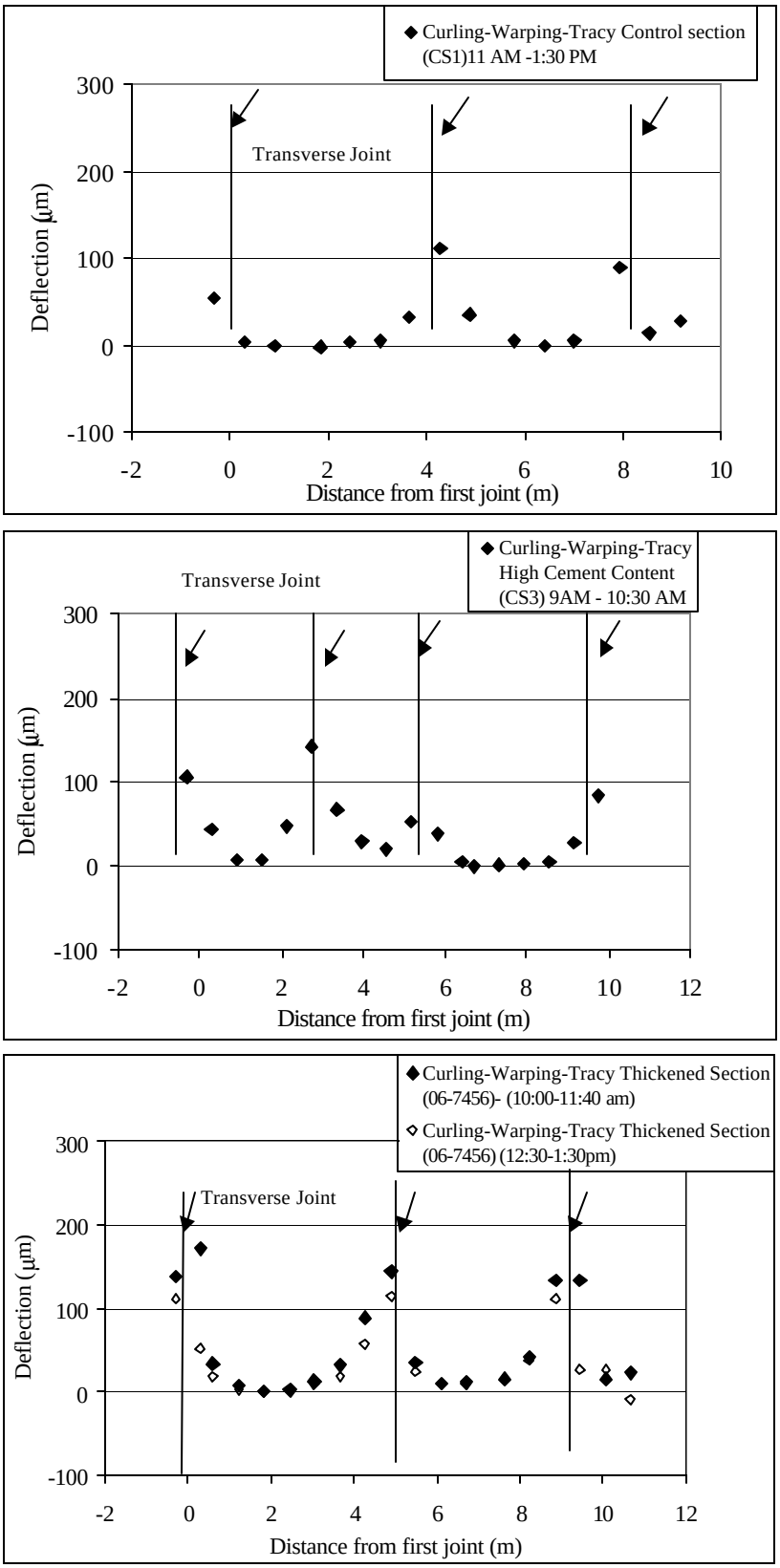

Figure 7.1.1 *Deflection profiles due to curling-warping of from the Experimental test road at Tracy, California.*

Figure 7.1.2 *Eroded CTB at joint. Decreasing erosion moving away from joint (left to right). Experimental test road at Tracy, California, with higher cement content.*

Moisture warping is also believed to have increased faulting, loss of slab support, and accelerated transverse cracking for the Iowa section 19-3006. The moisture warping has developed due to a poorly draining CTB base. The Iowa section had corner breaks at nearly every slab corner, typical for extensive loss of slab support.

The importance of good subsurface drainage in avoiding upward curvature from high moisture content at slab base near joints was investigated by Poblete et al. (1990). Also, Hveem, in a Caltrans report dating back to 1949, used profilograph measurements to demonstrate that vertical movements at slab ends from temperature and moisture differences in JPCP's increase over time. As a result the slab ends are curled or warped upward most of the time creating non-uniformity of contact and slab support. This mechanism causes pumping related distress when free water accumulates beneath the ends of a slab.

Darter et al. (1995) predicted using finite element analysis that slab thickness is a major factor in reducing the top tensile stress in cases of upward slab curvature and loss of slab support from curling-warping. This would explain why the thicker section (06-7456) of the Tracy experimental project has not developed transverse slab cracking despite similar losses of slab support as the other Tracy test sections.

The other extreme case of upward curling/warping is a slab on a soft foundation (i.e. low CBR subgrade), granular base, and undowelled joints. The Wisconsin section 55-3008 had developed extreme permanent upward curvature and joint faulting, but with only one slab cracked within the 153 m test section. This suggests that a PCC slab can "float" without breakup from traffic loads if the foundation is soft enough to maintain full support from curling and warping effects. Except for faulting, no other distress was found in the Wisconsin section, which is attributed to combinations of slab thickness (277 mm), flexure strength (6 MPa), excellent freeze-thaw resistance, durable aggregates, and low permeability (<1000 Coulombs RCPT).

The Georgia section was a lower strength concrete and dowelled JPCP on CTB and ATB. It was an excellent performer as it had not developed pumping erosion and associated upward curling. This suggests that the slab and base act together as a monolith, similar to German pavement design.

In summary, in cases of good design and construction practices, along with avoidance of loss of slab support, lower strength concrete can produce excellent long-term performance. However, if loss of support (pumping erosion and curling-warping) becomes significant, then higher strength PCC and/or greater slab thickness may be needed to control transverse cracking.

Premature Mid-Slab Transverse Cracking

Premature transverse cracking in PCC pavements is often associated with combinations of higher temperature at the time of construction and unfavorable environmental factors. These factors can affect the rate of hydration, strength gain, and moisture loss.

Within the first week after construction, rapid development of PCC properties occurs. These properties include coefficient of thermal expansion, elastic modulus, creep, shrinkage, and tensile strength occurs. These properties combined with environmental exposure conditions, timing of joint sawing, and slab restraint are important in avoiding mid slab transverse cracking. Creep and stress relaxation properties are significant during this time period. Beyond the first week the stress relaxation property is considerably reduced.

Concrete with a higher coefficient of thermal expansion and a higher elastic modulus is more sensitive to thermal gradient stresses known as curling stresses and moisture induced gradients from combined surface drying and/or high moisture level at the slab base at joints. Moisture warping develops over time, while slab deflections from curling follow a daily and seasonal cycle, with the maximum upward curvature at joints and corners (leading to increased joint deflection during heavy vehicle loading) occurs in the spring and summer at early morning hours when maximum thermal gradients are present (Hveem, 1949). Curling-warping, combined under certain unfavorable conditions, causes a permanent upward curved slab shape at the joints and corners. This together with water trapped at the slab-base interface from poor drainage and heavy vehicle loading starts the pumping mechanism resulting in joint faulting, corner breaks, loss of joint support, and eventually slab cracking. To combat pumping-erosion (pumping of fines) California adopted the practice of stabilizing base layers, hoping they would be erosion resistant. Hveem and Tremper (1957) concluded that concretes with reduced CTE and drying shrinkage potential are favorable for California weather conditions (warm and dry) leading to less upward curvature and improved long-term performance.

Additionally, concrete having higher CTE will undergo larger initial joint movement leading to increased crack width at joints. For certain coarse aggregate characteristics (soft aggregate and smaller top size) this can result in reduced load transfer efficiency (LTE) associated with aggregate interlock.

No correlation could be found between CTE and mechanical properties or aggregate type, which is probably due to the major effect that the cement paste content has on the CTE of concrete. CTE of the cement paste is 1.5 to 2 times that of the aggregate (FHWA LTPP-Program Reference Guide, 1996). In addition, variations in CTE can be significant within each aggregate type depending on mineral composition (Zoldners, 1971). CTE for dolomites ranges from 7.0 to 10.0 x $10^{-6}/^{o}$C, whereas granites and gneiss range from 6.5 to 8.5 x $10^{-6}/^{o}$C. These aggregate types were found in several concrete pavements for this project.

CTE values for concretes in California with cement contents of 307 kg/m^3 were about 9.8 x $10^{-6}/^{o}$C, increasing to 13.7 x $10^{-6}/^{o}$C for the higher cement content (418 kg/m^3) mix used at the Tracy test Road section 06-CS3. A 40 percent increase in cement content has resulted in about a 40 percent increase of CTE. Also, as seen from table 3.3.1, section 06-CS3 had a 10 percent higher elastic modulus (34,679 MPa) compared to the control concrete 06-CS1 (31,429 MPa).

The drying shrinkage property could not be determined on older field concretes as this property is irreversible for long-term environmental exposure. As high quality aggregates were found in the California concretes, and because the aggregate volume fraction was similar (75 percent of concrete), it is reasonable to assume that ultimate drying shrinkage has been similar for the control section (06-CS1) and the thickened section (06-7456) on the Tracy Test Road. However, the higher cement content concrete (06-CS3) is estimated to have substantially increased drying shrinkage as well as an increased CTE, although the actual amount of drying shrinkage is impossible to estimate as it depends on several factors (ACI 209). Based on the classical Pickett relation for aggregate volume effect on concrete shrinkage (Pickett, 1956), the higher cement content concrete (06-CS3) is estimated to have about 20 percent higher ultimate shrinkage than the control concrete 06-CS1.

Increased CTE and drying shrinkage are factors believed to have played a major role in the development of premature transverse cracking for the higher strength and higher cement content section (Tracy experimental project.) Caltrans distress survey showed that within one year, 42 percent of these slabs were cracked (Wells, 1993), while no cracking had occurred in the control concrete section of similar thickness or in the thickened section. The cumulative traffic at that point was about 0.31 million ESAL's. The number of cracks in this section remained constant until surveys stopped in 1990, at which point the estimated total traffic was 8.23 million ESAL's. During the period between one year after construction (1972) and 1980, 25 percent of the slabs in the control section (CS1) had developed transverse cracking. Number of cracks for both sections remained constant until 1990.

These results suggest that transverse slab cracking in the higher strength section (containing higher cement content) occurred due to restraint against contraction from thermal and drying shrinkage, and possibly late sawing, or curing problems or a combination of these factors. Premature distress is consistent with the higher CTE and shrinkage associated with higher cement and paste content of the mix.

7.1.4 PCC Properties Needed for Good Long-Term Resistance to Joint Faulting

This study findings show that joint faulting is a consequence of pumping erosion and/or slab settlement on soft foundation. Amount of joint faulting is, for a given climate and base/foundation type, primarily affected by heavy vehicle loading (i.e. ESAL's). See chapter 4 for more detail. These findings are in good agreement with a recent study by Titus-Glover et al., 1999, based on a comprehensive analysis of the LTPP database. It is apparent that PCC properties and materials characteristics play a secondary role through factors, which affect the rate of pumping (i.e. aggregate interlock and upward curvature from curling/warping).

Observations can be made regarding long-term aggregate interlock in the presence of upward curled joints based on the California sections, as they were undowelled. One site worth noting is the 51 year old test section on westbound I-10, in San Bernadino Co., near Los Angeles, where joint load transfer values were high (78 to 95 percent). This concrete had large gravel-like aggregates with a maximum size of 50 to 62 mm. This suggests that some types of coarse aggregate can improve LTE as they enhance the load-bridging action across a crack (e.g. Colley and Humphrey, 1967; and Nowlen, 1968; and Abdel-Maksoud et al., 1998). However, high variability in LTE was observed for the Tracy test sections probably associated with high variability in joint faulting and joint crack width from slab to slab.

7.2 Concrete Materials Characteristics Required to Produce the Above PCC Properties and Their Levels

PCC material characteristics and their required levels for achieving the necessary levels of PCC properties were determined. The key PCC material characteristics were w/c ratio, cement type and content, and coarse aggregate characteristics. The following discussions describe these factors in terms of the observations of this study.

7.2.1 Water-Cement Ratio

Water-cement ratio is the key mix characteristic controlling concrete strength (tensile and compressive). In most cases, the range was found to be typical of regular strength concrete pavements. See table 6.1.1. Using the LTPP database values and estimated w/c ratio values from water absorption tests, the w/c ratio ranged from 0.35 to 0.46 in the WF region, with an average of 0.42. The California PCC's located in the DNF region and the Georgia PCC in the WNF region had considerably higher w/c ratios. A range of about 0.46 to 0.67 was observed. The average w/c ratio for these concretes was 0.52. The WNF zone concretes from Washington (53-3812 and 53-3011) have low w/c ratios of about 0.40.

Lower w/c ratios were also associated with improved transport properties in the concretes. The data here suggests that one avenue for achieving high durability is by using a low w/c ratio. This is particularly valuable in the WF zone, where freeze-thaw resistance is needed. In the other climatic zones low permeability levels may be desired in order to protect the PCC from chemical deterioration.

As discussed in section 7.1, in the warm regions, PCC's with higher w/c ratios were found to have a permeability gradient (highest permeability at the slab surface), likely due to higher w/c ratios at the top of the slab compared to the bottom of the slab. Thus, these concretes are more exposed to moisture penetration near the pavement surface. This is discussed in detail in section 5.6. Lower w/c ratio concretes were seen to be both less permeable and more uniform through their thickness.

In chapter 6 it was shown that the compressive strength correlates well with w/c ratio despite the large differences in climate, and aggregate type and content. As seen in figure 6.2.1, an R^2 value of 0.80 was observed using regression with a simple power-curve. The w/c ratio was also related to elastic modulus and splitting tensile strength. However, the correlations were not as strong for these properties, as the R^2 values were below 0.40 from power-curve regressions.

7.2.2 Cement Type and Content

Not surprisingly, Type II (lower heat of hydration) Portland cements were found in warmer climates such as California, Georgia and even Washington State. The test sections in the WF climate used primarily Type I cements. The cement contents in these studied sections ranged from 252 to 418 kg/m^3 and averaged 328 kg/m^3.

The three highest compressive strength sections in this study (53-3812, 55-3008 and 53-3011) had similar cement contents, 335 kg/m^3, which is typical for pavement concrete. This indicates that higher strength can be achieved with typical mix proportions. The higher strength was obtained from combinations of slightly lower w/c ratio, excellent curing conditions, and good aggregates.

Many SHA's have traditionally designed pavements for a given slump, and have used cement content as the mechanism for increasing strength. A typical concrete mix contains 5.5(California) to 6 sacks (Michigan) of cement per cubic yard of concrete (307 to 335 kg/m^3). Often higher design strengths are obtained by increasing the cement content substantially. This was observed for the 7.5 sack (418 kg/m^3) mix used in the Tracy, California test section 06-CS3. While this approach is indeed effective in raising the strength, it may increase the tendency to cracking from increased CTE and shrinkage properties, as was the case in this section.

7.2.3 Coarse Aggregate Characteristics

In this study, coarse aggregate characteristics were found to significantly impact concrete properties in several areas, including aggregate interlock, fracture properties, and concrete durability to environmental attack.

Three different coarse aggregate groups were observed in the studied concretes: silicate rock gravel, dolomite/limestone, and crushed silicate rocks. The dolomite/limestone aggregates were used exclusively in concretes from the WF zone, most likely because of their local availability (test sections 19-3006, 19-3055, 27-4054, and 55-3008). The Ohio section 39-3801 contained a variety of coarse aggregate types, ranging from silicates and sandstone to limestone. The Georgia sections, 13-GA1-5 and 1-6, contained crushed granitic to granodioritic aggregates while the California and Washington State concretes mainly contained gravel of silicate rocks (test sections 06-3017, 06-3021, 06-7456, 06-CS1, 06-CS3, 06-I-10, 53-3019m 53-3011, 39-3801, and 53-3812).

Petrographic analysis showed that the aggregates had primarily remained chemically inert during placing of the concretes and their subsequent use. However, minor ASR was occasionally observed in the fine aggregate, particularly in Iowa section 19-3055, and Ohio section 39-3801. In the coarse aggregates ASR was rare and was only observed in Washington section 53-3019, and Ohio section 39-3801. It is concluded that high quality aggregates that are not deleteriously reactive (i.e. non reactive and freeze-thaw resistant) are important for long-term performance, particularly in aggressive environments like the WF climate zone.

The coarse aggregate gradations were very similar in the California concretes, which were significantly coarser than the gradations encountered in the other sections. The nominal maximum aggregate size was typically 38 mm in these sections with one section, 06-I10 as high as 62 mm. In general, these older concretes had well-graded aggregates of larger maximum particle size than commonly found in modern pavements. The nominal maximum aggregate size for the other studied sections ranged from 25 mm for PCC's in the WF climate to 38 mm in concretes outside the WF region. The smaller aggregates used in the WF region are consistent with D-cracking considerations. The gradations generally fell within the gradation limits of ASTM C 33.

It is noteworthy that the California combined (coarse and fine aggregate) gradations have 19 to 25 percent retained on the 25 mm sieve, which is beneficial for maintaining high load transfer through aggregate interlock. LTPP test section 55-3008 in Wisconsin had 12 percent retained on the 25 mm sieve, which is more than typically observed in PCC's in the WF region. This section is heavily faulted. It is speculated that large faulting and crack widths associated with slab settlement overshadow the effect of improved load transfer from larger aggregate size. Other factors such as the slabs being undoweled have contributed as well.

The presence of dowels and stiff foundations have been effective in maintaining high load transfer for the Iowa section 19-3006, and the Minnesota test section 27-4054, despite having only 0 to 4 percent retained on the 25 mm sieve.

The California PCC's were found to have excellent fracture resistance related to their gravel characteristics (strong and large size). The 51 year old California test section 06-I10, is an example of a low distress pavement with high traffic level (>16 million ESAL's), consisting of lower compressive strength (37.6 MPa) PCC with good splitting tensile strength (4.0 MPa). The large and strong gravel mix (top size of 50 to 62 mm) has ensured excellent load transfer (88 percent average) at joints and cracks and high fracture resistance (230 N/m). See table 4.2.1 and table 5.5.1.

7.3 Mix Design Procedures for Improved Long-Term Performance

Additional design considerations are proposed in order to improve the long-term pavement performance in terms of spalling and premature cracking. These distresses are categorized as durability issues related to environmental loading. The additional durability design considerations can be incorporated into current mix design procedures for proportioning normal concrete mixes.

This study also confirms several of the mix design considerations on materials related factors, which influence the durability of concrete pavements, resistance to environmental as well as traffic loading (e.g. Forster, 1997). Table 7.3.1 lists the mix and material factors confirmed in this study to significantly affect PCC properties. The mix factors were aggregates, cement, additives, and w/c ratios. This study focuses on the factors related to long-term PCC performance, and therefore table 7.3.1 does not elaborate on factors related to PCC workability, constructability, and economy.

Table 7.3.1 *Mix and material factors affecting PCC properties observed herein*

Mix Categories	**Material Characteristics**	**Affected PCC Properties**
Aggregates	Gradation, Maximum aggregate size	Elastic modulus, drying shrinkage (%paste), fracture resistance, brittleness, aggregate interlock
	Soundness	AAR resistance
	Strength (hardness)	Fracture resistance, brittleness, aggregate interlock
	Type	Coefficient of thermal expansion
Cements	Content	Coefficient of thermal expansion, strength, drying shrinkage
	Type	rate of strength gain
Additives	Air entraining	F-T resistance of the paste
w/c	level of:	ultimate strength, permeability, and elastic modulus

7.3.1 Mix Design Considerations for Improved Durability

Resistance to spalling is improved with low PCC permeability. Current design procedures (e.g. ACI 211) typically enforce a maximum w/c ratio of 0.45 and durable aggregates when the PCC is subjected to severe environmental loads (e.g. WF climates). This study found that in addition to the w/c ratio requirement that the level of permeability must also be specified and determined.

Further, this study found that several PCC's in the dry regions had a significant permeability gradient through the slab thickness with the highest permeability at the slab surface. Permeability gradients are believed to be caused by the tendency towards a more porous concrete near the surface when the mix w/c ratio is about 0.40 or greater. A more uniformly low permeability concrete was found for w/c ratios of about 0.40 or less.

In some cases a high early strength mix design is desired. It is common practice by SHA's to increase the cement content in order to achieve high early strength. Although it is generally known that such mix designs will lead to concrete with higher thermal stresses from heat of hydration as compared to regular cement contents. These concretes were found to have increased CTE, which further increases their early age (first 72 hours) cracking susceptibility. Later on drying shrinkage adds to these stresses, and combined effects can lead to premature cracking.

High early strength can also be obtained by lowering the w/c ratio rather than increasing the cement content. The reduction in w/c ratio to obtain 28-day strength values of 30 – 40 MPa can be achieved using combinations of water reducing admixtures and mineral additives, while maintaining typical cement contents (279 to 335 kg/m^3) (PCA 1995).

7.4 Prototype Concrete Mix Designs for Good Long-Term Jointed Concrete Pavement Performance

In section 7.3 modifications to the design considerations and procedures were discussed based on the mix and material characteristics needed for long-term performance. This section builds on the findings regarding PCC properties and the materials characteristics required to achieve excellent pavement performance, as presented in sections 7.1 and 7.2 respectively. In combination with the mix designs discussed in section 6, it is now possible to provide recommendations for prototype concrete mix designs for improved durability (i.e. spalling and premature transverse crack resistance) and improved structural capacity (i.e. improved fatigue resistance).

It is paramount that good practices must be followed during construction to ensure that the concrete mix designs will provide the intended improvement in long-term performance. The interaction of the concrete with the environment and any loading at early ages must be considered. As an example, heat generated during hydration must be estimated and combined with the effects of expected environmental conditions. Hot weather concreting requires special consideration, and changes in mix proportions may become necessary to prevent excessive internal temperatures, thermal gradients, and thermal stresses.

If these and other factors during the early life of the concrete are not considered, damage may occur that will prevent the concrete from attaining the intended design properties or design life.

Prototype mix designs, which are expected to meet these improved durability and structural capacity criteria are presented in tables 7.4.1 and 7.4.2. They are divided into two different climate groups (WF/DF) and (WNF/DNF). With the exceptions of the Washington concretes, they are divided into normal strength PCC and high strength PCC, as the mix designs were found to be typical for normal strength concrete (i.e. design strength less than 41.4 MPa (6000 psi)). These concretes were found to have ultimate in-service compressive strengths of up to 75 MPa and estimated flexure strength of about 6.0 MPa. Their w/c ratios were below 0.40. These concretes appear to have high resistance to spalling (despite low air content) and fatigue cracking.

Table 7.4.1 *Prototype mix designs for durable PCC pavements*

Climate Region	**Range of W/Cementitious ratio**	**Range of Cementitious Content (kg/m^3 (lb/cyd))**	**Cement Type**	**Minimum Air content in Hardened concrete (%)**	**Range of Coarse Aggregate (kg/m^3 (lb/cyd))**	**Range of Fine Aggregate (kg/m^3 (lb/cyd))**	**Target C/F ratio**
Regular Strength Mix Designs:							
WF/DF	0.40-0.45	≈335 (564)	I/IA or equivalent	6.0	990 -1280 (1669-2159)	564-839 (951-1407)	1.6
WNF/DNF	0.40-0.60	279-335 (470-564)	II/IIA or equivalent	No requirements	990 -1280 (1669-2159)	564-839 (951-1407)	1.6
High Strength Mix Designs:							
All	0.35-0.40	335-418 (564-705)	I A/II A or equivalent	6.0 in WF/DF	990 -1280 (1669-2159)	564-839 (951-1407)	1.6

Table 7.4.2 *Ultimate PCC properties for good long-term jointed concrete performance by climate region*

Climate Region	Range of Ultimate Compressive Strength (MPa)	Range of Ultimate Flexure Strength Range (MPa)	Range of Ultimate Elastic Modulus (GPa (10^6 psi))	Maximum RCPT Rating[1] (Coulombs)	Recommended Maximum CTE ($x10^{-6}$/°C)
Regular Strength Mix Designs:					
WF/DF	45-60	5.0-5.5	27.6-35 (4.0 - 5.0)	1000-2000 or low	10
WNF/DNF	35-60	4.5-5.5	25-35 (3.6-5.0)	2000-4000 (Moderate)	10
High Strength Mix Designs:					
	60-75	5.5-6.0	35-47 5.0-6.8)	100-1000 (Very low)	10

[1] If mineral additives such as fly ash or ground granulated slag are used, the water sorption test is recommended as well

7.4.1 Prototype Concrete Mix Designs and Ultimate PCC Properties for Improved Performance in the WF/DF Region

A major finding of this study was that regular strength concrete mixes are sufficient to provide good long-term spalling resistance in highway concrete in WF climates. A w/c ratio of about 0.45 or less is sufficient as the PCC will develop low long-term permeability, and a compressive strength of about 45 to 50 MPa. The minimum air content is about 6.0 percent, and the aggregate must be sound with respect to freeze-thaw and other durability attack.

Improving Performance by Increasing Strength

Increased 28-day strength above the typical design value of about 4.5 MPa (650 psi) may require combinations of lower w/c ratio, higher cement content, and water reducers. High strength concrete mixes with a 28-day compressive strength of 41.4 MPa (6000 psi) or higher typically contain higher than normal (335 kg/m^3) cement and paste contents. This places special demand on construction and curing methods to avoid early cracking.

Lowering w/c ratio

Lowering the w/c ratio to about 0.40 provides a more homogeneous concrete. This reduces the permeability gradient through the concrete thickness, which can leave the exposed surface vulnerable to environmental attacks (e.g. improving salt scaling resistance).

Lowering the w/c ratio has added benefits in terms of increased long-term fatigue resistance, as these concretes are expected to reach and exceed 5.5 MPa in ultimate

flexure strength. This corresponds to an additional 10 percent increase in long-term flexure strength as compared to a 28-day design value of 4.5 MPa (650 psi).

Adjusting Cement Type and Content

In the WF region it is adequate to use a Type I Portland cement, and a mix containing about 335 kg/m^3 (6 sack mix) cementitious material.

To achieve a higher than normal strength level (typically 4.5 MPa in flexure) it may be necessary to increase the cement content beyond the typical range of 300 to 335 kg/m^3 found in this study. The 418 kg/m^3 (7.5 sack) cement content mix of the high strength Tracy test section 06-CS3 had a reported 28-day compressive strength of 31 MPa, compared to 26 MPa for the 307 kg/m^3 (5.5 sack) cement content of the control concrete 06-CS1 (Spellman et al., 1973).

The cement contents and w/c ratios for an experimental JPCP in Detroit and the test sections from this study agree well with the PCA guidelines for required cement content and w/c ratio to achieve the expected strength levels (PCA, 1995). As an example, for air-entrained concrete containing Type I cement and regular cement content (i.e. about 335 kg/m^3), a 28-day compressive strength of 30 to 35 MPa can be expected for a 0.40 w/c ratio.

It must be noted, however, that increasing strength by increasing cement content may be detrimental to performance with respect to transverse cracking and faulting. Increasing cement content can significantly increase concrete shrinkage and CTE properties. These higher PCC levels can lead to transverse cracking from curling/warping due to loss of support, and/or loss of load transfer from excessive joint opening.

Mineral Additives

Due to the age of the studied sections, none contained mineral additives like fly ash or blast furnace slag. The use of mineral additives was therefore not within the scope of these investigations. However, modern mix designs frequently contain mineral additions. There is a wealth of literature on the benefits and detriments of mineral additives. Generally, though, it has been the experience of the investigators that mineral additives can be used as a partial replacement of cement to provide benefits such as added protection against chemical attacks like ASR, and reduced heat development during hydration. Excellent strength and low permeability can be achieved through the addition of mineral additives.

Minimum Requirements to Air Void System

For severe exposure conditions, ACI 211.1-91 recommends that the minimum total air content of concrete with a maximum aggregate size of 25 to 38 mm be in the range of 5.5 to 6 percent. Furthermore, air void spacing factor of less than 200 microns and specific surface area of air voids of 24 mm^2/mm^3 or greater are recommended. The air-entrained concretes from the WF climate region in this study all fall within these limits. These properties have sufficiently protected the studied pavements from freeze-thaw damage. Except in one case, where long-term saturation rendered the air void structure ineffective.

Aggregate Characteristics to be Considered in All Climates

Aggregate Soundness

Aggregate soundness is imperative for durable concrete. Aggregate soundness is the aggregate's resistance to all aspects of weathering and typically encountered chemical reactions. The weathering aspect includes heating and cooling, wetting and drying, and freezing and thawing. The chemical durability concerns reactions such as AAR. Thus aggregate soundness is important in all climates.

Aggregate Content, Size, and Gradation

In addition to aggregate soundness, the characteristics of the aggregates that have an important influence on proportioning concrete mixtures are particle size and distribution, content, and the shape and surface texture (PCA, 1998).

The aggregate volume content was found to be about 70 percent. This is consistent with low shrinkage. In addition, the weight ratio of coarse to fine aggregate was typically close to 60 percent coarse and 40 percent fine aggregates (C/F ratio about 1.6). These ratios are typical mix designs designed for pavements according to ACI 211 and PCA (1998).

This study showed that the older and higher strength PCC's contained larger maximum aggregate size than is typically used in today's conventional highway concrete. A larger top size has several advantages. First it reduces water and paste demand, leading to less drying shrinkage. The general guidelines for cement and water content versus maximum aggregate size can be used. As an example, an increase in maximum aggregate size from 25 to 50 mm generally results in a 15 percent reduction in cement and water content. For a 25 mm maximum size and 75 mm slump, a 335 kg/m^3 is sufficient for a non-air entrained concrete. For the concretes with the maximum nominal aggregate size of 38.1 mm and no air-entrainment, approximately 307 kg/m^3 of cement is required for a 75 mm slump concrete. These cement content levels were generally observed in this study for the test sections in California (06-3017, 06-3021, 06-7456, 06-CS1, and 06-I10). Second, tougher and larger sized aggregates provide better aggregate interlock and load transfer at joints and cracks for crack bridging. Furthermore, lower cement and paste content reduces CTE, and thus reduces joint crack width. Smaller crack width is important for maintaining long-term load transfer for any aggregate type and size.

It should be noted, however, that in severe climates maximum aggregate size may need to be limited for durability reasons. Increasing aggregate size can increase susceptibility to durability attacks, particularly for marginal quality aggregates.

Both fine and coarse aggregates in this study were found to be well-graded, and typically within ASTM C 33 grading limits. Therefore existing guidelines for aggregates according to ASTM C 33 and ACI 211 are necessary and adequate.

7.4.2 Prototype Concrete Mix Designs and Ultimate PCC Properties for Improved Performance in the WNF and DNF Regions

In the WNF/DNF regions spalling is not as prevalent, and more porous concretes can be used successfully. Based on this study, if the aggregate are AAR resistant, a w/c ratio of up to about 0.60 can provide excellent spalling resistance. Fatigue resistance is the major design factor. An ultimate flexure strength of about 4.5 MPa appears to be adequate in conjunction with sufficient slab thickness. Substantial improvement in fatigue resistance and ultimate flexure strength is achieved by reducing the w/c ratio below 0.60. A wide range in cement contents was found in the WNF/DNF region to provide excellent long-term performance ranging from 279 to 335 kg/m^3 (5 to 6 sack).

Lowering w/c ratio

In these regions the importance of permeability appears to be reduced as deicing salts and freeze-thaw cycles are not factors. However, in these hot, dry climates the advantage of lowering the w/c ratio would be to achieve a more homogeneous concrete. This reduces the permeability gradient through the concrete thickness, which can reinforce the concrete against environmental attacks. At the same time, in hot, dry climates workability requirements should be considered when selecting w/c ratio values. As discussed in section 7.4.1, it is an advantage to lower the w/c ratio to increase the PCC's fatigue resistance.

Cement Type and Content

Concretes in warmer climates such as in the WNF/DNF climates typically use a lower heat of hydration portland cement (Type II). In addition, these regions can typically use lower cement contents averaging 307 kg/m^3 as the resistance to fluid transport is often less of a concern.

In particular in dry regions, the potential for drying shrinkage should be addressed through minimizing the total paste content. As in the WF region, it is recommended to keep the paste content around 25 percent. As is also valid in the WF discussion, increasing the cement content can significantly increase the CTE. It was found in this study that CTE should be as low as possible. The typical range of 9 to 10 x 10^{-6}/°C was adequate for good performance.

7.5 Test Methods for Quality Acceptance and Control

This study has established several threshold levels for PCC properties and material characteristics, which were associated with good long-term performance in terms of spalling, transverse cracking, and faulting. Considering these findings, additional test methods are recommended to improve quality control and acceptance protocols.

The recommended tests should be performed in addition to already established quality control and acceptance measures employed by the various SHA's.

7.5.1 Test Methods for Improved Spalling Resistance

From this study it has been established that joint deterioration related to transport properties and freeze-thaw damage can be avoided when certain PCC properties and material characteristics met critical levels. In particular,

- PCC fluid transport is low.
- Air void content is about 6 to 8 percent.
- Ultimate compressive strength exceeds about 45 to 50 MPa.
- w/c ratio below about 0.45.
- Aggregates are not deleteriously reactive and are freeze-thaw resistant.

Transport Properties (Permeability and Chloride Resistance)

Low fluid transport properties (such as permeability) are fundamental to improved resistance to joint deterioration. This study found a strong relation between ultimate permeability values and compressive strength. Low permeability was achieved when the compressive strength exceeded 45 to 50 MPa. This is similar to, but somewhat lower than findings by Armaghani and Bloomquist (1994), who stated that the compressive strength must exceed 55 MPa to ensure that the PCC indeed has low permeability. Because the required compressive strength for low permeability is also dependent on the test method used, it is recommended that pre-construction testing be performed on the project specific concrete to establish a relationship between permeability and compressive strength. Field quality control and acceptance criteria can then be developed based on compressive strength values of test cylinders.

There are many permeability and transport property tests available. Two fluid transport test methods can be recommended based on this study. These are the rapid chloride permeability test (RCPT) and the water absorption test. However, no single transport property test gives an intrinsic material permeability value, and it is wise to use more than one test method. The RCPT in particular should be used with caution because it is an electro-chemical index test, and does not physically measure the transport of fluids. When used with OPC concretes with typical pavement mix designs, the RCPT is highly repeatable and reliable. On the other hand, the use of modern cements containing mineral additives may influence RCPT results.

Transport Properties of Concretes Containing Mineral Additives

Because none of the studied pavement sections were designed to contain mineral additives, inferences about the effect of mineral additives on transport properties must be drawn from the literature and laboratory data available to the research team from another study.

Concretes with a number of blended cement systems containing fly ash and blast furnace slag were cast and tested using the RCPT at 63, 91 and 270 days, and 3 years. These mixes had typical pavement mix designs, and contained between 20 and 25 percent mineral additives as a cement replacement. The concretes were air entrained to be suitable for the WF climate zone. The mixes included two different class F fly ashes, one type C fly ash, and one ground granulated blast furnace slag (GGBFS).

In figure 7.5.1 the RCPT results of the various blended systems are plotted against compressive strength, along with those of OPC's from the field and the laboratory study. A significant reduction in RCPT results is noted for blends of low to moderate strength over OPC's at similar strengths. In the figure all blend systems are lumped together into one relation for convenience. However, it is likely that each type and amount of mineral additive would exhibit a different RCPT and different strength relation.

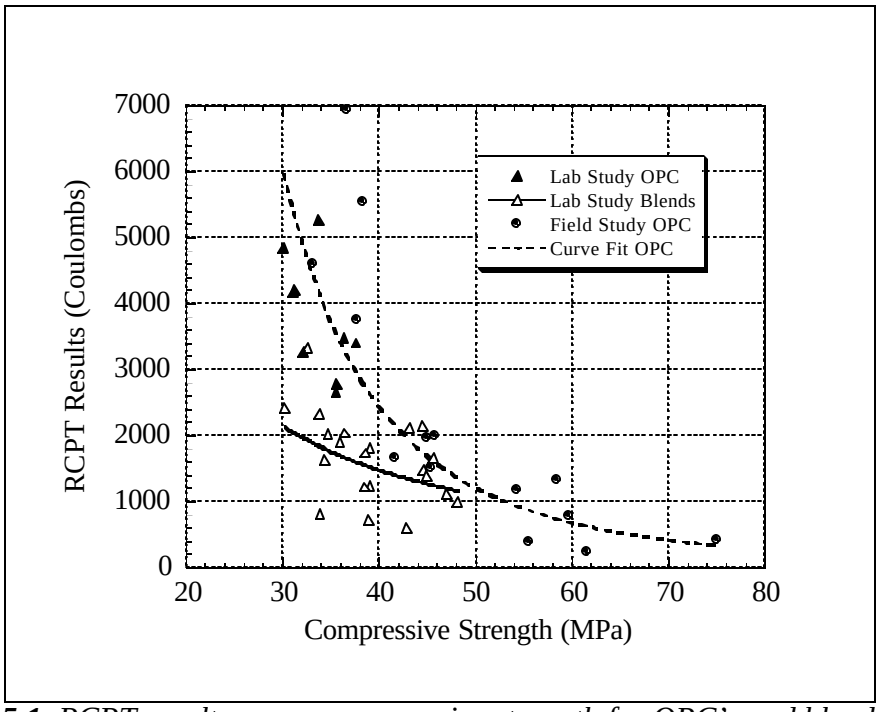

Figure 7.5.1 *RCPT results versus compressive strength for OPC's and blended cement systems from the field and laboratory studies.*

In recent years, though, a major concern has been raised about the RCPT. Researchers have found that the low RCPT measurements may not be caused by microstructure densification, but by changes in the pore solution chemistry (eg. Shi et al., 1998). These pore solution changes affect the electrical conductivity of the concrete, lowering measured RCPT values, but not the actual concrete permeability. As a result, a falsely low permeability is reported.

Figure 7.5.2 contains water absorption test data from the field study and from OPC and blended cement mixes in the laboratory study at 3 years. The significant decreases in transport seen with the RCPT are not visible here. All of the data here fall on one strength-permeability relation curve. Similar observations are made from the water permeability test. This indicates that the decreased RCPT results with blended systems are not primarily associated with a significant permeability decrease, but with some other mechanism. It is possible, for example that indeed the chloride ion penetration is significantly reduced with blended cements. However, permeability does not appear to be. A thorough study of the concrete microstructure and reaction processes would likely clear up the remaining uncertainty.

The absorptivity slope plotted here is obtained by taking the slope of the water uptake per unit area versus square root of time relationship, as described previously.

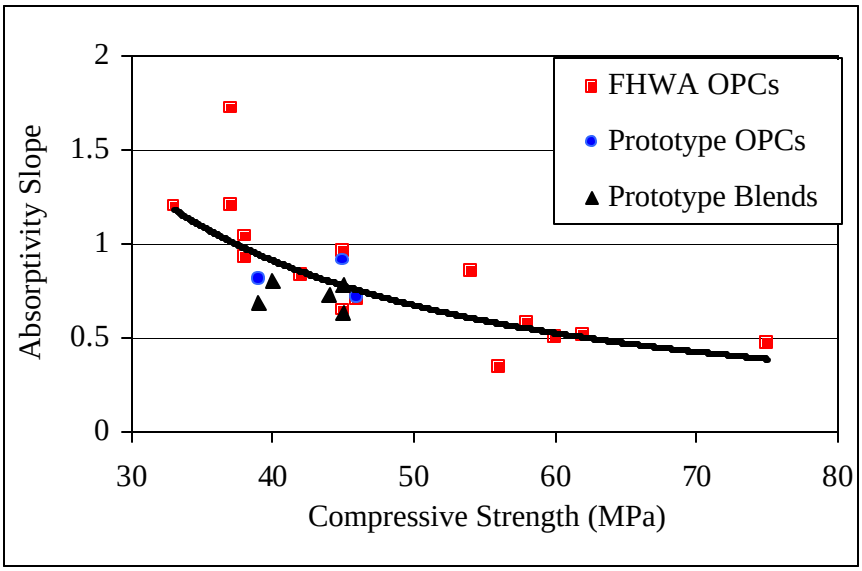

Figure 7.5.2 *Absorptivity slope versus compressive strength relation for field study and prototype mixes.*

Air Void System and Aggregate Soundness

Most SHA's already have established rigorous test methods for assuring adequate air void characteristics and sound aggregates. If post construction evaluation is desired, air void characteristics (air content, the spacing factor and specific surface area) can be determined in detail using the ASTM C 457 method. However, due to the detailed nature of this method, it is only recommended as a forensic tool. A good estimate of total air void content can also be gleaned from the relatively simple water absorption test, as described in chapter 6.

7.5.2 Test Methods for Improved Resistance to Transverse Cracking

This study found that transverse cracking could be avoided if the PCC slab has adequate strength and thickness, and if loss of support and large volumetric deformations are avoided as well. The observed PCC levels and material characteristics associate with improved resistance to transverse cracking are,

- PCC flexure strength exceeding 4.5 MPa when the slab thickness is adequate.
- Ultimate compressive strength exceeds about 33 MPa.
- CTE below 10.0 x 10^{-6}/°C.
- Drying shrinkage minimized with a paste content of about 25 percent (or about 28-30 percent including air).
- w/c ratio below about 0.60.
- Coarse aggregate tough and large sized.

Compressive Strength, Tensile Strength, and Elastic Modulus

Adequate strength is the controlling parameter for improved resistance to transverse cracking. The JPCP design procedures use the flexure strength as a design criterion. Current practice is often to establish a relationship between flexure strength and compressive strength, and then to base the field acceptance on the compressive strength measured from field cores. The main reasons for not using field beams are due to their large size and variability.

The PCC splitting tensile strength may serve as a better indicator of the PCC tensile capacity over its compressive strength. In general there is expected to be a stronger relation between flexure and splitting tensile strength, than between flexure and compressive strength.

It is, therefore, recommended that pre-construction testing be performed on the project specific concrete to establish a relationship between flexure strength and splitting tensile strength. Field quality control and acceptance can then be developed based on splitting tensile strength values of test cylinders from the field. Typically the same test equipment can be used to determine all the strength values. ASTM describes, in detail, the strength tests mentioned here.

In addition to PCC strength, the PCC elastic modulus is a key parameter in controlling the slab stresses. This study found that the ultimate elastic modulus increased proportionally to the ultimate compressive strength. This raises the need for determining the elastic modulus when higher strength concrete is used, as the elastic modulus increases more significantly than the increase in tensile capacity. This amplifies the significance of the elastic modulus as it could become a key input parameter for proper thickness design. Therefore, in the case of higher strength concrete, it is recommended that pre-construction testing be performed to establish the level of the elastic modulus associated with the PCC strength levels. The elastic modulus should be determined according to the current ASTM procedure.

Coefficient of Thermal Expansion

High CTE values were found associated with premature cracking. Therefore, it is recommended to keep CTE to a minimum. This study found that CTE values below 10.0 x $10^{-6}/^{o}$C were adequate. Based on the findings in this study, high CTE values become a concern when high cement contents are used. It is thus recommended to determine the concrete CTE when higher cement content is needed to obtain a desired level of strength. The test method is currently not an ASTM standard. However, the CTE test method developed by FHWA and used in this study has been accepted as a provisional standard by AASHTO. See chapter 2 for details.

PCC Resistance to Crack Propagation

Increasing strength has traditionally been viewed as increasing concrete brittleness. This study found that higher strength concrete may not become more brittle if tough coarse aggregates are selected. If higher strength is needed, the PCC fracture behavior can be optimized by proper coarse aggregate selection. The fracture energy test described in

chapter 2 of this report is an adequate measure of the resistance to crack propagation. This test is not currently an ASTM standard, however it is accepted and presented in detail by RILEM.

It was found that the ratio of fracture energy and splitting tensile strength can be used as an indicator of brittleness, and that the larger fracture energy to tensile ratio indicate tougher fracture behavior.

It is recommended that pre-construction tests be performed to establish which of the available aggregate sources would yield the toughest fracture behavior. The aggregates should be evaluated using the mix design and mix proportions intended for construction. The mix yielding the highest ratio should be selected, given that it also meets aggregate durability specifications.

7.5.3 Quality and Acceptance Control for Improved Resistance to Faulting

Faulting in this study has been linked primarily to foundation settlement and pumping erosion, both of which are structural level distresses. Thus, neither PCC properties nor material characteristics directly relate to faulting distress. At the same time, indirect relations to faulting are made with properties and materials characteristics that relate to improving load transfer across cracks and minimized pumping. As was described in the transverse cracking discussion above, the primary factors include large volumetric deformations and improved aggregate toughness. The test methods for these properties and characteristics have been discussed in section 7.5.2.

REFERENCES

AASHTO T 277 - 93 (1994). "Standard Method of Test for Electrical Indication of Concrete's Ability to Resist Chloride." *Standard Specifications for Transportation Materials and Methods of Sampling and Testing, Part II - Tests*, 16th Ed., American Association of State Highway and Transportation Officials, Washington, DC.

AASHTO (1986). *Guide for Design of Pavement Structures.* NCHRP Project 20-7/24, Vol. 2, American Association of State Highway and Transportation Officials.

AASHTO (1993). *Guide for Design of Pavement Structures - 1993*, Washington D.C. American Association of State Highway and Transportation Officials.

Abdel-Maksoud, M.G., Hawkins, N., and Barenberg, E. (1998). "Effect of geometric and mechanical properties of concrete joints on their cyclic shear response." Presented for the 1999 Federal Aviation Administration, Technology Transfer Conference.

ACI Committee 363 (1984). "State-of-the Art Report on High Strength Concrete." *ACI Journal*, Vol. 81, No. 4, Jul-Aug 1984, 364-411.

ACI Standard 211.1 (1989). "Recommended Practice for Selecting Proportions for Normal Weight Concrete." *ACI Manual of Concrete Practice, ACI*, Detroit, MI.

ACI Standard 318 (1994). "Durability Requirements, Section 4.2.1." *ACI Manual of Concrete Practice, ACI*, Detroit, MI.

ACI 360R-92 (1992). "Design of Slabs on Grade." Reported by ACI Committee 360, *ACI*, Detroit, MI.

Addis, B.J., ed. (1986). *Fulton's Concrete Technology.* Portland Cement Insitute, Midrand, South Africa.

Ahmad, S.H. (1994). "Short Term Mechanical Properties." *High Performance Concrete and Applications*, S.P. Shah and S.H. Ahmad, eds., Edward Arnold, London, UK, 27-64.

Aitcin, P.C., and Lessard, M. (1994). "Canadian Experience with Air-entrained High Performance Concrete." *Concrete International*, Vol. 16, No. 10, Oct 1994, pp. 35-38.

Aldea, C., Shah, S., and Karr, A. (1999). "Effect of Cracking on Water and Chloride Permeability of Concrete." *Journal of Materials in Civil Engineering*, Aug 1999, pp. 181-187.

Alungbe, G. D., Tia, M., and Bloomquist, D.C. (1990). "Effects of Aggregate, Water/Cement Ratio, and Curing on the Coefficient of Linear Thermal Expansion of

Concrete." *Transportation Research Record*, No. 1335, Transportation Research Board, pp. 44-51.

Armaghani, J., Romano, D., Bergin, M., and Moxley, J. (1994). "High Performance Concrete in Florida Bridges." *American Concrete Association Special Publication SP-140-1*, pp. 1-20.

Armaghani, J., and Bloomquist, D. (1994). "Development of Concrete Durability Specification and Ratings in Florida." *Transportation Research Record*, No. 1458, pp. 8-13.

Armaghani, J.M., and Bloomquist, D.G. (1993). "Durability Specification and Ratings for Concrete." *Concrete 2000*, R. Dhir and R. Jones, eds., E & FN Spon, pp. 23-36.

Armaghani, J.M., Larsen T.J., and Romano, D.C. (1992). "Aspects of Concrete Strength and Durability." *Transportation Research Record*, No. 1335, pp. 63-69.

ASTM C 39 - 94 (1995). "Standard Test Method for Compressive Strength of Cylindrical Concrete Specimens." *1995 Annual Book of ASTM Standards*, Vol. 04.02, Philadelphia, Pennsylvania.

ASTM C 457 - 90 (1995). "Standard Test Method for Microscopical Determination of Parameters of the Air-Void System in Hardened Concrete." *1995 Annual Book of ASTM Standards*, Vol. 04.02, Philadelphia, Pennsylvania.

ASTM C 469 - 94 (1995). "Standard Test Method for Modulus of Elasticity and Poisson's Ratio of Concrete in Compression." *1995 Annual Book of ASTM Standards*, Vol 04.02, Philadelphia, Pennsylvania.

ASTM C 496 - 90 (1995). "Standard Test Method for Splitting Tensile Strength of Cylindrical Concrete Specimens." *1995 Annual Book of ASTM Standards*, Vol. 04.02, Philadelphia, Pennsylvania.

ASTM C 856 - 83 (Re-approved 1988) (1995). "Standard Test Method for Petrographic Examination of Hardened Concrete." *1995 Annual book of ASTM Standards*, Vol. 04.02, Philadelphia, Pennsylvania.

ASTM C-1084 (1995). "Standard Test Method for Portland Cement Content of Hardened Hydraulic-Cement Concrete." *1995 Annual Book of ASTM Standards*, Vol. 04.02, Philadelphia, Pennsylvania.

ASTM C 1202 - 94 (1995). "Standard Test Method for Electrical Indication of Concrete's Ability to Resist Chloride Ion Penetration." *1995 Annual Book of ASTM Standards*, Vol. 04.02, Philadelphia, Pennsylvania.

Bache, H.H., and Vinding, I. (1990/1992). "Fracture Mechanics in Design of Concrete Pavements." *Proceedings, Second International Workshop on the Design and*

Evaluation of Concrete Pavements, CROW/PIARC, 4-5 October, Siguenza, Spain, pp. 139-164. (Also CBL reprint, CtO Aalborg Portland, Denmark -- in Danish.)

Benkelman, A.C. (1933). "Tests of Aggregate Interlock at Joints and Cracks." *Engineering News Record*, Vol. 3, No. 8, August 1933, pp. 227-232.

Bentz, D. et al. (1999) "Transport Properties and Durability of Concrete: Literature Review and Research Plan", NISTIR 6395, September 1999, pp.1-41.

Long, B., and Shatnawi, S. *"An Evaluation of Experimental PCC Pavement Design Features in California"*, TRB, 2000, pp.1-28.

Bjontegaard, O. (1999). "Thermal Dilation and Autogeneous Deformation as Driving Forces to Self-Induced Stresses in High Performance Concrete." Doctoral Thesis, The Norwegian University of Science and Technology.

Bradbury, R.D. (1938). *Reinforced Concrete Pavements.* Wire Reinforcement Institute, Washington, DC.

Bruinsma, J.E., Raja, Z.I., Snyder, M.B., and Vandenbosshe (1995). "Factors Affecting the Deterioration of Transverse Cracks in JRCP." Final Report, Contract 90-0973, to Michigan Department of Transportation. Michigan State University.

Buch, N., Frabizzio, M.A., and Hiller, J.E. (2000). "Factors Affecting Shear Capacity of Transverse Cracks in Jointed Concrete Pavements (JCP)." Final Report to Michigan Department of Transportation. Michigan State University.

Byrum, C.R., Hansen, W., and Kohn, S. (1997). "The effect of PCC Strength and Other Parameters on the Performance of PCC Pavements." *Sixth International Purdue Conference on Concrete Pavement Design and Materials for High Performance*, Vol. 1, pp. 373-393.

Carpinteri, A. (1986) "Mechanical Damage and Crack Growth in Concrete," Martinus nijhoff, Dordrecht. – as reference in Karihaloo (1995) p. 141.

Carrasquillo, R.L., Nilson, A.H. and Slate, F.O. (1981). "Properties of High Strength Concrete Subject to Short-Term Loads." *ACI Journal*, May-June 1981, pp. 171-178.

Colley, B.E., and Humphrey, H.A. (1967). "Aggregate Interlock at Joints in Concrete Pavements." *Highway Research Record*, No. 189, National Research Council, pp. 1-18.

Cramer, S.M., Hall, M., and Parry, J. (1995). "Effect of Optimized Total Aggregate Gradation on Portland Cement Concrete for Wisconsin Pavements." *Transportation Research Record,* No. 1478, July 1995, pp. 100-106.

CTA-Composite Testing and Analysis, Inc. (1998). *Design of Thermal Expansion Units,* Ann Arbor, Michigan.

Darter, M.I. (1977). *Design of Zero-Maintenance Plain Jointed Concrete Pavement: Vol. I-Development of Design Procedures.* FHWA, Report No. FHWA-RD-77-111.

Darter, M.I., and Barenberg, E.J. (1977). *Design of Zero-Maintenance Plain Jointed Concrete Pavement*. Report No. FHWA-RD-77-111., Vol. 1.

Darter, M.I., Peshkin, J.M., Snyder, M.B., and Smith, R.E. (1985). "Portland Cement Concrete Pavement Evaluation Systems – COPES." *National Cooperative Highway Research Program Report*, No. 227, Transportation Research Board, Washington DC.

Darter, M.I., Smith, K.D., and Peshkin, D.G. (1991). "Field-Calibrated Mechanistic-Empirical Models for Jointed Concrete Pavements." *Transportation Research Board,* No. 1307, National Research Council, Washington DC, pp. 143-153.

Darter, M.I., Hall. K.T., and Kuo, C-M (1994). *Support Under Concrete Pavements – Appendix E.* Prepared for National Cooperative Highway Research Program, Transportation Research Board, National Research Council, University of Illinois at Urbana-Champaign.

DataPave 97 (1997). *Long Term Pavement Performance (LTPP) Program Database*. US Department of Transportation, Federal Highway Administration.

Emborg, M. (1989). "Thermal Stresses in Concrete Structures at Early Ages." Doctoral Thesis, Lulea University of Technology.

FHWA (1996). *Determination of The Coefficient of Thermal Expansion of Portland Cement Concrete.* Draft.

FHWA (1995). *Performance of Concrete Pavements Containing Recycled Concrete Aggregate: Task B Draft Interim Report.* Prepared for the Federal Highway Administration by the University of Minnesota and ERES Consultants, Inc.

FHWA-SA-93-012-1992 (1992). *Report on the 1992 U.S. Tour of European Concrete Highways.* Federal Highway Administration, Publication No. FHWA-SA-93-012-1992.

Field Permeability Test (FPT) User's Manual. March, 1993.

Forster, S.W. (1997). "Concrete Materials and Mix Design for Assuring Durable Pavements." *Sixth International Purdue Conference on Concrete Pavement Design and Materials for High Performance,* Vol. 1, pp 111-118.

Foxworthy, P.T. (1985). "Concepts for the Development of a Nondestructive Testing and Evaluation System for Rigid Airfield Pavements." Ph.D. Thesis, University of Illinois at Urbana-Champaign.

Frabizzio, M.A., and Buch, N.J. (1999). "Investigation of Design Parameters Affecting Transverse Cracking in Jointed Concrete Pavements." *Transportation Research Board*, No. 1668, National Research Council, Washington DC, pp. 24-32.

Gan, G-L, Spry, P.G., Cody, R.D., and Cody, A.M. (1996). "Rim Formation in Iowa Highway Concrete Dolomite Aggregate: The Effects of Dedolomitization Reactions." *Environmental & Engineering Geoscience*, Vol. 2, No.1, Spring 1996, pp. 59-72.

Garboczi, E. (1990) "Permeability, Diffusivity, and Microstructural Parameters: A Critical Review," Cement and Concrete Research, Vol. 20, pp.591-601.

Giaccio, G., and Zerbino, R. (1998). "Failure Mechanism of Concrete – Combined Effects of Coarse Aggregates and Strength Level." *Advanced Cement Based Materials*, Elsevier Science Ltd., Vol. 7, pp. 41-48.

Gillespie, T.D., Karamihas, S.M., Sayers, M.W., Nasim, M.A., Hansen, W., and Ehsan, N. (1993). *Effects of Heavy-Vehicle Characteristics on Pavement Response and Performance.* Transportation Research Board, NCHRP Report 353, National Research Council, National Academy Press, Washington, DC.

Hansen, W., and Jensen, E.A. (2000). "Fracture Energy and Brittleness of Highway concrete: Effect of Coarse Aggregate Type and PCC Strength Level." *Cementing the Future, Center for Advanced Cement-Based Materials*, Spring 2000, Vol. 11, No. 2.

Hansen, W., Definis, A., Jensen, E., Byrum, C.R, Mohamed, A.R., Mohr, P., and Grove, G. (1998). *Investigation of Transverse Cracking On Michigan PCC Pavements over Open-Graded Drainage Course.* Final Report submitted to MDOT, University of Michigan.

Hansen, W., Mohamed, A. R., Byrum, C. R., and Jensen, E. (1998). "Effect of Higher Strength on Pavement Performance." *Proceedings, Materials Science of Concrete: The Sidney Diamond Symposium*, pp. 191-204.

Hearn, N., Hooton, D., and Mills, R. (1994). "Pore Structure and Permeability." *Tests and Properties of Concrete*, ASTM C 169, pp. 240-262.

Hillerborg, A. (1983). *Fracture Mechanics of Concrete.* "Chapter 4.1 Analysis of one single crack." Wittman, ed., Elsevier Science Publisher B.V., Amsterdam, pp. 223-249.

Holbrook, L.F., and Kuo, W.H. (1974). *General Evaluation of Current Concrete Pavement Performance in Michigan: Jointed Concrete Pavement Deterioration Considered as a Probability Process.* Michigan Research Laboratory Section, Michigan

Department of State Highways, Research Project 69 F-110, Research Report No. R-905.

Huang, Y. H. (1993). *Pavement Analysis and Design*. Prentice Hall, Englewood Cliffs, New Jersey.

Hveem, F.N. (1949) *"A Report of an Investigation to Determine Causes For Displacement and Faulting at the Joints in Portland Cement Concrete Pavements on California Highways"*, Caltrans, May 17, 1949.

Hveem, F.N., and Tremper, B. (1957). "Some Factors Influencing shrinkage of Concrete Pavements", ACI Journal, pp. 781-789, 1957.

Ioannides, A.M., and Korovesis, G.T. (1990). "Aggregate Interlock: A Pure Shear Load Transfer Mechanism." *Transportation Research Record*, No. 1286, Transportation Research Board, National Research Council.

Jensen, E.A, and Hansen, W. (2000). "Fracture Energy Test for Highway Concrete-Determining the Effect of Coarse Aggregate on Crack Propagation Resistance." *Transportation Research Record 1730,* pp. 10-16.

Kan, Y-C, and Swartz, S.E. (1995). "The effect of mix variables on concrete fracture mechanics parameters." *Fracture Mechanics of Concrete Structures, Proceedings FRAMCOS-2*, F.H. Wittmann, ed., AEDIFICATIO Publishers, Freiburg, Germany, pp. 111-118.

Karihaloo, B.L. (1995). *Fracture Mechanics & Structural Concrete.* Concrete Design & Construction Series, Longman Scientific & Technical, John Wiley & Sons, Inc., New York.

Kelleher, K., and Larson, R.M. (1989). "The Design of Plain Doweled Jointed Concrete Pavement." *Proceedings of the Fourth International Conference on Concrete Pavement Design and Rehabilitation*, Purdue University, West Lafayette, IN, April 1989.

Kleinschrodt, H.-D., and Winkler, H. (1986). *The Influence of Maximum Aggregate Size and the Size of Specimen on Fracture Mechanics Parameters, Fracture Toughness and Fracture Energy of Concrete.* F.H. Wittmann, ed., Elsivier Science Publishers B.V., Amsterdam, pp. 391-402.

Kosmatka, S.H., and Panarese, W.C. (1988/1992*). Design and Control of Concrete Mixtures.* 13th ed., PCA, Skokie, IL.

Kosmatka,S.H., Panarese W.C., Gissing,, K.D.,and MacLeod, N.F., (1995). *"Design and Control of Concrete Mixtures"*, Portland Cement Association. 1995.

Lane, S. (1994) "Thermal Properties of Aggregates," In *Significance of Tests and Properties of Concrete and Concrete-Making Materials*, Ed. Klieger, P., and Lamond, J.F. ASTM 04-169030-07, pp.438-445.

de Larrard, F., and Malier, Y. (1992). *High Performance concrete: From material to structure*. Y. Malier, ed., E & FN Spon, pp. 85-114.

Larson, R.M., Suneel, V., Forster, S. (1993). *Summary Report - U.S. Tour of European Concrete Highways (U.S. Tech) -- Follow-up tour of Germany and Austria*. FHWA-SA- 93-080, pp. 1-108.

"*Long-Term Pavement Performance-Program Reference Guide*"; Version 1.0, March 1996, Pavement Performance Division, Federal Highway Administration, 34 pp.

Mahoney, L.J., Pierce, L., Jackson, N., and Barenberg, E. (1991). "Urban Interstate Portland Cement Concrete Rehabilitation Alternatives for Washington State." WA-RD 202.1, p.350.

Marks, V.J. (1990). "An Overview of D-Cracking." *Nation D-Cracking Workshop Procedings,* Conducted by Kansas DOT and FHWA.

Marzouk, H. and Chen, C.W. (1995). "Fracture Energy and Tension Properties of High-Strength Concrete." *Journal of Materials in Civil Engineering*, Vol. 7, No. 2, May 1995, pp. 108-116.

Metha, P. (1990). "Durability of High Strength Concrete." Paul Klieger Symposium on Performance of Concrete, ACI SP-122, pp.19-27.

Mehta, P.K., and Aitcin, P.C. (1990). "Microstructural Basis of Selection of Materials and Mix Proportions for High-Strength Concrete." *High- Strength Concrete: Second International Symposium*, T.H. Weston, ed., ACI SP-121, pp. 89-108 and pp.265-286.

Mehta, P. and Monteiro, P.J.M. (1993). *Concrete: Structure, Properties, and Materials*. Second Edition, Prentice Hall, Inc., Englewood Cliffs, New Jersey.

Meyers, S.L. (1950). "Thermal Expansion Characteristics of Hardened Cement Paste and of Concrete." *Materials and Construction, Proc. Highway. Resesearch*., Board 30, 193.

Mindess, S., and Young, J. F. (1981). *Concrete.* Prentice-Hall, Inc., Englewood Cliffs, New Jersey.

Mobasher B., and Mitchell, T.M. (1988). "Laboratory Experience with the Rapid Chloride Permeability Test." *Permeability of Concrete,* ACI SP-108, pp. 117-144.

Mohamed, A.R., and Hansen, W. (1996). "Prediction of Stresses in Concrete Pavement Subjected Non-Linear Gradients." *Journal of Cement and Concrete Composites*, Vol. 18, pp. 381-387.

Mohamed, A.R., and Hansen, W. (1999). "Micromechanical Modeling of Crack-Aggregate Interaction in Concrete Materials." *Journal of Cement and Concrete Composites*.

Monteiro, P.J.M., and Helene, P.R.L. (1994). "Designing Concrete Mixtures for Desired Mechanical Properties and Durability, Concrete Technology: Past, Present and Future." *Proceedings of V.M. Malhotra Symposium*, K. Mehta, ed., ACI SP-144, pp. 519-543.

Neville, A.M. (1975). *Properties of Concrete.* Pitman Publishing Inc.

Neville, A.M. (1981). *Properties of Concrete.* Pitman Publishing Inc.

Neville, A.M. (1983). *Properties of Concrete.* 3rd Edition, The English Language Book Society and Pitman Publishing, London.

Neville, A.M. (1997) "Properties of Concrete", Wiley, pp.1-844.

NCHRP 1-26, (1990) *Calibrated Mechanistic Structural Analysis Procedures for Pavements.* Vol. 2, Appendices D.2.2-34, University of Illinois at Urbana-Champaign.

Nowlen, W.J. (1968). "Influence of Aggregate Properties on Effectiveness of Interlock Joints in Concrete Pavements." *Journal of the PCA*, Research and Development Laboratories, Vol. 10, No. 2, May 1968, pp. 2-8.

Ollivier, J., Massat, M., Parrot, L. (1995). "Parameters Influencing Transport Characteristics." *Performance Criteria for Concrete Durability*, RILEM Report No. 12, H. Hilsdorf and J. Kropp, eds., pp.33-96.

Owusu-Antwi, E.B., and Darter, M.I. (1994). "Early Results of the LTPP Concrete Pavement Data Analysis." *Third International Workshop on Design and Evaluation of Concrete Roads*, Vienna, Austria.

Packard, R.G., and Tayabji, S.D. (1985). "New PCA Thickness Design Procedure for Concrete Highway and Street Pavements." *Third International Conference on Concrete Pavement Design and Rehabilitation*, Purdue University, pp. 225-236.

PCA (1984). *Thickness Design for Concrete Highway and Street Pavements.* Portland Cement Association.

PCA (1988/91). "Design and Construction of Joints for Concrete Highways." *Concrete Paving Technology*, Portland Cement Association.

Peshkin, D.G., Smith, K.D., Darter, M.I, and Arnold, C. (1994). "Performance Evaluation of Experimental Pavement Designs at Clare, Michigan." *Transportation Research Record*, No. 1227, pp. 24-32.

Petersson, P. (1981). *Crack Growth and Development of Fracture Zones in Plain Concrete and Similar Materials*. Division of Building Materials, Lund Institute of Technology, Lund, Sweden.

Philleo, R.E. (1986) "Freezing and Thawing Resistance of High-Strength Concrete", NCHRP Report 129, pp.1-31.

Pickett, G.O., (1956). *"Effect of Aggregate on Shrinkage of Concrete and a Hypothesis Concerning Shrinkage"*, ACI Journal, January 1956, pp. 581-590.

Pittman, D.W. (1996). "Factors Affecting Joint Efficiency of Roller-Compacted Concrete Pavement Joints and Cracks." *Transportation Research Record*, No. 1525, National Research Council, Washington DC, pp. 10-20.

Poblete, M., Salsilli, R., Valenzuela, R., Bull, A., and Spratz, P. (1989). "Field Evaluation of Thermal Deformations in Undoweled PCC Pavement Slabs." *Transportation Research Record*, No. 1207.

Poblete, M., Ceza, P., Espinosa, D.R., Garcia, A., and Gonzalez, J. (1991). "Model of slab cracking for portland cement concrete pavements." *Transportation Research Record*, No. 1307, Transportation Research Board, National Research Council, Washington, DC.

Powers, T.C. (1945). "A Working Hypothesis for Further Studies of Frost Resistance of Concrete." *Proceedings*, American Concrete Institute, Vol. 41, pp. 245-272.

Powers T.C. & Brownyard T.L., (1948) "Studies of the Physical Properties of Hardened Portland Cement Paste", PCA Bulletin 22.

Powers, T.C. (1949). "The Air Requirement of Frost-Resistant Concrete." *Proceedings of the Highway Research Board*, Vol. 29, Highway Research Board, National Research Council, Washington, DC, pp. 184-211.

Price, W.H. (1951). "Factors Influencing Concrete Strength." *ACI Journal*, Feb 1951, pp. 417-432.

Rauhut, J. B., Lytton, R.L, and Darter, M.I. (1984). *Pavement Damage Functions for Cost Allocation*. Four Volumes, Report No. FHWA/RD-84/017-020, Federal Highway Administration, U.S. Department of Transportation, Washington, DC.

Rhodes, C.C. (1949). *Curing Concrete Pavements.* Michigan State Highway Department, Project 42 B-14(2), Report 145.

RILEM Committee FMC 50 (1985). "Determination of the fracture energy of mortar and concrete by means of the three-point bend tests on notched beams." Mater. Struct., 18.

Roesler, J.R., and Barenberg, E.J. (1998). "Fatigue of Concrete Beams and Slabs." Final report FHWA-IL-UI-265. University of Illinois Urbana, Illinois.

Roy, D.M., Silsbee, M.R., Sabol, S., and Scheetz, B.E. (1995). "Superior Microstructue of High-Performance Concrete for Long-Term Durability." *Transportation Research Record,* No. 1478, July 1995, pp. 11-19.

Schonlin, K., and Hilsdorf, H.K. (1988). "Permeability as a Measure of Potential Durability of Concrete - Development of a Suitable Test Apparatus." *Permeability of Concrete,* ACI SP-108, pp. 99-116.

Sellevold E.J., (1986) "Hardened Concrete-Determination of air/macro and gel/capillary porosity (PF-Method)," Report 01731, Norwegian Building Institute.

Senadheera, S.P., and Zollinger, D.G. (1994). "Framework for Incorporating Spalling in the Design of Concrete Pavements." *Transportation Research Record*, No. 1449, Transportation Research Board, National Research Council.

Senadheera, S.P. and D.G. Zollinger. (1995). "Influence of Coarse Aggregate in Portland Cement Concrete on Spalling of Concrete Pavements." Research Report 1244-11, Texas Transportation Institute, College Station, TX.

SHRP-P-338 (1993). *Distress Identification Manual for the Long-Term Pavement Performance Project*. Strategic Highway Research Program, National Research Council, Washington, DC.

Simpson, A.L., Rauhut, Jordahl, P.R., Owusu-Antwi, E.B., Darter, M.I., and Ahmad, R. (1994). "Early Analysis of LTPP General Pavement Studies Data, Volume 3: Sensitivity Analysis for Selected Pavement Distresses." Report No. SHRP-P-393. Strategic Highway Research Program, Washington, DC.

Smiley, D.L. (1995). "Michigan Department of Transportation-First Year Performance of The European Concrete Pavement on Northbound I-75-Detroit, Michigan." Research Report No. R-1338, pp. 1-20.

Smiley, D.L. (1996). "Michigan Department of Transportation-Second Year Performance of The European Concrete Pavement on Northbound I-75-Detroit, Michigan". Research Report No. R-1343, pp. 1-13.

Smiley, D.L. (1997). "Michigan Department of Transportation-Third Year Performance of The European Concrete Pavement on Northbound I-75-Detroit, Michigan." Internal MDOT document, March 18, pp. 1-6.

Smith, K.D., Peshkin, D.G., Darter, M.I., Mueller, A.L., and Carpenter, S.H. (1990). "Performance of Jointed Concrete Pavements: Volume I-Evaluation of Concrete Pavement Performance and Design Features." Report No. FHWA-RD-89-136, U.S. Department of Transportation, Federal Highway Administration.

Smith, K.D., Wade, M.J., Peshkin, D.G., Khazanovich, L., Yu, H.T., and Darter, M.I. (1995). *Performance of Concrete Pavements, Volume II - Evaluation of Inservice Concrete Pavements*, Report No. FHWA-RD-95-110, Federal Highway Administration, Washington, DC.

Smith, K.D., M.J., Wade, H. T. Yu, and M.I., Darter (1997). "Design Considerations for Improved JPCP Performance." *Sixth International Purdue Conference on Concrete Pavement Design and Materials for High Performance,* Vol. 1, pp. 89-109.

Soares, J.B., and Zollinger, D.G. (1997). "Strength Characterization and Basis for Sawcutting Requirements for Jointed Concrete Pavements." *Sixth International Purdue Conference on Concrete Pavement Design and Materials for High Performance*, Vol. 2.

Spellman, D.L.; Woodstrom, J.H.; Neal, B.F.; Mason, P.E. (1973) "Recent Experimental PCC Pavements In California", Caltrans, June 1973, pp.56.

Stark, D. (1991). *Handbook for the Identification of Alkali-Silica Reactivity in Highway Structures*. SHRP-C/FR-91-101, Nation Research Council, Washington, DC.

Sutherland, E.C., and Cashell, H.D. (1945). "Structural Efficiency of Transverse Weakened-Plane Joints." *Public Roads*, Vol. 24, No. 4, Apr-June 1945.

Tachibana, D., Imai, M., Yamazaki, N., Kawai, T., and Inada, Y. (1990). "High-Strength Concrete Incorporating Several Admixtures." *High- Strength Concrete: Second International Symposium*, ACI SP-121, T.H. Weston, ed., pp. 309-330.

Teller, L.W., and Bosley, H.L. (1930). "The Arlington Curing Experiments." *Public Roads Journal of Highway Research*, USDA, Vol. 10, No. 12.

Teller, L.W., and Sutherland, E.C. (1935). "Observed Effects of Variations in Temperature and Moisture on the Size, Shape, and Stress Resistance of Concrete Pavement Slabs." *Public Roads Journal of Highway Research*, USDA, Vol. 16, No. 9.

Till, R., Smiley, D., and Van Portfliet, R. (1994). "Demonstrating Innovative Concrete Pavement Concepts in Michigan" *Transportation Research News*, No. 174, pp. 14-18.

Titus-Glover, L., Owusu-Antwi, E.B., and Darter, M.I. (1999). "Design and Construction of PCC Pavements" FHWA-RD-98-113, U.S. Department of Transportation, Federal Highway Administration.

Titus-Glover, L., Owusu-Antwi, E.B., and Darter, M.I. (1999). "Design and Construction of PCC Pavements – Volume III: Improved PCC Performance Models." FHWA-RD-98-113, U.S. Department of Transportation, Federal Highway Administration.

Torrent, R. (1992). *A Two-chaber vacuum cell for measuring the coefficientof air-permeability of the concrete cover on site.* Materials & Structures, v. 25m n. 150, 1992, pp. 358-365

TRB (1986). *Strategic Highway Research Program - Research Plans.* Transportation Research Board, Final Report, Washington, DC.

Ulfkjær, J.P., Brincker, R., and Krenk, S. (1990). "Analytical Model for Complete Moment-Rotation Curves of Concrete Beams in Bending, Fracture Behavior and Design of Materials and Structures." (Proc 8th European Conf on Fracture, Turin, Italy 1990.) D. Firrao, ed., Engineering Materials Advisory Services, Warley, UK, Vol. 2, pp. 612-617. Also published elsewhere in 1992.

Van Dam, T.J. (1995). "The Impact of Climate, Load, and Materials on the Performance and Deterioration of GA Airports in Illinois." Ph.D. Thesis, University of Illinois Urbana-Champaign.

Van Wiji, A.J., Larralde, C.W.L., and Chen, W.F. (1989). "Pumping Prediction Model for Highway Concrete Pavements." *Journal of Transportation Engineering*, Vol. 115, No. 2, pp. 161-175.

Vervuurt, A. (1997). "Interface Fracture in Concrete." Ph.D Thesis, CIP-GEGEVENS KONINKLIJKE BIBILOTHEEK DEN HAAG.

Vesic, A.S. and Saxena, S.K. (1969). "Analysis of Structural Behavior of Road Test Rigid Pavements." *Highway Research Record*, No.291, pp. 156-158.

Weinfurter, J.A. et al. (1994). "Michigan Department of Transportation Construction of European Concrete Pavement on Northbound I-75-Detroit, Michigan." Research Report no. R-1333, pp. 1-27.

Wells, G.K. (1993). "Summary Report to Improve Jointed Plain Concrete Pavement (JPCP) Performance," Dec. 29.

Westergaard, H.M. (1926). "Stresses in Concrete Pavements Computed by Theoretical Analysis." *Public Roads Journal of Highway Research*, USDA, Vol. 7, No. 2.

Westergaard, H.M. (1927). "Analysis of Stresses in Concrete Roads Caused by Temperature." *Public Roads Journal of Highway Research*, USDA, Vol. 8, No. 3.

Yu, H.T., Darter, M.I., Smith, K.D., Jiang, J., and Khazanovich, L. (1996). "Performance of Concrete Pavements, Volume III – Improving Concrete Pavement Performance,

Final Report." Contract No. DTFH61-91-C-00053. Federal Highway Administration, McLean, VA.

Zia, P., Leming, M. L., and Ahmad S. H. (1991). *High Performance Concretes - A State of-the-Art Report*. Strategic Highway Research Program, SHRP-C/FR-91-103, National Research Council, Washington, DC.

Zhou, F.P., Barr, B.I.G., and Lydon, F.D. (1995). "Fracture Properties of High Strength Concrete with Varying Silica Fume Content and Aggregates." *Cement and Concrete Research*, Vol. 25, No. 3, pp. 543-552.

Zoldners, N.G. (1971). "Thermal Properties of Concrete Under Sustained Elevated Temperatures", Temperature and Concrete" in *Temperature and Concrete*, ACI SP-25, Detroit, MI, pp. 1-31.